THE CROSS-FLOW CHROMATOGRAPHIC SEPARATION OF CARBOHYDRATE MIXTURES

A thesis submitted by

CHRISTOPHER LESLIE THIRKILL, BSc

for the degree of Doctor of Philosophy

THE UNIVERSITY OF ASTON IN BIRMINGHAM

August 1987

THE UNIVERSITY OF ASTON IN BIRMINGHAM

DEPARTMENT OF CHEMICAL ENGINEERING & APPLIED CHEMISTRY

THE CROSS-FLOW CHROMATOGRAPHIC SEPARATION OF CARBOHYDRATE MIXTURES

Mr Christopher Leslie Thirkill

Doctor of Philosophy
August 1987

Summary

Reviews are given of the theoretical aspects of chromatography and of continuous chromatographic techniques.

A pilot-scale rotating annular chromatograph has been constructed consisting of two concentric cylinders which form an annulus 1.4m in length and 12mm wide. The annular space is filled with ion-exchange resin. The upper and lower surfaces of the annulus are enclosed by stainless steel flanges. The entire bed is rotated slowly at speeds of up to four revolutions per hour. Feed solutions are introduced via a stationary inlet distributor into a layer of glass beads at the upper surface of the column packing. Deionised water as eluent is also introduced to the upper surface of the packing. Each component in the feed mixture has a different retention time within the resin. The rate of travel of each solute combined with the rotation of the annulus causes each component to exit the annulus at a different position. Products pass through the lower stainless steel flange and into a stationary collector beneath the annulus.

Several carbohydrate mixtures have been separated with varying degrees of success. Glucose has been separated from its isomer fructose in synthetic solutions and in inverted beet molasses. Mixtures of glucose, fructose and sucrose have also been resolved quite successfully. These separations were carried out on Purolite PCR 833 ion exchange resins in the Ca^{2+} form. Sucrose has been separated from betaine and other non-sugars in ordinary beet molasses using Duolite C211/2558 ion exchange resin in the Na^{+} form.

A total throughput of 540g h^{-1} sugar solids has been shown to be readily achievable to give 300g h^{-1} glucose (4.8% w/v concentration, 90% purity) and 240g h^{-1} fructose (2.6% w/v concentration, 90% purity). This corresponds to a specific throughput of 56.8 Kg sugar solids m^{-3} resin h^{-1}.

A computer simulation program has been developed which can be used to predict quite accurately the peak positions and peak bandwidths of solutes leaving the annulus, product purities, yields and throughputs.

KEYWORDS: Continuous chromatography; carbohydrate; annular, molasses; multicomponent.

Dedicated to my
family and friends

ACKNOWLEDGEMENTS

The author wishes to thank the following:

Dr E. Smith and the Department of Chemical Engineering and Applied Chemistry for making available the facilities for research.

Professor PE Barker, who supervised the work for his advice and guidance.

Mr N Roberts, Mr M Lea and all the members of the Department technical staff who assisted in the construction of the equipment.

The directors of British Sugar plc for the provision of funds for equipment and consumables. Mr GC Jones,Mr N Broughton , Mr D Sargent and other members of the British Sugar research group for the helpful advice and assistance.

Fellow research students in the separation and purification group for many useful discussions.

Mr S Bridges for the work carried out on the computer program.

The University of Aston for the provision of a scholarship.

CONTENTS

LIST OF FIGURES AND TABLES

PHOTOGRAPHS

CHAPTER ONE

INTRODUCTION

The increasing demand for pure chemicals has stimulated research into developing more novel separation processes such as electrodialysis, ultrafiltration, electrophoresis and chromatography.

Chromatography is a method of separating various components from a mixture of chemical substances. The method has been broadly applied to organic and inorganic substances. It is particularly useful if the compounds involved have very similar chemical or physical properties. Chromatography involves the partitioning of differing solutes by a variety of means which are discussed in Chapter 2 between a mobile phase and a stationary phase. The degree to which a solute is retarded by the stationary phase governs the rate at which it progresses through a chromatographic column. The difference in retention time of solutes effects the separation.

The application of chromatography to industrial preparative operation was for many years hampered by several factors. Among them the need for batch separations and the problems associated with large diameter columns. To a large extent this has restricted chromatography to low throughput systems or use for sensitive systems.

Chromatography has the advantages of versatility and high resolution over other separation techniques and in the last thirty years various attempts have been made to increase the capacity in chromatography. Several reviews of methods which attempt to achieve

continuous chromatographic separations have appeared in the literature, eg. Rendell (1), Sussman and Rathore (2), Sussman (3) and Barker (4). These methods include counter-current moving bed systems, simulated moving bed type systems and cross-current flow type systems. This work concentrates on the cross-current flow type of system.

The aims of this research were;

(1) To design a continuous rotating annular chromatograph suitable for the separation of multicomponent mixtures of carbohydrates.

(2) To commission and test the chromatograph in order to evaluate its performance in comparison with batch and semi-continuous chromatographic equipment.

(3) To assess the capabilities of the chromatograph for resolving multicomponent feedstocks and in particular beet molasses.

Beet molasses is the uncrystallizable viscous liquid which remains after the sugar refining process. It consists of mainly sucrose and a large number of other carbohydrates, amino acids, minerals etc in low concentration. It is normally sold as animal fodder at a small percentage of the cost of pure sucrose. The sucrose present cannot be crystallized by normal means due to the impurities

present. Chromatography offers a method of removing other components in the mixture to give a crystallizable solution of sucrose and a solution which has a much greater protein/carbohydrate ratio than the original molasses and hence a better animal food.

(4) To model the technique and develop a computer simulation program which can be used to predict throughputs, yields and purities of products under any operating conditions.

CHAPTER TWO

CHROMATOGRAPH THEORY AND TERMINOLOGY

2 Chromatographic Terminology and Theory

2.1 Scope

The literature survey included in this thesis has been mainly divided into two sections. Chapter Two discusses the theory and terms involved in chromatography and in particular the theory of annular chromatography. Chapter Three contains a review of continuous chromatographic equipment and techniques.

A review of the chromatographic extraction of sucrose from beet molasses is covered in Chapter Seven.

2.2 Introduction to Chromatography

Chromatography is a separation technique in which a mobile phase containing two or more components is allowed to pass through a stationary phase. Each component has a different affinity for the stationary phase and therefore each component proceeds through the stationary phase at a different rate. A chromatographic separation is the result of specific interactions between sample molecules and the stationary and mobile phases. These interactions may be physical or chemical. This thesis is concerned with liquid chromatography, which can be defined as any chromatographic process in which the mobile phase or eluent is a liquid.

2.3 Types of Liquid Chromatography

Categorisation of liquid chromatography is usually carried out according to the mechanism of retention of solutes passing through the stationary phase. The categories are:

(i) Ion exchange chromatography

(ii) Ligand exchange chromatography

(iii) Ion exclusion chromatography

(iv) Exclusion chromatography

(v) Partition chromatography

(vi) Adsorption chromatography.

In ion exchange chromatography the retention mechanism involves the formation of complexes between the cations on the stationary phase and the solute molecules. Ion exchange mechanisms were used to effect the separation of mixtures of glucose and fructose. Chapter Six describes this in detail.

Ion exclusion chromatography involves the charged species on an ion-exchange resin having the effect of repelling similar species in the mobile phase. These ions in the mobile phase are therefore not retained and are eluted rapidly. The separation of sucrose from beet molasses as discussed in Chapter Six was effected by this technique.

Separation in exclusion chromatography is based on molecular size. Larger molecules are less likely to penetrate the pores of the packing. The more frequently that a molecule can penentrate these pores, the more highly retained the molecule will be. Larger molecules are therefore eluted at a faster rate and smaller molecules are eluted more slowly.

Partition chromatography is dependent upon the adsorption of solutes by an inert solid support coated with a liquid stationary phase.

Adsorption chromatography involves the retention of molecules by association either physically or chemically with active sites on the stationary phase.

Ligand exchange chromatography is a form of adsorption chromatography whose retention mechanism relies on the association of the solute with a suitably charged ion-exchanger on the stationary phase; no ion-exchange actually occurs.

Process and liquid chromatography do not always fit neatly into one or other category. The separation of components in a mixture may be effected by two or more of these mechanisms simultaneously. For instance in the separation of sucrose, glucose and fructose mixtures on Purolite PCR833 ion exchange resin it was noted that sucrose was eluted before the lighter glucose and fructose molecules; a size exclusion effect. Glucose was however eluted before its isomer fructose, since fructose forms a weak complex with the calcium ions in the resin. This is a ligand exchange effect.

2.4 Conventional Chromatographic Theory

Differential migration rates for compounds in the mobile phase is the basis for separation in liquid chromatography and results from the equilibrium distribution of these compounds between the stationary and the moving phase. Figure 2.1 demonstrates this.

$$K = \frac{(X)_s}{(X)_m} \qquad \text{..... 2.1}$$

where

K = distribution coefficient

$(X)_s$ = No of moles per litre of X in the stationary phase

$(X)_m$ = No of moles/l of X in the mobile phase

If compound X is found mainly in the stationary phase at equilibrium, ie. the distribution coefficient for X is high.

If compound Y is found mainly in the mobile phase, ie. K is low then the migration rate for compound Y is greater than that for compound X. At the extreme, if the distribution coefficient for a compound is equal to zero, then the compound is present only in the mobile phase. Such a compound would have the same velocity as the solvent.

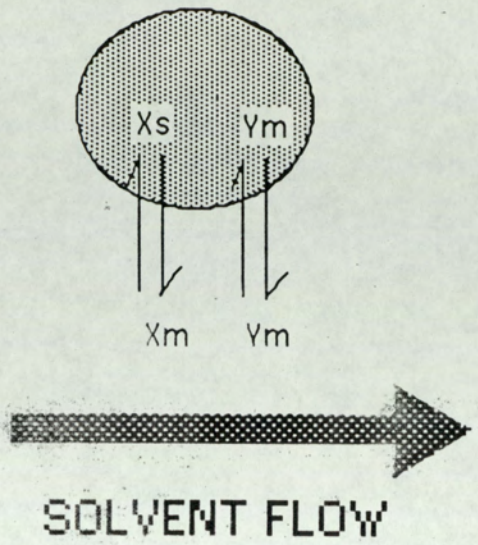

Figure 2.1 distribution of solutes between the stationary and mobile phases.

If a solvent passing through a column has a velocity equal to u and the average velocity of a solute X is u_x, then u_x depends on the fraction R of molecules X in the mobile phase and upon u, ie:

$$u_x = uR \qquad \text{..... 2.2}$$

If the capacity factor k' is defined as:

$$K' = \frac{\text{The total number of moles of X in the stationary phase}}{\text{The total number of moles of X in the mobile phase}}$$

$$= \frac{n_s}{n_m} \qquad \text{..... 2.3}$$

it can be shown that:

$$R = \frac{n_m}{n_s + n_m} = \frac{1}{1 + k'} \qquad \text{..... 2.4}$$

and therefore

$$u_x = \frac{u}{1 + k'}$$

The average velocity of solute X; u_x can be related to column length, L and retention time, t_R. t_R is the time taken for solute X to pass from one end of the column to the other.

$$t_R = L/u_x \qquad \text{..... 2.5}$$

If t_o is the time taken by the solvent to traverse the column, then:

$$t_o = L/u$$

and hence

$$t_R = t_o (1 + k') \qquad \text{..... 2.6}$$

or by rearrangement

$$k' = \frac{t_R - t_o}{t_o} \qquad \text{..... 2.7}$$

Retention can also be measured in terms of volume. Retention volume, V_R is the total volume of mobile phase required to elute a given band X and can be expressed as:

$$V_R = t_R F$$

where F = flowrate of solvent through the column.

The total volume of solvent within the column;

$$V_m = t_o F$$

Eluminating F

$$V_R = V_m t_R / t_o$$

$$= V_m (1 + k') \qquad \text{..... 2.8}$$

Rentention volume values can be more useful than retention times because V_R is independent of flowrate. The capacity factor K' is related to V_m as follows:

$$k' = \frac{(X)_s V_s}{(X)_m V_m} = \frac{K V_s}{V_m} \qquad \text{..... 2.9}$$

where V_s = the volume of stationary phase within the column

K = the distribution coefficient of X

Band spreading has been shown by various researchers to be dependent on many factors. Several concepts and theories have been used to explain the mechanisms involved.

2.4.1 The Theoretical Plate Concept

This concept first applied by Martin and Synge (5) envisages a chromatographic column consisting of a number of layers or plates. The solution issuing from each plate can be assumed to be in equilibrium with the mean concentration of solute in the stationary phase throughout the plate. It is also assumed that the diffusion of solute from one layer to another is negligible and that the mobile phase flow is discontinuous, consisting of stepwise additions of volumes of the mobile phase equal to the mobile phase volume per plate. Further assumptions are made in that at equilibrium, the distribution ratio of one solute between the two phases must be independent both of the absolute value of its concentration and of the presence of other solutes.

The Theory of Band Broadening

Bandwidth, t_w can be expressed in terms of the theoretical plate number N of the column:

$$N = 16\left(\frac{t_R}{t_w}\right)^2 \qquad \text{..... 2.10}$$

For a given set of conditions N can be considered constant for different bands in a chromatogram. Therefore N can be used to measure the efficiency of a column. N can be related to column length L by the following equation:

$$N = L/H \qquad \text{..... 2.11}$$

where H is a constant known as the height equivalent to a theoretical plate or HETP value. Small H values mean more efficient columns, ie. larger numbers of theoretical plates.

The efficiency, defined by the plate height, H is expressed as:

$$H = \frac{d\sigma_z^{\,2}}{dZ} = \frac{\sigma^2(L)}{L} \qquad \text{..... 2.12}$$

where σ_z^2 = length based second moment

Z = distance along a column of length L

This assumes that the single solute band has spread into a Gaussian distribution curve. The second moment term describes the degree of spreading or variance of the curve.

For a given solute:

$$C = C_o \exp\left(\frac{V_o - V_R^2}{2\sigma^2}\right) \qquad \text{..... 2.13}$$

where C = solute concentration

C_o = concentration at the peak

V_o = mobile phase velocity

V_R = retention volume of solute i

σ^2 = peak variance in units of volume

Since the bandwidth is represented by the variance, the square root of the variance (standard deviation, σ) is proportional to the peak's width, W. Equation 2.13 can be rewritten in terms of the number of plates, N as:

$$C = C_o \exp\left(\frac{N\,(V_o - V_R)^2}{V_i}\right) \qquad \text{..... 2.14}$$

Therefore the relationship between the number of plates in a chromatographic column, the variance, the column length, L and the solute retention volume is as follows:

$$N = \frac{V_i^2}{\sigma^2}$$

$$H = \frac{L}{N} = L\left(\frac{\sigma^2}{V_R^2}\right) \qquad \text{..... 2.15}$$

Glueckauf (6) using a similar approach related the elution time, t_{Ri}, and the variance to the "apparent" number of theoretical plates, N* in the following form:

$$N^* = 8\left(\frac{t_R}{t_{w\,(h/e)}}\right) \qquad \text{..... 2.16}$$

where $t_{w(h/e)}$ was the bandwidth at a height equal to the peak height divided by the base of the national logarithm, e (Figure 2.2). The predictions arising from the plate theory can be summarised as follows:

- a Gaussian peak shape
- peak width increased linearly with retention volume
- the number of theoretical plates increases with column length

2.4.2.1 The Rate Theory

The rate theory which was originally developed by Lapidus and Amundson (7) visualizes the column as a continuous medium where mass

Figure 2.2 The relationship between the number of theoretical plates and the Peak Characteristics.

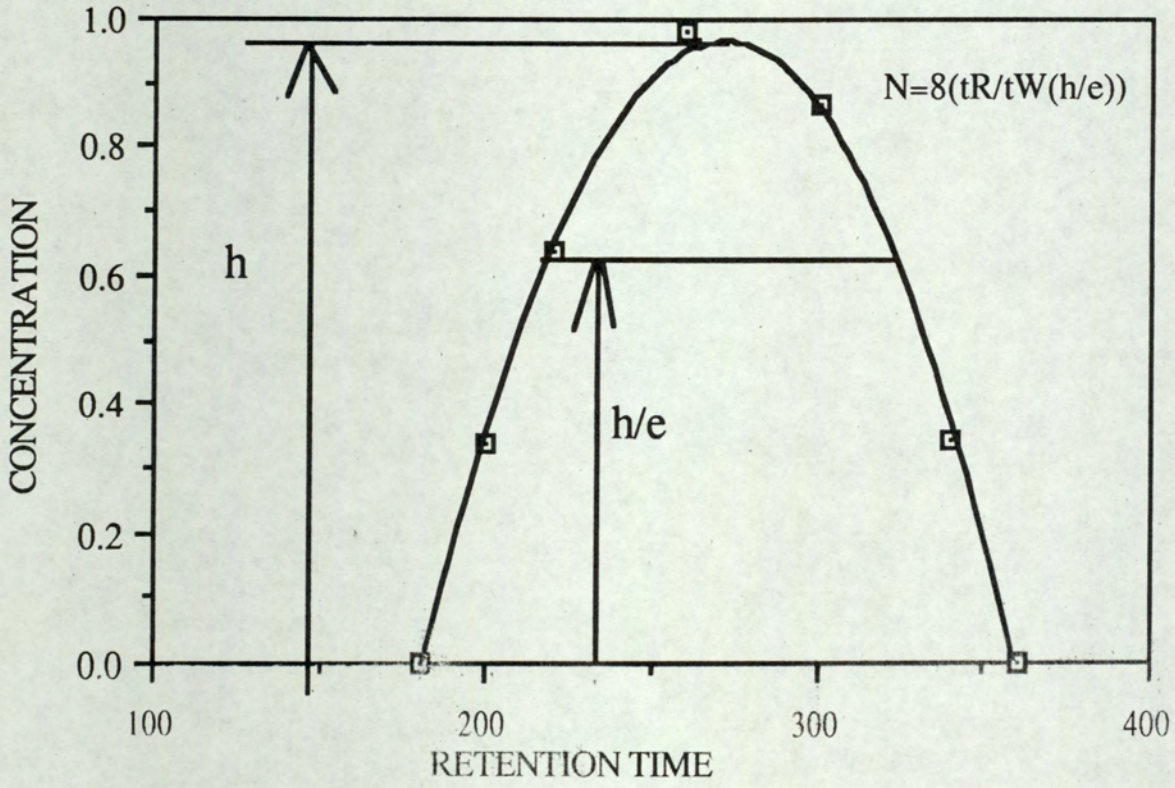

transfer and diffusion are accounted for. Van Deemter et al (8) took the model one stage further and took into account the effects of flow behaviour on a band in the column and the rte of adsorption or reaction.

The Van Deemter equation can be expressed as:

$$H=A+ B/u +Cu \qquad .....2.17$$

where

u = mobile phase velocity

A = eddy diffusion component

B = longitudinal diffusion terms

C = mass transfer term

Equation 2.17 can be represented as in Figure 2.3. The solid line in Figure 2.3 is the sum of the dispersion processes and shows a minimum in plate height (H_{min}) which corresponds to the "optimum" velocity (u_{opt}); at this velocity the column has the maximum separation efficiency. The C term in the equation is the sum of the contributions from three possible processes:

(i) extra-particle effects (C_m)

(ii) stagnant mobile phase effects (C_{sm})

(iii) conventional liquid chromatography stationary phase mass transfer effects involving the basic sorption process (C_s)

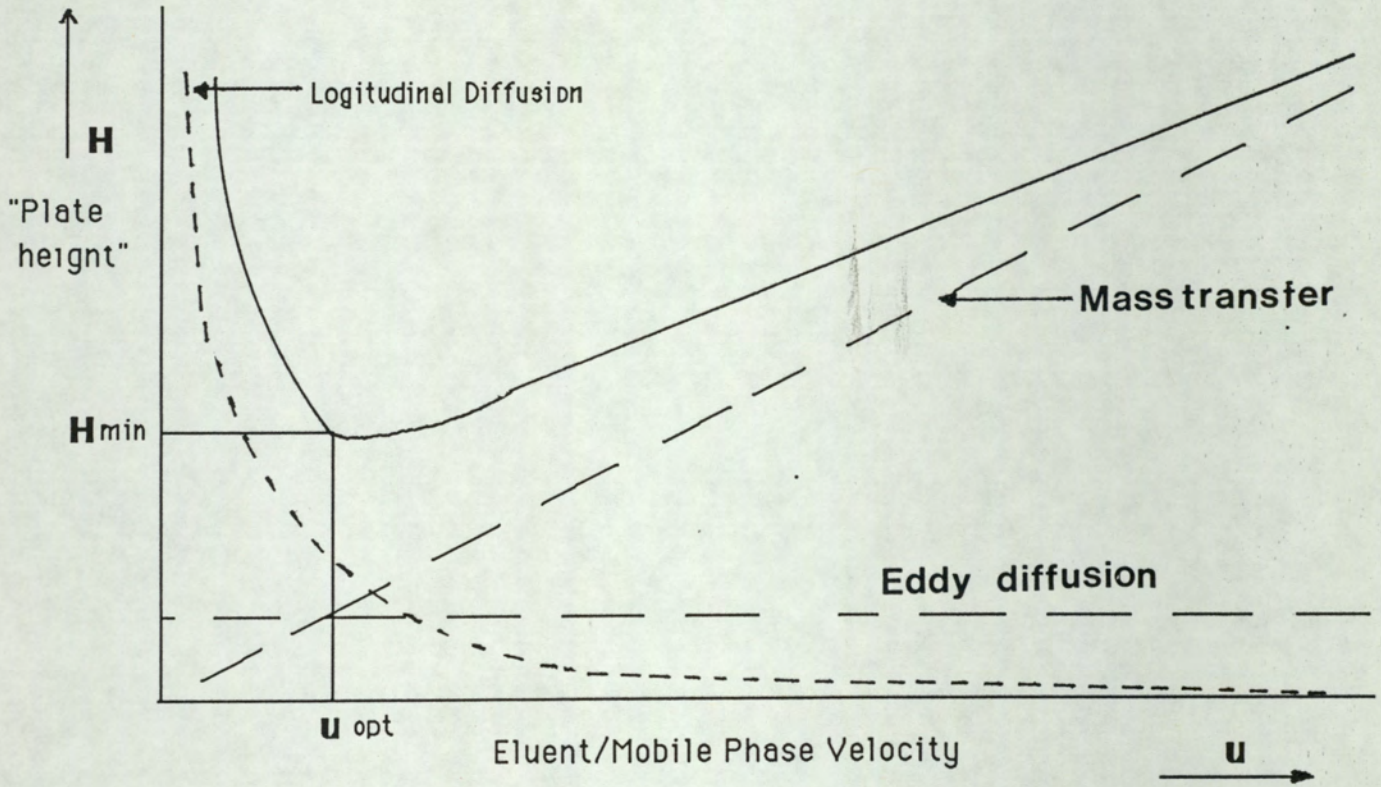

Figure 2.3 The Theoretical Van Deemter Graph

If the Van Deemter equation is expanded equation 2.18 is obtained

$$H = A + \frac{B}{u} + C_{mu} + C_{sm}u + C_s u \qquad \text{..... 2.18}$$

2.4.1.3 Random Walk Theory

Equation 2.18 shows a linear increase of plate height with increasing mobile phase velocity. In practice at high mobile phase velocities the plate height begins to level off. The random walk theory or coupling theory takes into account the eddy and lateral-diffusion terms ignored in classical plate height theory. This gives:

$$H = \frac{B}{u} + C_{sm}\,u + C_s\,u + \left(\frac{1}{A} + \frac{1}{C_m u}\right)^{-1} \qquad \text{..... 2.19}$$

Giddings (9) described a more detailed equation which includes a term for the extraparticle dispersion effect.

$$H = \frac{D_m}{u} + C_{sm}\frac{ud_p^2}{D_{sm}} + C_s\frac{ud_f^2}{D_s} + \left(\frac{1}{ad_p} + \frac{D_m}{c_m u d_p^2}\right)^{-1} \qquad \text{..... 2.20}$$

2.4.2 Resolution

The degree of separation between two solutes in chromatography is known as the resolution. The resolution, R_S of two adjacent bands X and Y is defined as the difference in retention time for X and Y divided by the average bandwidth, where retention time is defined as the time taken after injection for a solute peak maximum to exit the column.

$$R_S = \frac{t_y - t_x}{[1/2\ (tw_x + tw_x)]} \qquad \text{..... 2.21}$$

where

t_x = retention time of component x

t_y = retention time for component y

tw_x = bandwidth for component x = time taken for all of component x to exit the column

tw_y = bandwidth for component y

Resolution defines the separation; the greater the value of R_S the better the separation. Snyder and Kirkland (10) have also shown that Rs is a function

of a, the separation factor:

$$\alpha = \frac{k_y}{k_x} \qquad \text{..... 2.22}$$

where k_x and k_y are k' values for components x and y. R_S is also a function of N, the number of theoretical plates and of k', the average value of k_x and k_y, ie:

$$R_S = 1/4\,(\alpha - 1)\; N\left[\frac{k'}{(1 - k')}\right] \qquad \text{..... 2.23}$$

2.5 The Theory of Continuous Annular Chromatography

2.5.1 The Plate Model

Moskvin and his co-workers (11) were able to modify conventional plate theory by making the dimensional translation from time to angular position

$$\bar{\theta} = \omega t$$

$\bar{\theta}$ = angular displacement(degrees)

ω = rotational rate(degrees h^{-1})

t = time(h)

Assuming an infinitely small feed bandwidth, the following expressions were obtained:

$$\bar{\theta} = \frac{\omega L}{V} (1 + K_d \, q_1/q_2) \qquad \text{..... 2.25}$$

$$W_e = \bar{\theta} \sqrt{8/N} \qquad \text{..... 2.26}$$

where

$\bar{\theta}$ = position of the peak maximum(degrees)

L = bed length(m)

V = superficial eluent velocity(mh^{-1})

Kd=Distribution Ratio(l solution/l sorbent)

q_1/q_2 = ratio by volume of the stationary and mobile phases

W_e = solute bandwidth at a height of $1/\sqrt{e}$ (0.607) of maximum

Using these equations a reasonable agreement was obtained between theory and experimental results using elution of copper at various rotation rates. However, bandwidths achieved experimentally were always greater than the theory predicts.

Wankat (12) described a relationship between a conventional chromatographic column and a rotating annular chromatograph. He noted that conventional chromatography is an unsteady-state one-dimensional process which separates a feed mixture on a time basis, whereas in annular chromatography a two-dimensional steady-state process occurs, separating the feed mixture in a spatial direction.

If the radial gradients in velocity and concentration are ignored, the mass balance on a differential element in a conventional packed bed with constant eluent velocity gives rise to the following equation:

$$\frac{\partial C}{\partial t} + \left(\frac{1-\varepsilon}{\varepsilon}\right)\frac{\partial n}{\partial t} = D_z\frac{\partial^2 C}{\partial z^2} - \frac{V\partial C}{\varepsilon \partial z} \qquad \ldots\ldots 2.27$$

where

C = solute concentration in the liquid phase(mol/l of solution)

n = solute concentration in the solid phase(mol/l of sorbent)

$$\varepsilon = \text{void fraction} = \frac{\text{volume of voids}}{\text{empty column volume}}$$

t = time

D_z = dispersion coefficient in the z-direction

V = superficial velocity of eluent

Initial conditions are:

(1) for t = 0, all Z: C=n=0

boundary conditions are:

(2) for z = 0, $0 < t < t_f$: C = C feed

(3) in the limit C = 0 as Z ——> ∞

t_f = time of feed injection on to column

C_{feed} = feed conc

In a rotating annular chromatograph, ignoring radial gradients, the following expression can be derived from the steady state mass balance:

$$\frac{\omega \partial c}{\partial \theta} + \omega \left(\frac{1 - \varepsilon}{\varepsilon} \right) \frac{\partial n}{\partial \theta} - D_\theta \frac{\partial^2 C}{\partial \theta^2} = D_z \frac{\partial^2 C}{\partial_z{}^2} \qquad \text{..... 2.28}$$

where ω = rotational speed

D_θ = dispersion coefficient in q-direction

θ = angular co-ordinate.

The boundary conditions are:

(1) for $\theta = 0$, all Z: c=n=0

(2) for z=0, $0<\theta<\theta_f$ $C = C_{feed}$

(3) at $z = -\infty$, $0<\theta<360$ deg: C=0

Comparing equation 2.27 with 2.28 it can be seen that there is a term for term correspondance between the two if the axial dispersion term is considered negligible.

Working independently of Moskvin, Scott and his co-workers (13) were able to derive several key equations by adapting the plate theory. The following equation

$$\bar{\theta} = \frac{\omega L}{V} [\varepsilon + (1 - \varepsilon) K] \qquad \text{..... 2.29}$$

was obtained using equations 2.6 and 2.24 where

$$K = \text{distribution coefficient, } \frac{\text{moles dm}^{-3} \text{ in solid phase}}{\text{moles dm}^{-3} \text{ in liquid phase}}$$

A rearrangement of equation 2.29 gives a method of determining the distribution coefficient K, under varying conditions of eluent flowrate, rotations speeds etc:

$$K = \left[\frac{\theta V}{\omega L} - \varepsilon \right] / (1 - \varepsilon) \qquad \text{..... 2.30}$$

2.5.1.1 Exit Bandwidth

An expression for the exit bandwidth which incorporated the effect of the initial feed bandwidth, W_o, was derived:

$$W_e = \sqrt{W_o^2 + 8\theta^2/N} \qquad \text{..... 2.31}$$

2.5.1.2 Resolution in Annular Chromatography

The definition of resolution was altered to suit a rotating annular chromatograph as follows:

$$R_S = \frac{\bar{\theta}_y - \bar{\theta}_x}{1/2\,(W_x + W_y)} \qquad \text{..... 2.32}$$

W_x and W_y are exit bandwidths in degrees.

Figure 7.2 describes this. A resolution value of 1 indicates virtually no overlap between solute bands and no dead volume either.

2.5.1.3 Dilution Factors

As solutes travel through a chromatographic column dilution is equal to the ratio of the exit bandwidth to the initial feed bandwidth, ie:

$$D_f = \frac{W}{W_o} \qquad \text{..... 2.33}$$

2.5.1.4 Efficiency

The number of theoretical plates can be calculated from the equation:

$$N = \frac{16\,\bar{\theta}^2}{W^2 + W_o^2} \qquad \text{..... 2.34}$$

This is analogous to equation 2.10 and is simply a rearrangement of equation 2.30.

Initial Feed Bandwidth

Begovich (10) showed that a good estimate of the initial feed bandwidth could be made using the relationship:

$$W_o = 360\, Q_f/(Q_f + Q_E) \qquad \text{..... 2.35}$$

where Q_f = feed flowrate, cm^3h^{-1}

Q_E = eluent flowrate, cm^3h^{-1}

This equation does assume that the velocity of the feed and the eluent are perfectly matched and that the feed is uniformly distributed over the entire calculated bandwidth. The usefulness of this equation is therefore dependent on the position of the feed nozzle in the annulus.

CHAPTER THREE

CONTINUOUS CHROMATOGRAPHIC EQUIPMENT AND TECHNIQUES

3 Continuous Chromatographic Equipment

Scale-up of a chromatographic process can be achieved by two basic methods, these are:

(i) Direct scale-up of batch or co-current systems

(ii) Development of continuous systems

3.1 The Co-current Process

The use of batch columns for production scale processes has been carried out successfully in industry for many years. Columns of up to 12m in height and 3.5m in diameter have been used by the Finn Sugar Company for the extraction of sucrose from molasses (15). Column utilisation and therefore throughput is increased by introducing a "repeated injection" technique. Batch samples are injected at as frequent an interval as the total on-column band width of the preceeding sample permits without extensive overlap.

3.2 The Continuous System

The inherent advantages of the continuous mode of operation over batch operation have been well established. Consequently, since the introduction of continuous chromatography many mechanical devices have

been constructed whereby continuous operation is achieved. These fall into two categories:

(i) Counter-current flow processes

(ii) Cross-current flow processes

3.2.1 Counter-current Flow Processes

Many attempts have been made to increase throughput over more conventional co-current systems using counter-current flow processes.

In counter-current systems the stationary phase is moved in the opposing direction to that of the mobile phase by a variety of methods. These include:

(i) Moving bed systems

(ii) Moving column systems, and

(iii) Simulated moving bed systems

3.2.1.1 Moving Bed Systems

In moving bed systems the column packing moves in the opposite direction to the mobile phase. Components which are highly retained move with the packing. Components which are less strongly retained exit the column with the mobile phase (Figure 3.1). An example of this type of system is the Hypersorption process developed by the Universal Oil

Figure 3.1 Counter current flow chromatography

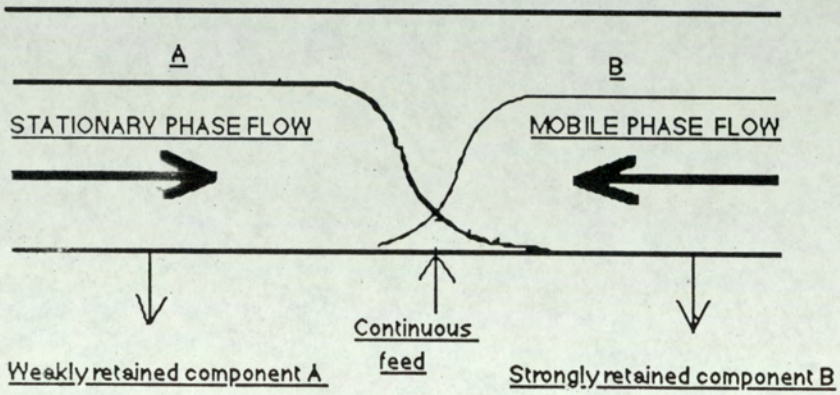

Products, California (16).

3.2.1.2 Moving Column Systems

This type of system (17,18,19) usually consists of a circular arrangement of parallel columns which are rotated past stationary ports which interconnect the columns.

3.2.1.1 Simulated Moving Bed Systems

In these systems a number of stationary interlinked columns are employed. Counter-current movement is achieved by sequentially moving the inlet and outlet ports in the direction of the mobile phase.

Barker and co-workers (20,21,22,23) have developed a system known as semi-continuous chromatographic refining. In this technique the counter-current movement was simulated by the simultaneous opening and closing of specially constructed valves connected to the inlets and outlets of each column.

A review article by Barker (4) gives full details of the above techniques.

3.2.2 Cross-Current Flow Processes

Cross-current flow processes involve the movement of the chromatographic bed laterally to the mobile phase. The chromatographic bed can be arranged as a circular array of parallel tubes, an annular disc (see figure 3.2) or as a single annular cylinder. Rotation of the annulus about its centre, as the mobile phase flows in the axial or radial direction results in each component describing a helical path from the point of entry to each individual component exit port. Martin (24) was the first to propose a scheme based on this principle in 1949. Martin suggested a device consisting of two cylinders, one placed inside the other, concentrically to form an annulus. The annulus is packed with chromatographic medium and is rotated slowly, usually at speeds of the order of one revolution per hour. A solution of the mixture to be separated is introduced at a fixed point above the packed annulus while eluent is introduced continuously above the whole surface of the bed. A chromatographic packing is selected such that each component in the feed mixture will have a different affinity for the packing. Each solute therefore travels at a different rate from the top of the annulus to the bottom. When this is combined with the rotation of the chromatograph it is clear that individual components in the feed will exit the chromatograph at different angles of displacement from the feed entry point. Products are then collected at fixed points beneath the annulus (see Figure 3.3). Each solute will display a stationary helical band which joins the feed entry point to the product exit point for that feed component. Dunnil and

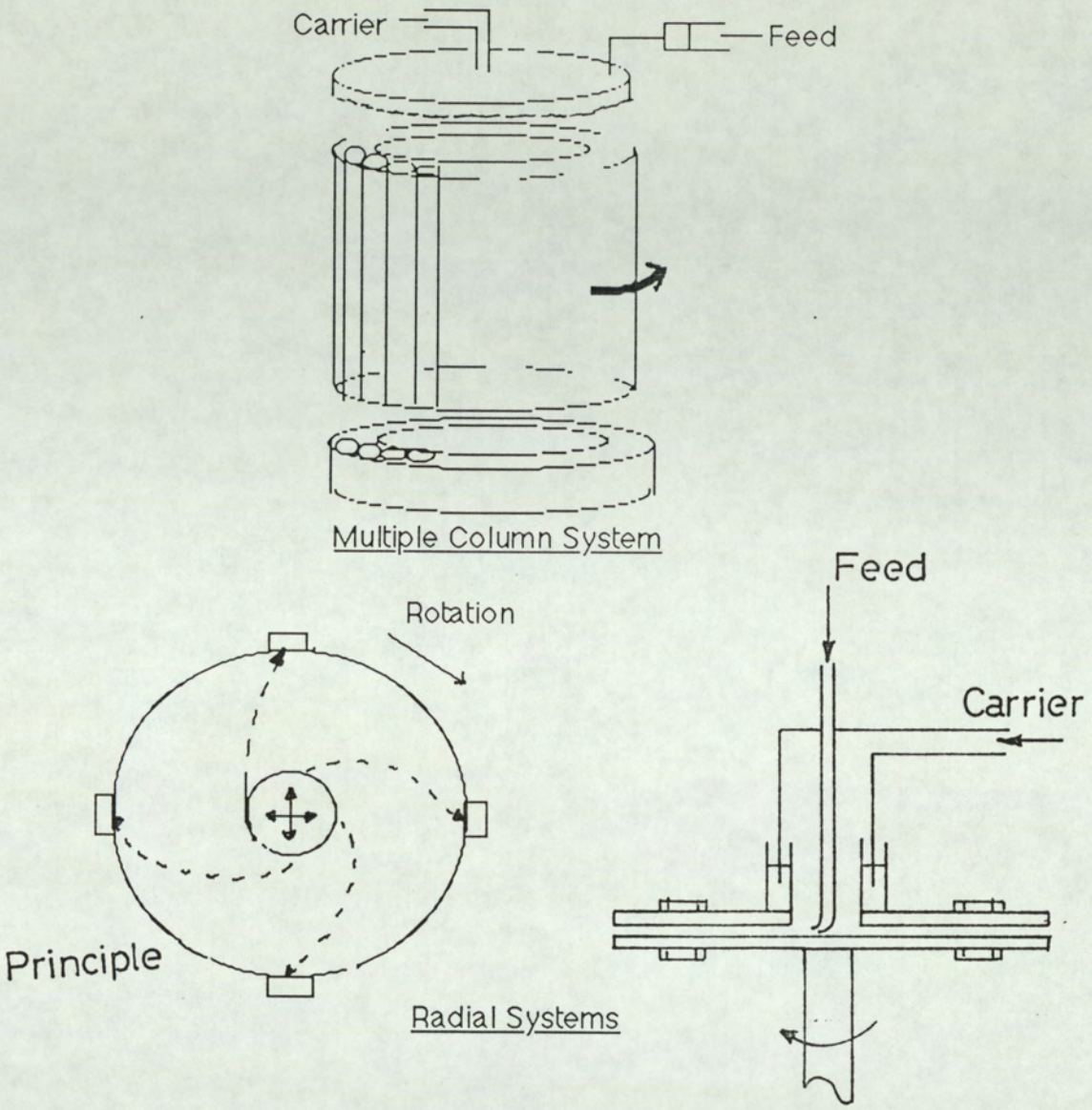

Figure 3.2 Cross-current Flow Systems

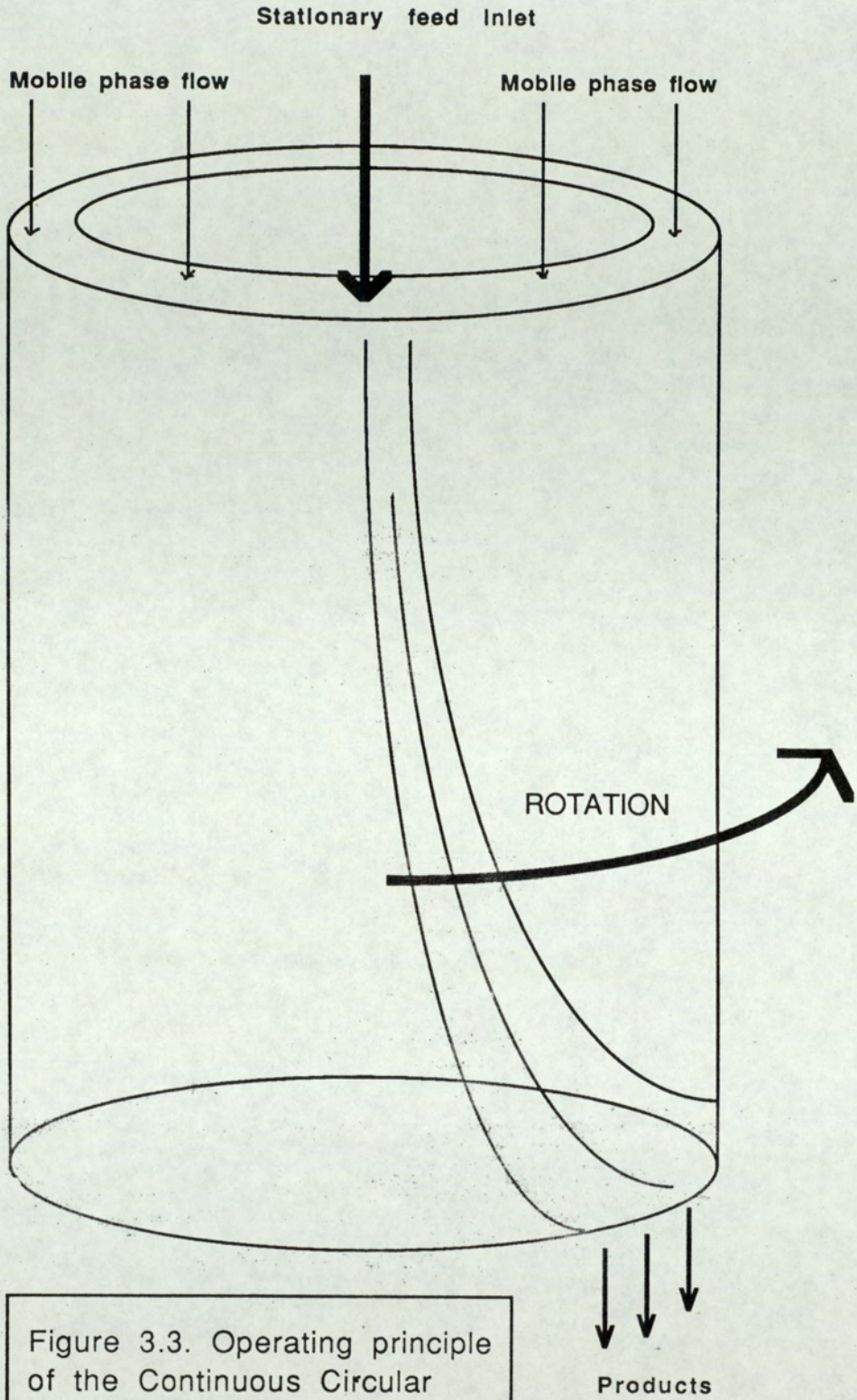

Figure 3.3. Operating principle of the Continuous Circular Chromatograph.

Lilley (25) showed that it is possible although more complicated to use a stationary annulus and moving feed and outlet points since the relative movement is the same. Dunnil and Lilley used their device to separate skimmed milk proteins and to purify cow heart myoglobin on Sephadex G75 using gel permeation chromatography.

Cho and co-workers (26) developed a continuous chromatographic reactor which consisted of a packed stationary annulus with a rotating feed port (see Figure 3.4). The equipment was used for the acid catalysed hydrolysis of aqueous methyl formate. Separation of the products namely formic acid and methanol supressed the reverse reaction causing conversions to be significantly greater than equilibrium conversions.

Byali and Ganitskii (27) in a 1969 patent described an apparatus based on a carousel of columns in which the feed position and fraction collectors were rotated. Wichterle and Coupek (28) in a 1974 patent described a similar system, however in this equipment multiport switching valves were use to simulate movement of the feed point and product collectors. This arrangement was found to be suitable for gel chromatography and was used for the preparative separation of alkylphenols.

Andrew (29) in 1979 devised a continuous apparatus using a stationary annulus and suggested a method of handling the problem of rotating feed and product collection points. This involved feeding the distributors from rotating funnels with overflows and collecting the products

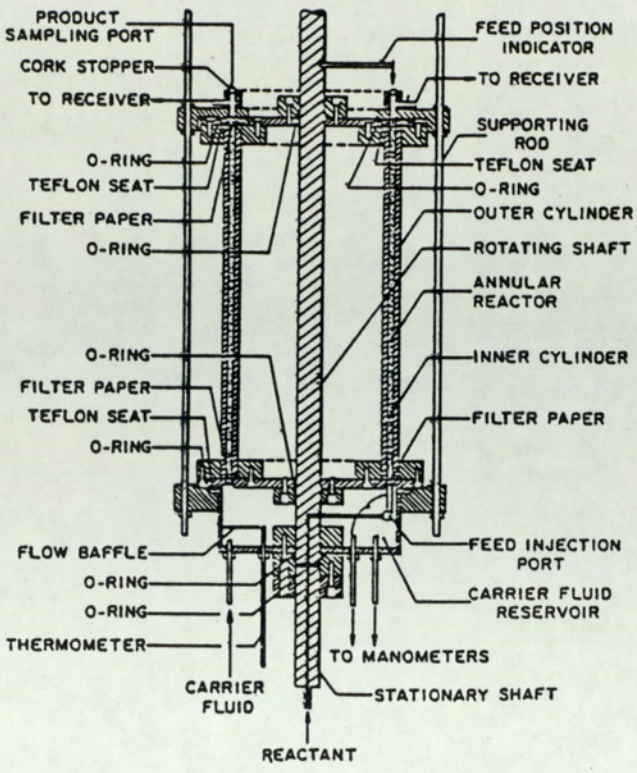

Figure 3.4 - Cho's Reactor Separator

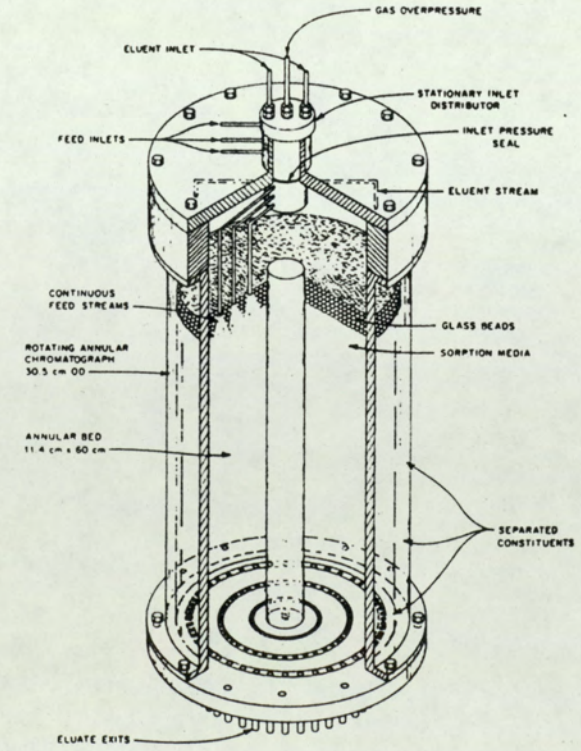

Figure 3.6 - Begovich high capacity annular chromatograph

into stationary funnels, thus avoiding the rotating valves used by Dunnil and Lilley.

The rotating annular chromatograph allows feed to be pumped in continuously and separated components withdrawn for any desired period of time. This makes the process a truly continuous one.

Laboratory equipment using cross-current flow rotating beds for liquid chromatography was first reported by Svensson and Brattsen (30) and by Grassman and Hanig (31). Svensson (32) used both packed annular beds and circular arrays of parallel columns. A continuous cross-flow gas chromatographic apparatus with 100 x 6mm diameter tubes, 1.2 metres long, arranged in a circle was constructed by Dinelli et al (33) (see Figure 3.2). This arrangement was used successfully to separate cyclohexane and benzene at experimental feed rates up to 200 cm^3h^{-1}. The carousel was rotated at speeds ranging from 1 to 50 revolutions per hour. Carrier gas was fed to all columns except the one which feed was being injected into. Another application for this equipment was the separation of n-heptane from toluene. They found that in this case a 99% product purity could be achieved at a feed rate of 500 $cm^3\ h^{-1}$ with a carrier gas flowrate of 1.05 lh^{-1}.

Polezzo and Taramasso (34) extended this work to determine the relationship between column length and maximum feed rate in the separation of two components. They proposed that the maximum possible feed rate increases very rapidly initially with increases in bed length, but

approaches a maximum as bed length is further increased.

In a later paper Taramasso (35) discussed optimum conditions for multicomponent preparative gas separations. The conditions included the use of columns between 1m and 3m in length and carrier gas and temperature selected to give short retention times. Several applications were discussed by Taramasso including the separation of cis- and trans-isomers of pentene, the separation of isoprene from methyl butenes, the separation of methallyl clhoride, isocrotyl chloride, t-butyl chloride and isobutylene, purification of terpene mixtures and the separation of mixtures of iso-pentene and n-pentene.

Continuous paper chromatography, using paper cylinders has been described by Solms (36) and others (37,38,39).

Patents on rotating bed cross-flow devices have been granted to Heaton (40), Moshier (41) and Hall (42) although no operating data on these devices is available.

Sussman (43-46) constructed a practical system called a continuous surface chromatograph. This system utilised two parallel annular discs. Separation occurs between a stationary phase coated onto surfaces between 50 μm and 150 μm apart. The primary application of this system was in the continuous monitoring and multi-component analysis of gases.

Fox et al (47-49) used a device which consisted of two acrylic cylinders clamped to a "plexiglas" baseplate. The outer cylinder was cut

from tubing of 30.5cm outside diameter and 29.2cm internal diameter. The inner cylinder had an external diameter of 27.3cm giving an annulus width of 0.95cm. Both cylinders were 30.5cm in length. 100 exit orifices were drilled on a circumference in the centre space around the annulus base. To support the packing media a ring of course grade filter paper was clamped between the bottom edges of the two cylinders and the baseplate, and compressed tightly to prevent leakage. The equipment was again used for the separation of myoglobin from heart extract using the Sephadex G75 gel at pH 8.1.

Tuthill (50,51) conceived a cross-flow chromatographic process in 1970 termed a "chromatographic slab", (Figure 3.5). This equipment was used to achieve a high degree of separation by the phased cycling of mobile phase flow and temperature within a packed bed.

Moskvin et al (52) were the first to report the use of gradient elution in a rotating annular chromatograph. Gradient elution involves alteration of the composition of the eluent or mobile phase at different angular regions of the annulus. A crude separation of calcium and strontium was achieved by making step changes in the concentration of their ammonium acetate eluent from 0.5M to 1.8M to 2.7M.

At the Oak Ridge National Laboratory in the United States (53,54,55) work has been carried out for several years on continuous annular chromatography.

Multicomponent separations of copper, nickel and cobalt from an

Figure 3.5

Chromatographic Slab

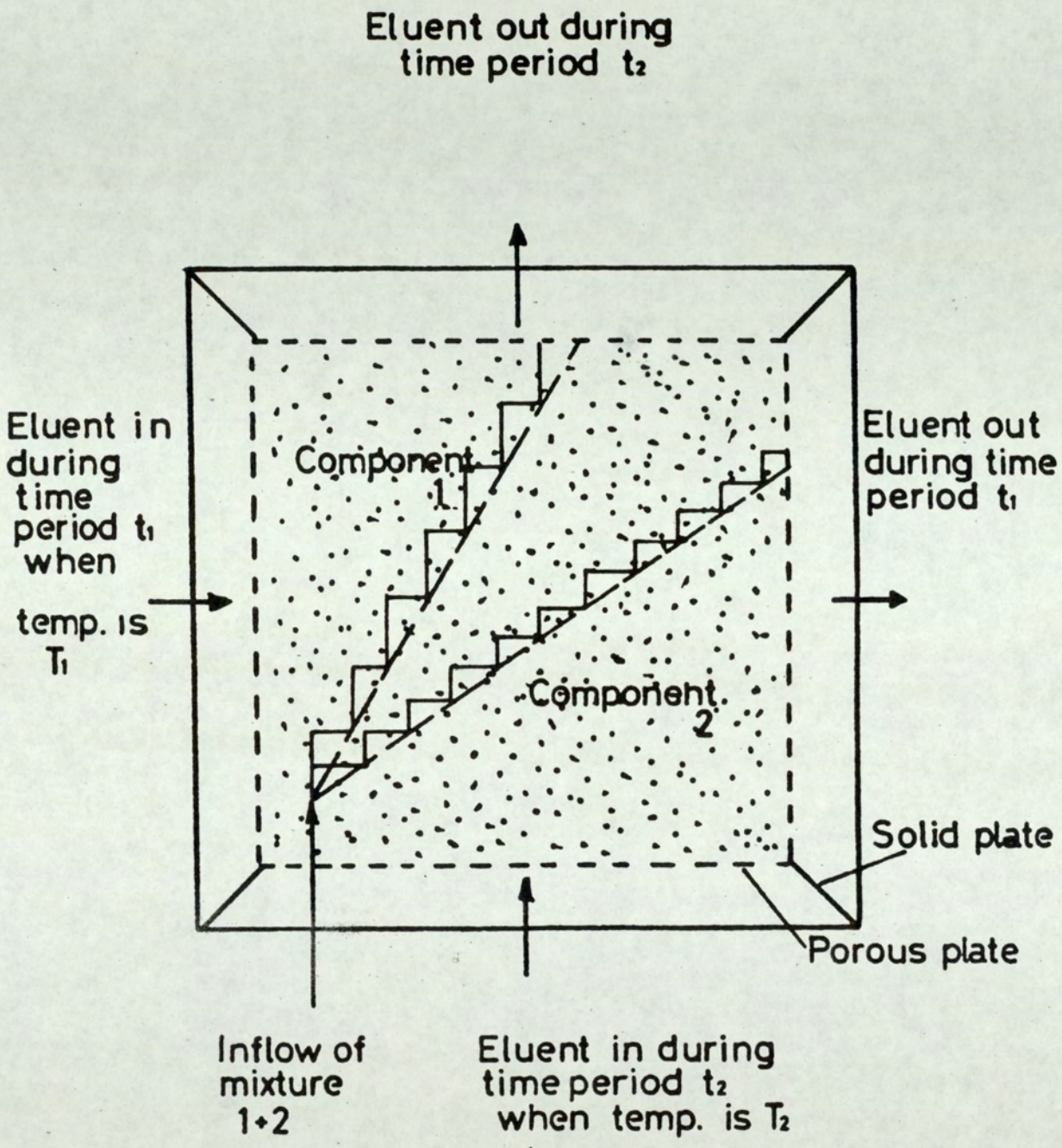

ammoniacal leach liquor were used to evaluate the capabilities of a variety of chromatographs. The experimental units ranged in diameter from 89 to 445mm and in annulus width from 6 to 114mm. A study was carried out of the effects of feed rate, feed concentration, rotation rate, eluent velocity and column size. An abundance of experimental data was used to assess the validity of three theoretical models. The equipment used was operated in the gradient elution mode during the separation. Use of different solvents at different regions of the annulus allows the separation of solutes with similar distribution coefficients in one solvent but in other solvents the distribution coefficients change giving much greater scope for separation of multicomponent mixtures. An annulus of 111mm diameter and width 35mm was constructed. A 60-90 mesh cation exchange resin was used as packing to a depth of 55cm and rotated at speeds up to 785deg/h. In this system a rotating sorbent bed was used in conjunction with stationary top and bottom plates. Different eluents could be fed in at different sections of the annulus. Step changes were made in the concentration of the ammonium acetate eluent. Pressures of up to 1135 kPa (150 psig) have been used in order to increase throughput.

A high capacity chromatograph was developed by Begovich et al (56). This unit had an annulus width of 114mm. This allowed 96% of the available surface area within the outer cylinder to be used. Three feed nozzles positioned on radii of 44, 83 and 121mm were employed to evenly distribute feed solution across the annulus. To ensure even draining, the

bottom plate of the annulus contained three rows of exit holes positioned to coincide with the feed nozzles. These holes were of diameter 5.2mm (outer row), 4.3mm (middle row) and 3.2mm (inner row).Figure 3.5 shows this.

CHAPTER FOUR

EQUIPMENT DESIGN AND EXPERIMENTAL PROCEDURE

4.1 Introduction to Equipment Design

The equipment which has been constructed was based on the design of Scott et al (52) but adapted for use with carbohydrates. It was decided to construct the annulus of the first equipment using a high quality glass outer shell to enable observation of the chromatographic packing to be made. Problems arising from air pockets and fissures within the resin, disturbance of the glass bead layer by sudden changes in pressure, the need to check that the feed solutions were entering the chromatograph correctly and the growth of micro-organisms have subsequently shown this to be a very worthwhile decision.

The use of a glass outer shell created several problems however. The first problem was in finding glass pipes made to a sufficiently high tolerance on the internal diameter. A glass pipe supplied by Schott Process Plant Ltd, Stafford was chosen since the internal diameter was accurate to ±4.0mm which was better than any other manufacturer could match. The longest pipe available in the diameter required was selected, this was 1500mm in length. Another big problem with the use of glass is its inability to withstand high pressures. The glass pipe chosen had a wall thickness of 8.0mm ± 1.5mm and was rated to a safe maximum working pressure of 101 kNm^{-2}. Therefore liquid flowrates and hence throughputs were restricted

by the comparatively low pressure limit. It was considered however that the visual benefits of using glass outweighed the limitations to its use.

4.2 Equipment

4.2.1 The Annulus

The CCC or Continuous Circular Chromatograph was constructed from an outer borosilicate glass column 297mm internal diameter and 1.5m in length (Figure 4.1A, Plate 1). This enclosed a type 304L stainless steel pipe (RGB Stainless Ltd, Smethwick) of outside diameter 273mm (Figure 4.1B) and 1.40m in length to form an annulus. Two 25mm thickness, type 316L stainless steel flanges (Figure 4.1C,D) were used to support the pipes at the top and the bottom. The inner stainless steel pipe (B) was blanked off at its upper surface by a flat stainless steel flange (E). The inner pipe was 1.40m in length and so provided a headspace of 10cm at the top of the chromatograph. The headspace gave sufficient height to include a liquid level controller and allowed a substantial volume of space above the packing to minimise fluctuations in pressure from the liquid being pumped in. These components (A,B,C,D,E) formed the rotating annulus.

When the various parts of the apparatus were under construction a stainless steel outer shell having a greater diameter than the glass column was also constructed as a direct replacement for later studies. The purpose of the stainless steel pipe was to increase the annulus area and hence enable increase of volumetric throughput to be obtained. The stainless

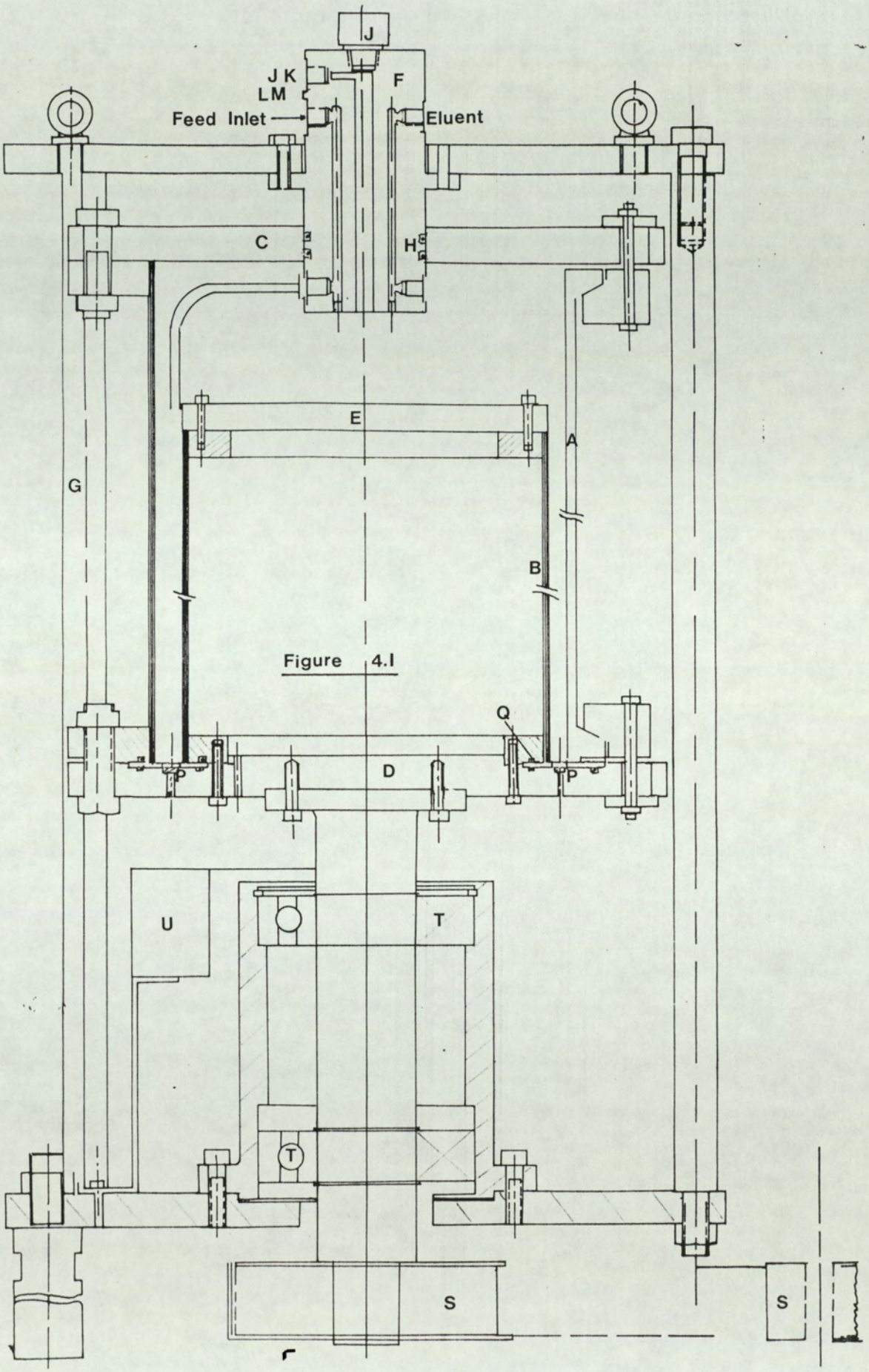

Figure 4.1

KEY

A -Glass outer column

B -Inner stainless steel column

C -Upper stainless steel flange

D -Lower stainless steel plate

E -Stainless steel blanking flange

F -Inlet distributor

G -The outer framework

H -O-Rrings

I -Liquid level controller

J -Pressure relief valve

K -Overflow pipe

L -Pressure guage

M -Safety solenoid valve

N -Manual pressure release valve

O -Safety relief valve

P -porous polyethylene discs

Q -Stainless steel ring for securing discs

R -Motor

S -Drive pulleys and belt

T -Ball bearings

U -Polypropylene product collector

V -Eluent storage tank

PLATE 1

THE CONTINOUS CIRCULAR CHROMATOGRAPH

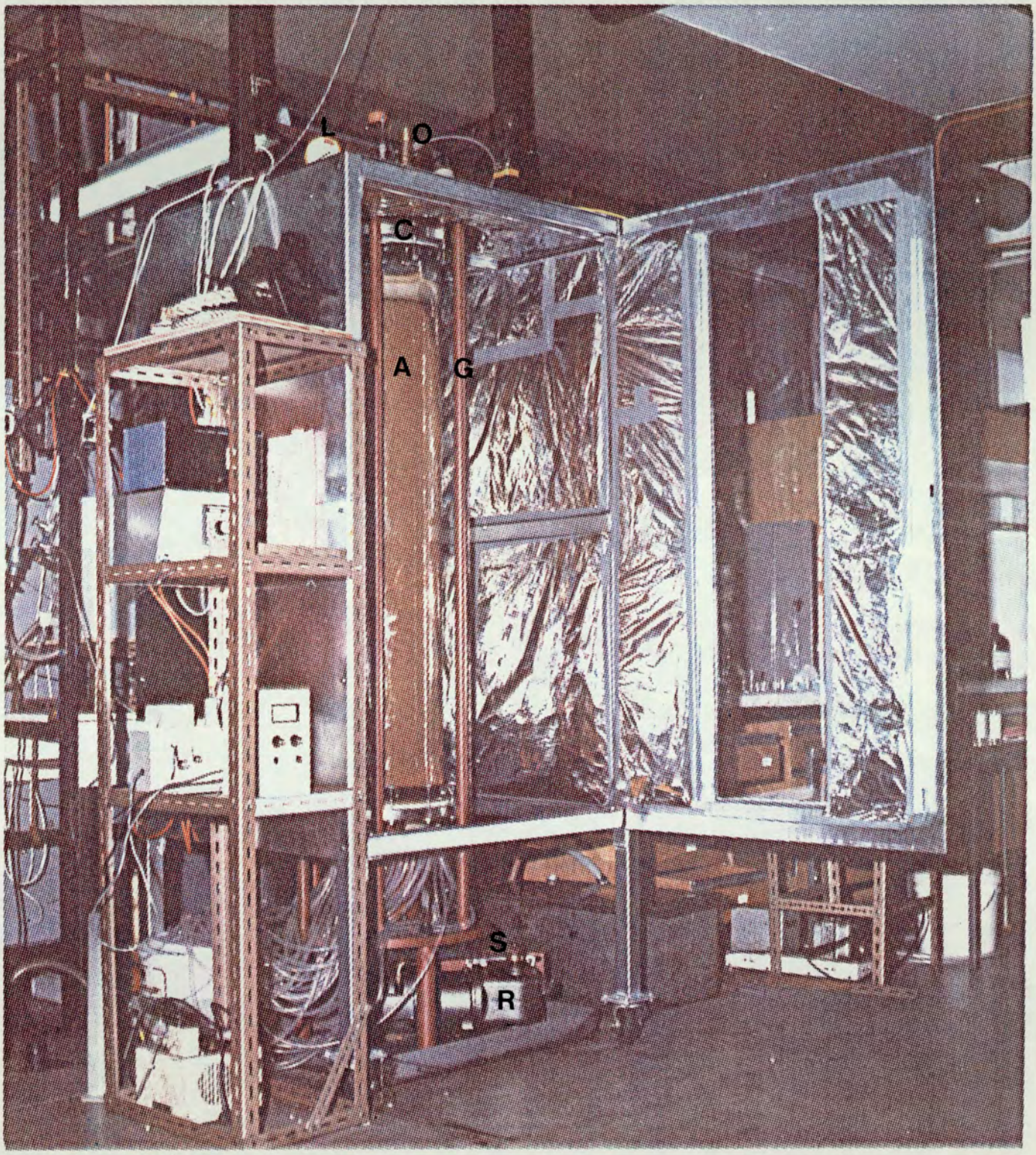

Table 4.1 - Dimensions of CCC and SCCR Equipment

CCC

Internal diameter of glass outer shell	297mm
External diameter of inner stainless shell	273mm
Annulus width	12mm
Annulus length	1.40m
Height of chromatographic packing	1.35m
Volume occupied by packing	14.5 l
Cross-sectional area of bed	107 cm^2
Equivalent diameter of annulus	11.7cm
Internal diameter of stainless steel outer shell	315cm
Annulus width using stainless steel outer shell	21mm
Annulus length using stainless steel outer shell	1.35m
Volume of annulus available for packing	26.2 l
Cross-sectional area with stainless steel outer shell	194cm^2
Equivalent diameter of annulus	15.7cm

SCCR 7

Number of columns	12
Diameter of column	5.08cm
Cross-sectional area of a column	20.3cm^2
Column length	0.70m
Total column length	8.40m
Total column volume	17.0 l

Number of columns	10
Diameter of a column	10.16cm
Cross-sectional area of a column	81.1cm^2
Column length	0.66m
Total column length	6.6m
Total column volume	53.52 l

4.2.2 The Distributor

The upper stainless steel flange (C) had a centrally placed circular hole (9cm diameter) in which the stainless steel inlet distributor (Figure 4.1F, Plate 2) was fitted. The distributor was held stationary by the outer framework which enclosed the apparatus (G). Two nitrile 'O' rings (H) were fitted into the groves around the distributor. These formed a gas-tight seal as well as the bearing on which the upper flange turned.

The distributor allowed the influx of deionised water as eluent, feed solution and compressed air via various ports drilled through it. The inlet distributor also housed the probes for an electronic liquid level control device (I), a pressure relief valve (J), an overflow pipe (K), a pressure gauge (L), a safety solenoid valve, (M) and a manual valve for releasing the pressure built up in the apparatus during a run (N). The column is also fitted with a safety relief valve (O) set at 95 kNm^{-2} to protect the glass column.

PLATE 2

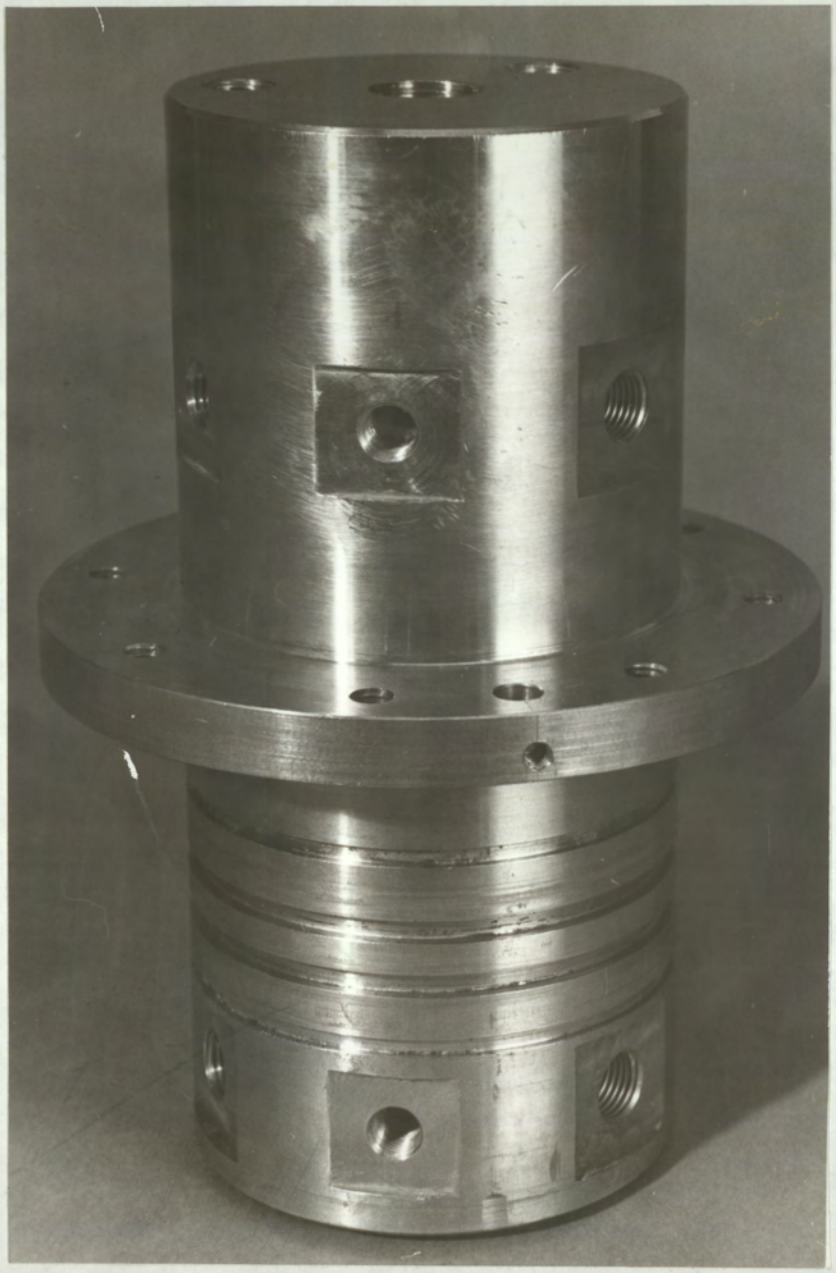

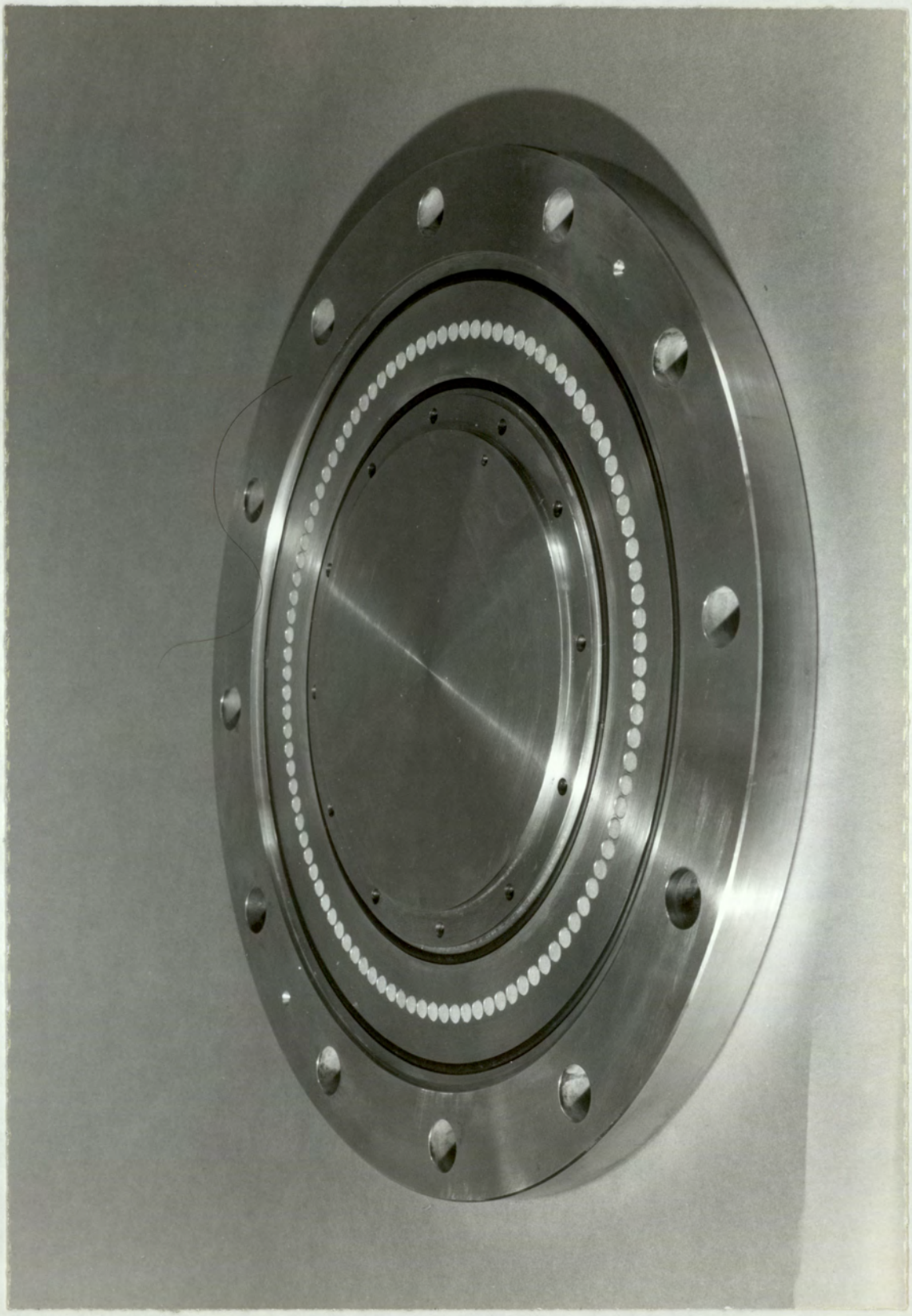

pulleys different speed ranges could easily be achieved. The chromatograph rotated about two 150mm diameter ball bearings (T) situated underneath the chromatograph.

4.2.5 Product Collection

Collection of product fractions from the CCC was achieved using a stationary polypropylene annulus (U). This was attached to the tie-bars on the supporting structure of the apparatus by three moveable clamps. The clamps allowed the stationary product collector to move up or down in order that access could be gained to the underside of the chromatograph. Fifty countersunk 10mm diameter holes were drilled into the collector each having a length of PVC tubing attached underneath to allow separation of the product fractions. The PVC tubing passed to a large perspex tank containing 50 x 150cm^3 Sterilin sample bottles (Plate 4) (Appleton Woods, Selly Oak).

4.2.6 Temperature Control

The equipment was surrounded by an air bath (1.66 x 1.02 x 0.92m) (Plate 1) which was designed to operate at temperatures of up to 70°C. The temperature was controlled accurately by means of a DU82A temperature controller (Diamond H Controls Ltd, Norwich). Two 1kW heating elements (Elton Ltd, London) and a fan (Woods of Colchester, Essex) were used to distribute the heat evenly. The oven also provided

Plate 4

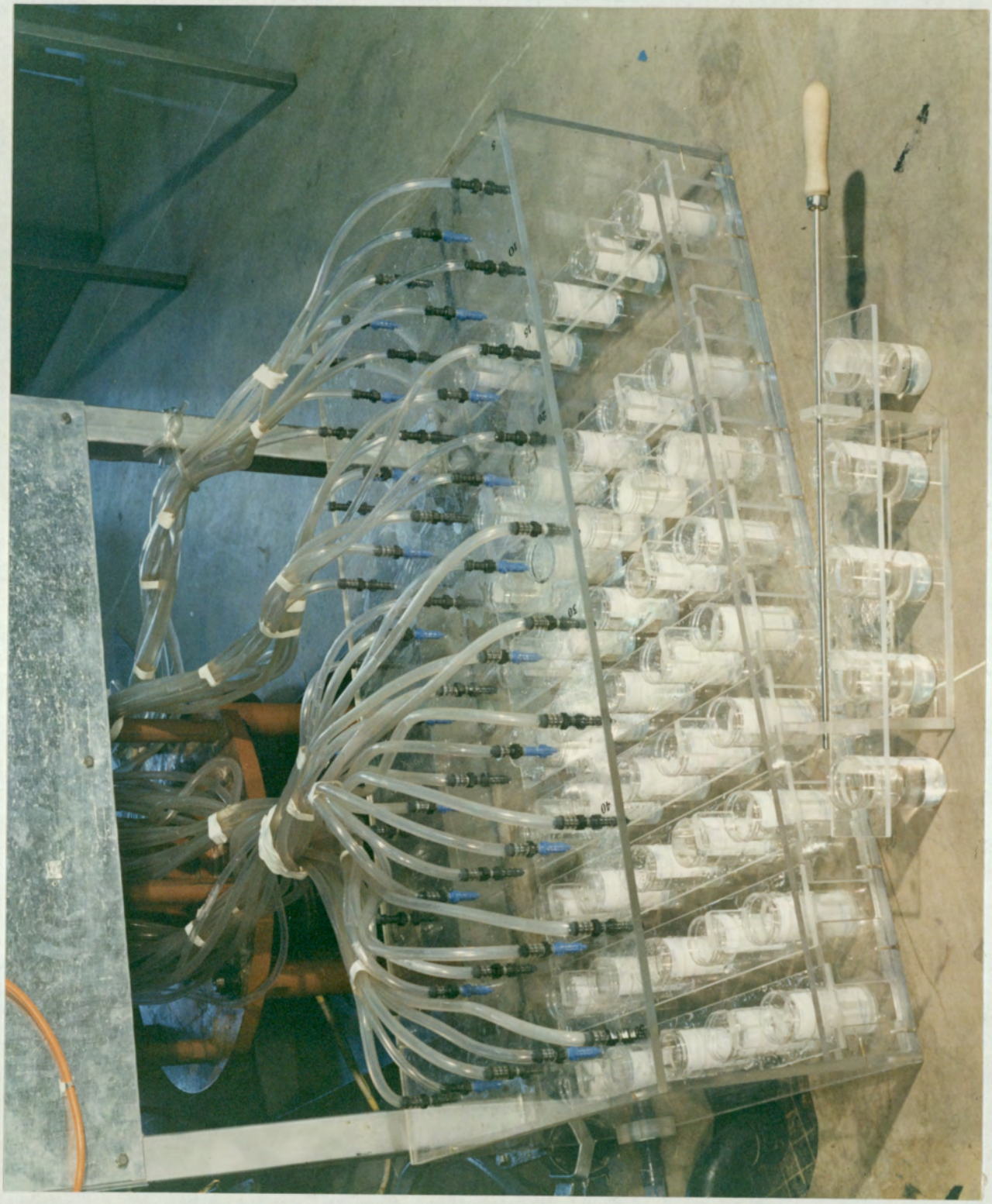

useful protection should the glass column shatter. A perspex screen mounted in the door allowed observation of the annulus during a run. A Baird and Tatlock thermal cut-out was used as a safety measure in the event of the temperature controller malfunctioning. The temperature of the feed and eluent was also controlled.

Deionised water was used as eluent and could be transferred to the stainless steel eluent storage tank (V) either directly from the deioniser (The Elga Group, Bucks) or through an immersion heating vessel. Since the heating vessel was situated several metres from the CCC apparatus a Techne TE-7 heater/stirrer (Techne, (Cambridge) Ltd) was used to maintain the correct temperature of water entering the chromatograph.

Feed solutions were maintained at a constant temperature in a water bath.

4.2.7 Liquid Level Control

Ion-exchange resins have to be kept moist to prevent damage occurring to the particles. It is also important to prevent air entering the bed as this causes channelling in the packing.

It was found to be extremely difficult to prevent water draining from the annulus through one hundred individual outlets. Experimenting with small bungs was found to be very time consuming and not very effective; half circular plates with rubber gaskets and clamps also were tried without success. Eventually it was decided to simply let the water drain out and

control the liquid level above the packing. An electrical level controller with three probes was used. One probe was simply a common earth at the lowest level possible and the other two for high and low level. When the water level had dropped below the low level probe the eluent pump was activated. The pump was switched off again once the water level had reached the upper level probe. An improvement on this was made when a back-up system using two further probes was used. One probe was again used at a permanently low level the other was set to approximately 1cm below the original low level probe. If the level controller or the eluent pump failed a solenoid valve opened and deionised water from the storage tanks passed into the upper part of the chromatograph until the water level had reached the emergency probe. At this point the solenoid valve closed again preventing any further water passing into the chromatograph.

4.3 Experimental Procedure

An experimental run was carried out as follows:

1 The molasses to be used was analysed by HPLC in order to prepare a feed having exactly 30g sucrose per $100cm^3$ solution.

2 The stainless steel baseplate underneath the annulus which contained the exit holes was cleaned using ethanol and dried using tissues. This was necessary to prevent movement of liquids across the underside of the baseplate to other collection points.

3 The vent valve on the top of the stationary distributor was closed to allow pressure to build up inside the apparatus.

4 The motor drive to the column was started and the speed controller set at the speed required. A check on the rotational speed was made using calibrated graph paper around the perimeter of the baseplate of the annulus and a pointer attached to one of the stationary tie bars. A mark was made on the graph paper adjacent to the pointer, with the motor turning. After an accurately timed interval of about one hour another mark was made on the graph paper to determine the exact angle turned through in that space of time.

5 The eluent pump was then set to approximately the correct stroke required. The eluent inlet pipe was then removed from the inlet distributor and the pump switched on. A measuring cylinder was used to check the volume delivered in a given time and the pump was adjusted accordingly.

6 When the pump had been accurately set, the inlet pipe was reconnected to the distributor, and the pump was started. The pump was started by disconnecting one of the terminals from the probes of the level controller.

7 Time had to be allowed for the internal pressure to reach a maximum. This was necessary before an accurate determination of the feed flowrate could be made.

8 A digital "Pelton wheel" type flowmeter was used during a run. The flowmeter was used in series with the outlet pipe from the eluent tank to the eluent pump. After calibration of the flowmeter to the initial eluent flow, frequent checks were made to ensure no deviation occurred in the flowrate.

9 To enable accurate determinations of feed flowrate to be made the pressure generated by the eluent pump had to have reached its maximum. This was necessary to gain accurate feed flowrates since it was found that although a high pressure metering pump was used to pump the feed, slight reductions in flowrate occurred when the back pressure was increased.

A burette ($50cm^3$) was used in conjunction with a three way valve. The three-way valve allowed liquid entering the pump to pass from the burrette instead of the feed container. The time for the liquid level to drop from $50cm^3$ to $0cm^3$ was measured and the pump adjusted until the correct flowrate was achieved.

10 The three-way valve was switched back to the feed container and the run allowed to commence.

11 The apparatus was rotated by at least two revolutions to ensure all components in the feed mixture had been eluted. A minimum amount of time was also required for the apparatus to reach equilibrium, this was dependent on the eluent flowrate used and the feed mixture in question. As an example when using glucose and fructose mixtures at $12lh^{-1}$ at least one hour after the first

revolution had to be allowed to ensure complete elution of the fructose at all parts of the annulus.

12 When it was certain that equilibrium had been obtained product samples could be taken.

Sample bottles ($150cm^3$) were arranged in the perspex tank mentioned previously. To save time with analysis not all the sample points were used since it was found that only very small differences in product concentration occurred between adjacent sample bottles. However if a detailed study of one small region was required then a greater number of samples could be obtained in that region. Sample bottles were removed from the perspex tank when full.

13 Carbohydrate solutions can act as a very good substrate for micro-organisms and therefore product samples, unless being immediately analysed, were transferred to the freezer. Once equilibrium had been obtained tracking of the products using on-line monitoring could be carried out. This proved to be a good method of ensuring that equilibrium had been achieved and of showing where the key products appeared. It was also a useful qualitative guide to the resolution between the ionic content peak

and the refractive substrate peak when using beet molasses as a feed.

A small diameter pipe of the correct outside diameter was inserted into one of the exit holes beneath the chromatograph. This was connected to a peristaltic pump which was set up to deliver exactly 1/100th of the total eluent flowrate (100 exit holes) to a Refractive Index detector or a conductivity meter which was connected to a chart recorder.

The small diameter pipe rotated with the annulus. A plot of concentration versus angular displacement from the fixed feed point was produced as the pipe moved across the solute bands.

Care had to be taken to ensure that the tube leaving the chromatograph did not tangle itself as the apparatus revolved.

14 After an experimental run had been completed, the feed pump was switched off. The feed container was rinsed with hot water and then refilled with a 0.02g cm^{-3} solution of sodium azide. This was pumped through the feed inlet pipe until it had been well flushed out. Cleanliness was of great importance since bacteria and fungi flourish in the dilute sugar solutions remaining in the

tubing. Sodium azide was used as a sterilizing agent.

15 The eluent pump was left running until all the feed solution was removed from the packing. Sodium azide solution (0.02g cm^{-3}) was prepared in the eluent storage tank and left to pump through the chromatograph for several hours.

16 The motor and feed pump were switched off and the liquid level controller was reconnected. The vent valve was opened to release any remaining pressure within the chromatograph. For safety it is important that when the chromatograph was pressurized the door to the air bath was firmly closed.

The pressure relief valve was tested from time to time to ensure correct operation.

NB: Since sodium azide is very poisonous great care was exercised with its use.

CHAPTER FIVE

ANALYSIS

5.1 Introduction

This chapter describes the analytical equipment which has been used in this project.

Analyses were carried out quantitatively on individual product samples and qualitatively using on-line measurements during experimental runs.

5.2 Sample Collection

There are one hundred exit holes drilled into the stainless steel baseplate which supports the annulus. Product samples passed through these into a static product collector. The latter consisted of a solid polypropylene block in which there were fifty funnel shaped holes, positioned directly below the exit holes in the baseplate. Product fractions flowed through fifty lengths of PVC tubing into individual sample containers housed in a perspex tank (1m x 0.5m x 0.4m), see plate 4.

One hundred outlets were considered necessary to give even flow out of the annulus with little side to side mixing however taking only fifty product samples was found not to compromise the accuracy of the results obtained as the differences in concentration from one outlet to the next were found to be negligible.

5.3 HPLC System - description

High performance liquid chromatography has been used successfully as a method of determining the carbohydrate content of the product samples obtained.

Analytical columns from three manufacturers have been tested with varying degrees of success. These columns were all packed with particles (5-10μm) of calcium charged ion-exchange resin. The columns tested were each 30cm in length. All were operated at a temperature of 85°C using deionised water as eluent at a flowrate of $0.5cm^3\ min^{-1}$.

Initially the equipment used consisted of an MPL series II eluent pump operated at $0.5cm^3\ min^{-1}$ (MPL Ltd, Feltham, Middlesex); a SUGAR PAK I analytical column (Waters Associates, Millipore UK Ltd, Harrow, Middlesex) maintained at 85°C using a glass water jacket and a C400 water heater/circulator (TECHNE, Cambridge). A Waters type R401 differential refractometer (Millipore UK Ltd) was used to detect product peaks, in conjunction with a type 3390A Integrator (Hewlett Packard Ltd, Altringham, Cheshire).

The analytical work carried out on this equipment involved the determination of glucose and fructose. It was discovered, however that with one sugar present in high concentration and the other present in low concentration the results obtained could be a little ambiguous, ie. the equipment occasionally failed to resolve the two peaks. This lack of resolution of the two peaks was believed to be due to a combination of the

pulsations produced by a single-headed reciprocating pump and poor column performance.

This equipment was replaced by a Bio-Rad HPLC system consisting of a Bio-Rad HPLC 1330 pump (Bio-Rad UK Ltd, Watford); a dual piston pump with very accurate control over flowrates under large differences in pressure and which operates without pulsations in pressure; a Bio-Rad Amnex HPX-78C analytical column (30 x 0.65cm); a Bio-Rad 1750 refractive index detector; a Spectra-Physics SP4720 Integrator (St Albans, Herts); and a Talbot ASI-3 Autosampler (Talbot UK, Alderley Edge, Cheshire).

The problems of poor resolution using the early system were eliminated using the Bio-Rad system. The installation of Alltech 700 CH analytical columns (Alltech UK Ltd, Carnforth, Lancashire) improved resolutions even more, however one of the Alltech columns tested was found to invert any sucrose in the samples to glucose and fructose. It was therefore decided to revert to Bio-Rad columns which gave good performance without inversion problems.

5.3.1 Experimental Procedure

A $2cm^3$ sample for analysis in a syringe was filtered using a 0.45µm Gelman filter (Brackmills, Northampton) and introduced into a 20µl injection loop contained in the sample injection valve.

Deionised water containing 0.2g l^{-1} calcium nitrate solution was heated to 80°C. This removed most of the dissolved gas and prevented the solution degassing in other parts of the equipment. This solution was stored in a round flask (1l) and used as eluent. Eluent was passed through a sintered stainless steel filter and a debubbler (Anachem, Luton, Bedfordshire) into the eluent delivery pump (see Figure 5.1). Samples were injected and the integrator was activated simultaneously. Results were interpreted as areas under plotted peaks obtained on the integrator and compared to areas for standard solutions to obtain exact sugar concentrations. Graphs could then be plotted to show individual sugar concentrations at different angles from the feed entry points.

5.4 In-line Monitoring

The separation performance of the CCC could be obtained qualitatively using beet molasses as a feedstock by connecting a refractive index detector (Jobling Laboratories) and an Alpha 800 conductivity meter (Aqua Scientific Ltd) to one of the outlets in the baseplate of the annulus via a length of small diameter tubing (Figure 5.2). As the chromatograph rotates, the tubing also rotates passing across the "stationary" solute bands generating a chromatogram on a chart recorder. The flowrate through the RI detector and conductivity meter was controlled by a peristaltic pump. The flowrate is set by using special tubing of various diameters. To get an accurate representation of the conductance band and the refractive

Figure 5.1 The Analytical HPLC System.

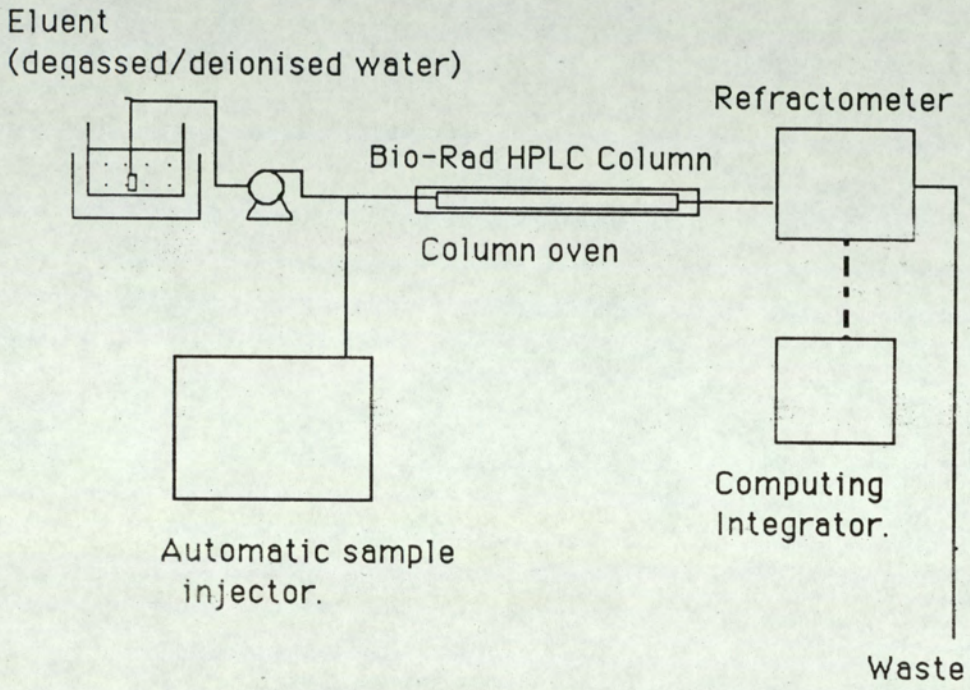

Figure 5.2 In-line Monitoring.

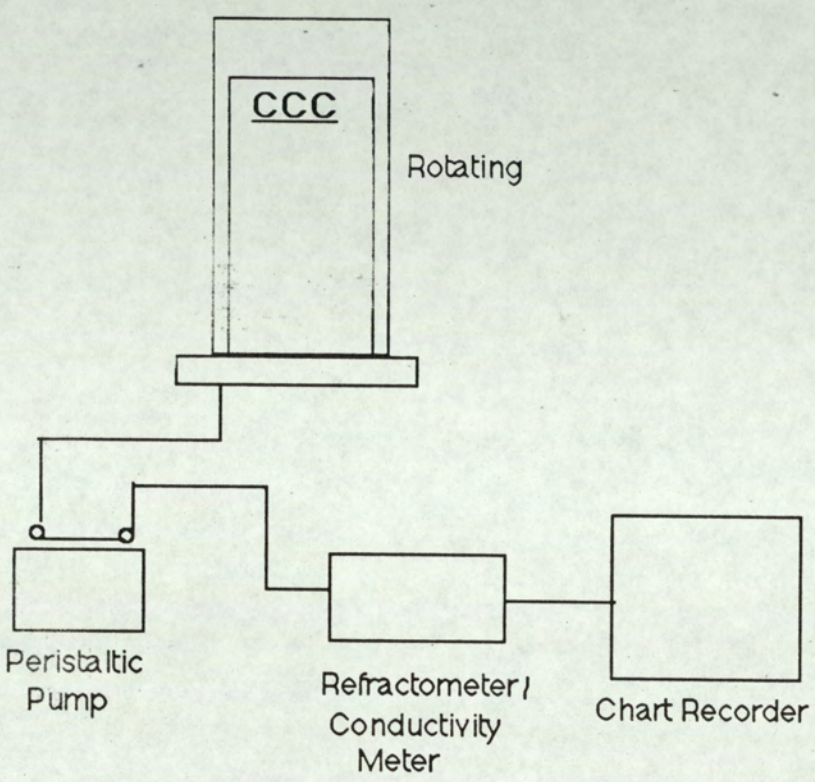

substance band it was necessary to use a flowrate exactly equal to the normal liqud flow through each exit hole to prevent the bands appearing artificially small or large. The conductivity meter detects the ionic fraction in the molasses. The refractive index detector measures the relative quantity of refractive dry substance. Since a good separation of sucrose from the mineral ions is essential to this separation this technique acts as a useful check on resolution when using different operating parameters.

5.5 Analysis of Beet Molasses

Beet molasses is a complex mixture of organic and inorganic components. Sucrose is present in by far the greatest proportion at approximately 63% of the dry matter. Table 5.1 gives an indication of the relative quantities of each of the main types of compounds found in molasses (57). Obviously quantities of each component will vary depending upon plant variety, maturity, climate and soil conditions.

To analyse each sample produced on the CCC apparatus for each component would be extremely time consuming and difficult. It was therefore decided to limit analysis to a combination of refractive dry substance measurement, conductivity measurements and HPLC analysis for sucrose and with the help of British Sugar Research Laboratories to have one set of samples analysed in detail. The British Sugar analysis also included colour absorbance measurements using a UV visible spectrophotometer set at 420nm in a 1cm cell, having been filtered through

Table 5.1 - Composition of Beet Molasses

Sucrose		63%	
Reducing sugars		0.3-1.5%	
Raffinose		0.7-2.6%	
Organic non-sugars	nitrogen compounds	betaine 5%	
		glutamic acid 3%	
		others	
	non-nitrogen compounds	organic acids	14%
		hemicelluloses	
Sulphated ash	Potassium K^+	6%	14%
	Sodium Na^+	0.4%	
	Calcium Ca^{2+}	0.4%	
	Chlorine Cl	1.2%	
	Phosphorus	0.5%	
	Others	5.5%	

a 0.45μm membrane and adjusted to pH 7. Potassium and sodium ions were analysed for by flame photometry. Calcium ions were detected by atomic absorption spectrometry. Anions present were detected using a Dionex ion chromatograph. Figure 5.3 shows the detailed analysis of a run carried out using enzyme inveted molasses.; feed flowrate $120cm^3h^{-1}$, eluent flowrate 12 lh^{-1} and rotational speed of 144 deg^{-1} using a feed solution with 30g sugar per $100cm^3$ of solution.

5.5 HPLC Analysis of Molasses

HPLC analysis of beet molasses was carried out on the Bio-Rad HPLC system at 85°C using the Aminex HPX 87C carbohydrate analytical column. No pretreatment of the molasses was required apart from filtration using a 0.45μm filter and dilution of samples to a solid concentration of less than $3g/100cm^3$. Problems involved in analysing molasses stem chiefly from the relative quantity of sucrose to other components in the mixtures. The large sucrose peak can overlap other small peaks in the vicinity. With care, accurate sucrose concentrations can be obtained for individual product samples as well as other components of interest, eg. betaine.

The results of a series of experiments carried out by British Sugar suggests that most, if not all of the major molasses constituents can contribute to the HPLC chromatogram. Figures 5.4 and 5.5 show typical chromatograms for diluted beet molasses and enzyme-inverted beet molasses obtained on Bio-Rad HPLC system. Table 5.2 indicates the

Degrees	Glucose	Fructose	Betaine	Ionics	Colour	RDS	K+	Na+	Ca++	NO -	SO -	Cl-
0	0	0	0.05	0.02	0.36	0.0	.1	2.0	59	3	0	1
14.4				0.01		0.0						
28.8	0	0	0.09	0.01		0.0						
43.2				0.01	0.36	0.0	.1	3.5	18	5	10	16
57.6				0.04		0.2						
72.0				0.11	0.65	0.0	.1	7.5	44	6	11	21
86.4	0.01	0.05	0.04	0.04	0.108	0.2	.1	12.0	142			
100.8				0.07	0.192	0.2	.1	11.5	168	20	47	71
108.0				0.07		0.2						
115.2				0.09	0.396	0.2	.1	25.0	299	22	57	136
122.4	0.16	0.06	0	0.10		0.2	.18					
129.6				0.17	0.880	0.5	.5	31.5	669	58	73	431
136.8	0.98	0.07	0	0.29		1.2						
144.0	1.60	0.10	0	0.36	0.82	1.5	.3	61.0	1464			
158.4				0.27		2.2	.			224	690	349
165.6	1.432	0.10	0	0.21		2.1	.1	41.5	1161			
172.8				0.23		1.8	.1	46.0	1282			
187.2	0.93	0.71	0	0.09	0.183	1.8	.15	31.0	805	52	356	28
201.6	0.19	1.22	0	0.07		1.6						
216.0	0.23	0.93	0	0.05		1.2				16	95	11
230.4				0.04		1.1						
244.8	0.165	0.92	0	0.04	0.80	1.0						
259.2				0.04	0.80	1.2	.9	9.5	225	3	38	11
273.6	0.02	0.72	0	0.05	0.80	0.8						
288.0				0.06	0.65	0.8						
302.4				0.04	0.58	0.4						
316.8				0.04		0.4						
331.2	0	0.04	0.04	0.02		0.0	.1	3.5	110	3	5	7
345.6				0.02	0.41	0.0	.1	3.5				
360.0				0.02								

Units:-

Colour:- absorbance at 420 nm and pH7 after filtration through .45µm membrane (1 cm cell).

Fructose/
Glucose/ :- g/100 cm^3

Betaine

Conductivity :- m Siemens

$K^+/Na^+/Ca^{2+}/Cl^-/No_3^-/SO_4^{2-}$:- ppm

Figure 5.3

Figure 5.4 Chromatogram for Experiment 8-SM

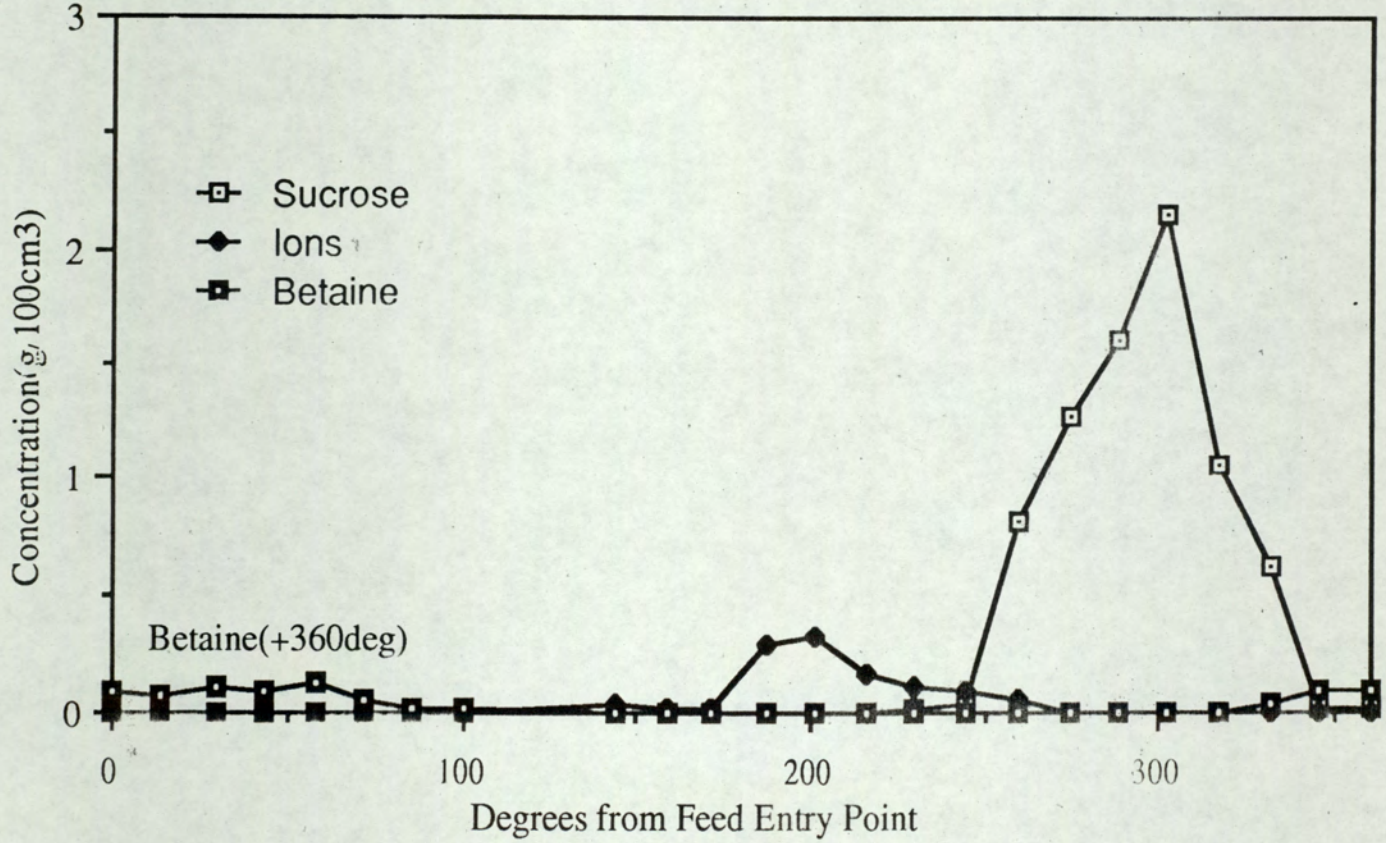

Figure 5.5 Chromatogram for Inverted Molasses Experiment

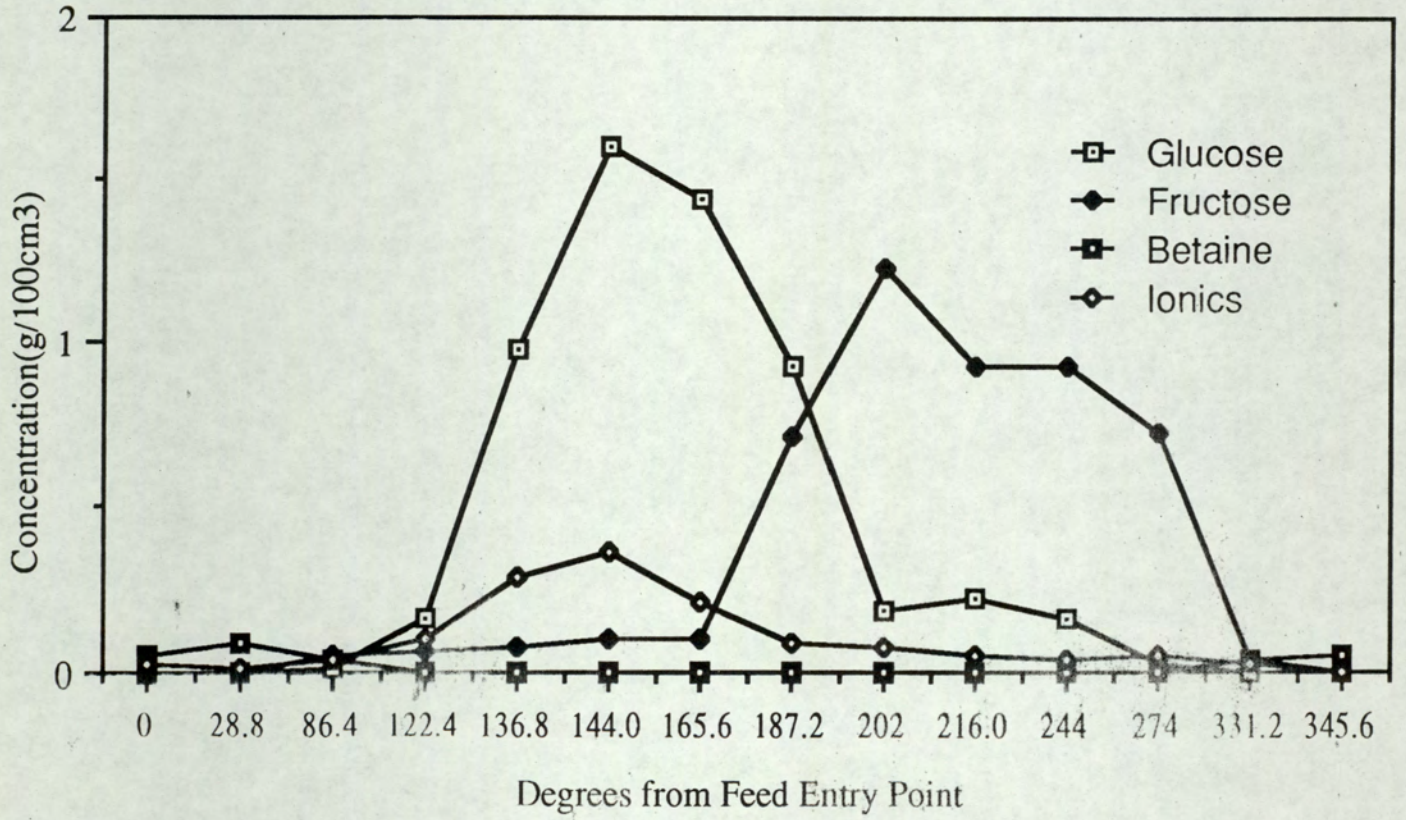

Table 5.2 - HPLC times for important molasses constituents

	Relative retention time	Typical concentration % w/v
Potassium chloride	0.65	0.7
Pyrollidone carboxylic acid	0.70	3.5
Disodium citrate	0.71	0.3
Citric acid	0.72	0.3
Sodium sulphate	0.74	1.0
Raffinose	0.80	1.0
Aspartic acid	0.82	<0.05
Glutamic acid	0.83	0.5
Lactic acid	0.97	1.1
Sucrose	1.00	62
Glucose	1.22	0.5
Fructose	1.52	0.5
Betaine	3.19	6
Glutamine	3.26	<0.5
Alanine	3.57	<0.5
Glycine	3.64	<0.5
Leucine	5.15	<0.5
Adenosine	6.8	<0.5

relative retention times of some of the more important molasses components taking sucrose as having a relative retention time of one.

Results were obtained using a Waters SUGAR PAK I HPLC column but should be similar for all calcium charged carbohydrate analytical columns.

5.6 RDS

Refractive Dry Substance (RDS) determination was carried out on a refractometer (Bellingham and Stanley Ltd, London). The procedure for using the refractometer was as follows:

The instrument was set up using a sodium lamp shaded to eliminate extraneous light. Water was circulated through the jackets of the prisms at a temperature of 20°C. Two or three drops of the sample were placed on the face of the lower prism and the two prisms brought together slowly and clamped. The prism was then rotated until the edge of the shadow passed exactly through the cross wires when viewed through the eyepiece. This allowed a reading to be taken on the Vernier by viewing through the other eyepiece. Tables were then used to obtain the refractive index value of the solution and hence total refractive dry substance concentration. The prisms were then cleaned and dried before re-use.

British Sugar Analysis of Experiment 8-SM

Degrees	Sucrose	Ionic	Betaine	Colour	K+	Na+	RDS
0		0.062					0
14.4		0.038			4.7	4.3	0
28.8		0.034					0
43.2		0.027					0
57.6		0.032		0.006			0
100.8		0.087			6.9	14.8	0
115.2	0	0.060	0	0.027			0
129.6	0	0.245	0	0.122	61.9	68.2	0
144	0.17	1.55		0.527	56.2	474.0	0.20
172.8		1.85	0	0.460			0.20
187.2	0.2	2.20	0	0.673	508	353.4	0.40
201.6		7.20	t	0.691	1748	1335	2.00
216	0.89	1.45	0	0.185	314.6	209.7	2.80
230.4	2.49	0.450	0.09	0.094	108.4	83.5	2.20
244.8	2.03	0.600	0.07	0.086			1.00
259.2	0.82	0.380	0.06		84.2	41.5	0.55
273.6	0.43	0.235		0.036			0.30
288		0.160	0.03		32.8	15.2	0.20
302.4	0.09		0.07	0.024			0
316.8	0	0.125	0.09				0
331.2		0.077	0				0
345.6	0	0.040		0.013			0
360		0.060			7.7	6.9	0
		0.031					

CHAPTER SIX

ION-EXCHANGE RESINS

6.1 Properties and Principles of Ion-Exchange Resins

Ion exchange particles consist of a porous matrix having electrically charged functional groups which are covalently bonded. There are four main types of ion-exchanger:

(a) inorganic exchangers; usually based on aluminium silicates

(b) synthetic resins

(c) cellulose ion-exchangers

(d) ion-exchange polydextran

There are five principal classes of functional groups found on ion-exchangers:

(a) cation exchangers

(b) anion exchangers

(c) amphoteric and dipolar ion exchangers

(d) chelating ion exchangers

(e) selective (or specific) ion exchangers

This project has been carried out using synthetic cation exchangers which operate by the following mechanism.

$$R\text{-}X^+ + Y^+ \rightleftharpoons R\text{-}Y^+ + X^+$$

The foward reaction is known as adsorption and the reverse process desorption. The equilibrium position depends on the concentration of solute ions and the relative affinities of the ions for the exchanger.

The ionic form of a commercial resin is generally specified by the manufacturer. Cation and anion exchangers are classified according to the nature of the active groups, ie.

Ion Exchanger	Type	Usual functional group
Cation exchanger	Strongly acidic	Sulphonic
	Medium acidic	Phosphoric
	Weakly acidic	Carboxylic
Anion exchanger	Strongly basic	Quaternary ammonium
	Medium basic	Mixture of tertiary and quaternary ammonium
	Weakly basic	Amines

In chromatography synthetic ion exchangers are most widely used. These resins are solid insoluble high molecular weight polyelectrolytes consisting of a three-dimensional matrix with large numbers of attached ionizable groups as mentioned above. These matrices are produced by polymerisation of styrene cross-linked with

divinyl benzene (DVB) (58).

The degree of cross-linkage is an important factor in chromatography. The cross-linkage can be controlled and varies between 1% and 16%.

The degree of cross-linkage determines the mechanical strength of a resin. Resins with low cross-linkage tend to be more porous and exchange ions more rapidly but have the disadvantage of swelling and shrinking which can disturb chromatographic operations. Low cross-linkage resins cannot be subjected to as high pressures limiting liquid throughput. Low cross-linkages resins are also less selective ion-exchangers.

The choice of an ion-exchange resin for a particular application is influenced by a number of properties, these are:

(1) Capacity, the capacity of an ion exchanger is a measure of the total amount of ions the resin is able to bond to and is usually expressed in terms of milliequivalents per gram of dry resin (in the H^+ or Cl^- form) or in milliequivalents per gram of fully swollen wet resin. The available capacity of an ion-exchange resin is affected by the concentration and ionic strength of the eluent, the pH, the temperature, the accessibility of functional groups and the nature of the counter-ions.

(2) Affinity, affinity is the degree of adsorption of a solute ion by the exchanger. Ion exchange is generally a reversible process and therefore an equilibrium is obtained. Equilibrium depends not only on the relative affinities of ions for the exchanger, but also on the relative ionic concentrations, therefore ions of a low affinity for the exchanger can regenerate it and replace ions of greater affinity, if the former are present at a higher concentration.

The affinity of ions for an ion exchanger is sometimes called the "ion-exchange potential" and in dilute aqueous solutions it increases with the charge density on a particular ion, ie. small highly charged ions have the greatest exchange potential. The affinity sequence for some of the common cations is:

$$Li^+ < Na^+ < NH_4^+ < K^+ < Ag^+$$

and

$$Mg^{2+} < Ca^{2+} < Sr^{2+} < Ba^{2+}$$

A measure of the affinity is given by the affinity coefficient, ß

$$ß = \frac{X_A/Y_A}{X_B/Y_B} \qquad \text{..... 4.1}$$

where X_A and Y_A are the concentrations of the ion A in the solute and the

concentration of the ion A in the resin respectively and X_B and Y_B are the corresponding concentrations for ion B.

6.2 Particle Size

The size of the particles in ion exchange resins is of great importance. The particle size determines how quickly equilibrium is established and influences the resolution of a chromatographic separation. The smaller the particle size the sharper the separation. if the particles are too small, however, the flow resistances increase and higher pressures are required. Particle structure is also important. The particle should offer good mechanical properties, resistance to deformation, attrition and chemical stability. In chromatographic separations it is important to have a uniform flow at all points of a bed of resin. It is necessary therefore to use resins which have a narrow range of particle size.

6.3 Purolite PCR 833 Ion-exchange Resin

Purolite PCR 833 ion-exchange resin supplied by Duolite International, Hounslow, Middlesex was used in this project for the separation of gluocse and fructose mixtures and mixtures of glucose, fructose and sucrose. It was chosen since it is a direct replacement for the Zerolit 225, SCR14 resin used by previous workers (22,23,59) for the separation of glucose and fructose in the SCCR equipment and as such

gave a direct comparison of the performance of the two chromatographic techniques.

In order to check the specification of the resin a technique known as seive analysis is used. The following procedure is carried out:

1 The resin was thoroughly wetted. A sample was taken from midway down the bag of resin.

2 Approximately $100cm^3$ of resin was transferred onto the uppermost of a series of sieves (200mm diameter) sieves used were mesh size diameters

355µm	180µm
300µm	150µm
250µm	106µm
212µm	

3 Using a length of PVC tubing attached to a cold deionised water supply the resin was washed gently through the top sieve.

4 The uppermost sieve was then removed and operation 3 was repeated and so on. Care had to be taken to ensure that excess water collected in the bottom plate was decanted off without losing

any fines in the process.

5 The resin held in each sieve was washed into separate beakers.

6 The resin from each beaker was allowed to dry on watchglasses and each portion was weighed.

Figure 6.1 shows the analysis as a histogram.

Table 6.1

Particle size	Mass of resin(g)	% resin
> 335	1.4	1.3
300-355	3.8	3.5
250-300	15.4	14
212-250	31.2	28.8
180-212	39.6	36.6
150-180	10.6	9.8
106-150	5.5	5.1
106	0.7	0.65

In this case 85% of the resin is within the specification which was 150μm-300μm. To improve on this, fines were removed by flotation using an excess of deionised water and agitation by stirring.

Figure 6.1 Seive Analysis on Purolite PCR 833 Ion Exchange Resin

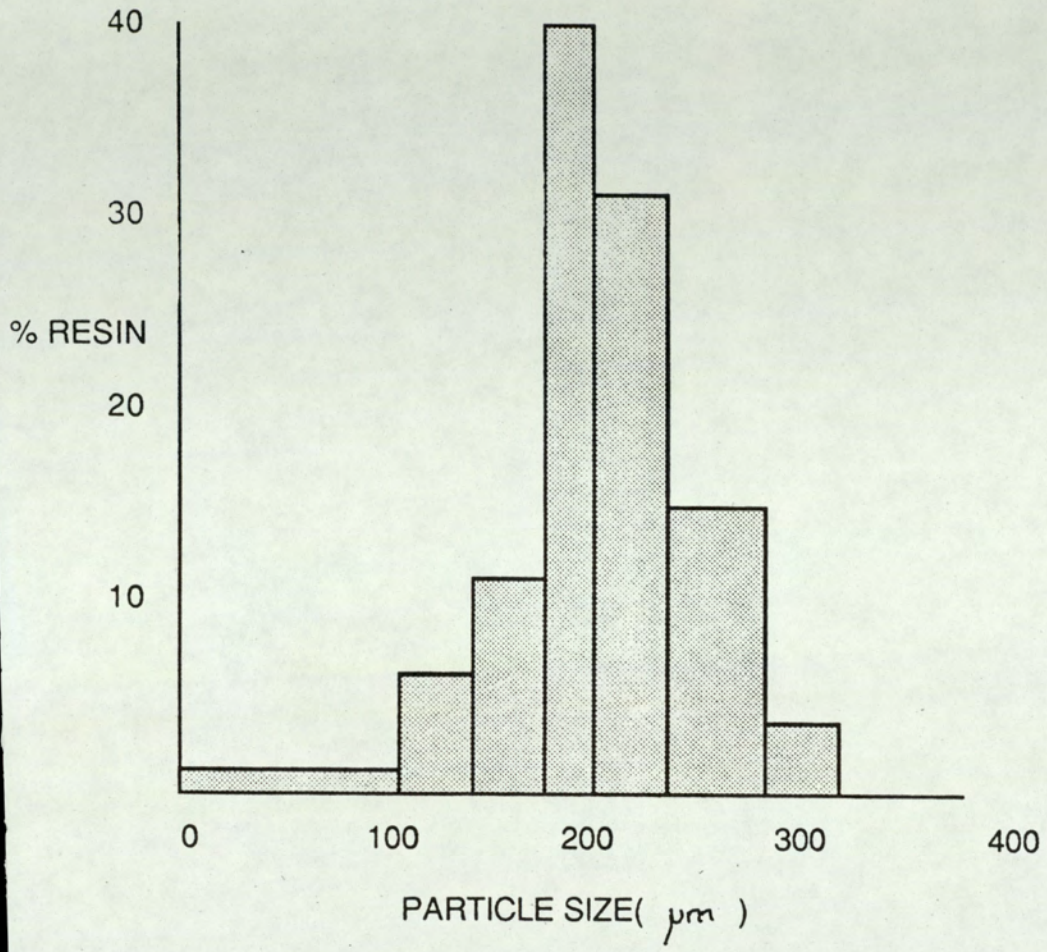

6.3.1 Regeneration

The Purolite resin has a particle size range of 150-300μm diameter and is 8% cross-linked with DVB giving good mechanical strength and resistance to shrinkage. The resin was supplied in its Na^+ form. For glucose and fructose separations the Ca^{++} form is required and so regeneration of the resin was necessary. This was carried out in two stages; hydrochloric acid (59l, 10% w/v) was passed through a 20 litre flask containing the resin (15 Kg) at a flowrate of 30 lh^{-1}. Deionised water was then passed through the flask at the same rate until the effluent was found to be neutral. The resin was then in its H^+ form, this is ncessary for conversion to the Ca^{++} form. Calcium chloride solution (65l, 10% w/v) was then passed through at the same flowrate (30 lh^{-1}).

6.3.2 The mechanism of separation of glucose and fructose

The formula for the isomers glucose and fructose is $C_6 H_{12} O_6$, the structures and molecular size of the two molecules is very similar (see Figures 6.2 and 6.3). Glucose and fructose have to therefore be separated by chemical means. Saltman and Charley (60) reported that Ca^{2+}, Ba^{2+}, Mg^{2+} and Sr^{2+} ions form soluble compounds in aqueous alkaline solution with various sugars including fructose. Angyal (61-66) suggested that only one form of the fructose forms the complex with the cations since it has an axial-equatorial-axial hydroxide group arrangement. This arrangement does not exist in the glucose forms

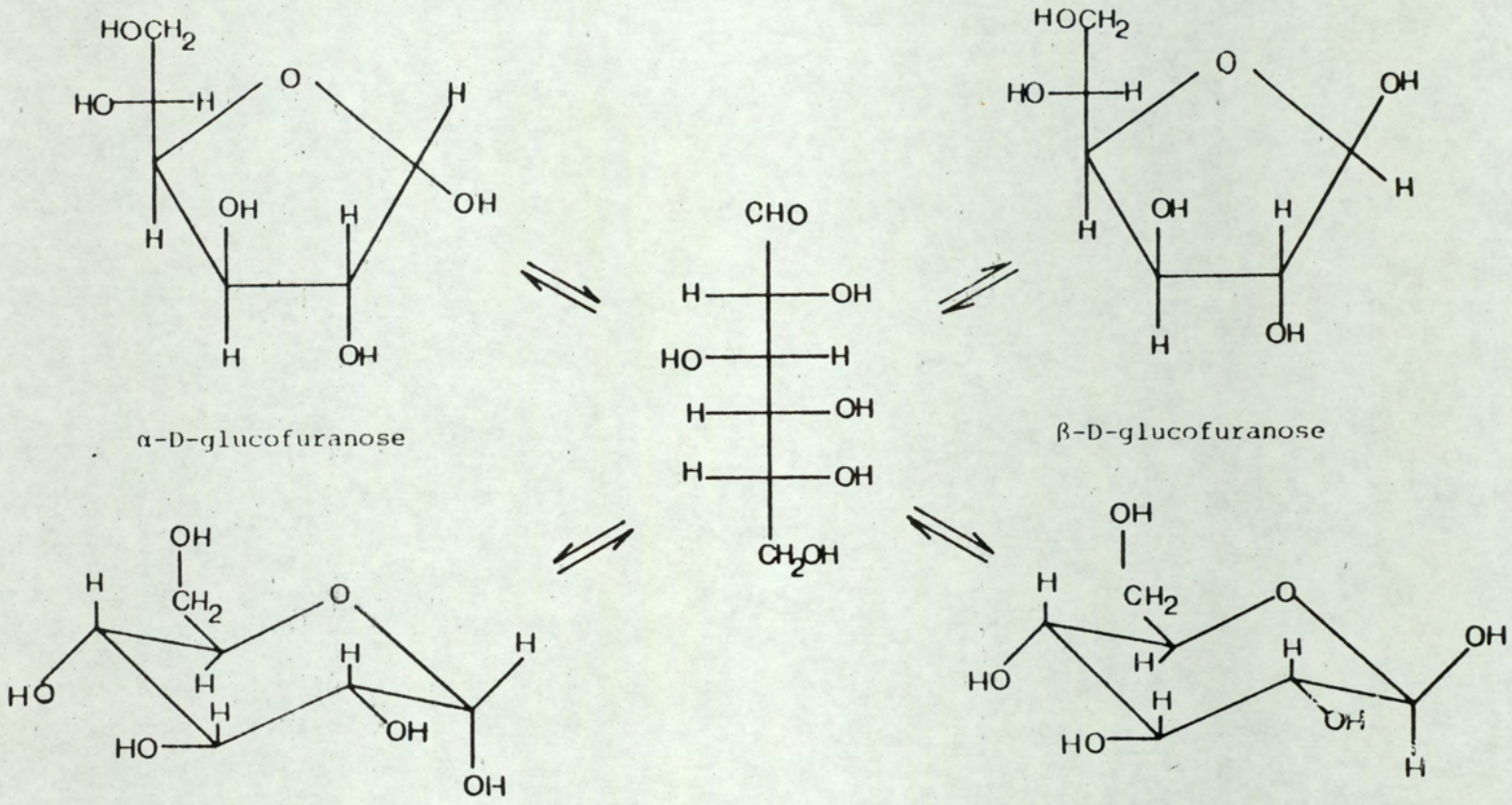
α-D-glucofuranose
β-D-glucofuranose
α-D-glucopyranose
β-D-glucopyranose

Figure 6.2

Figure 6.3

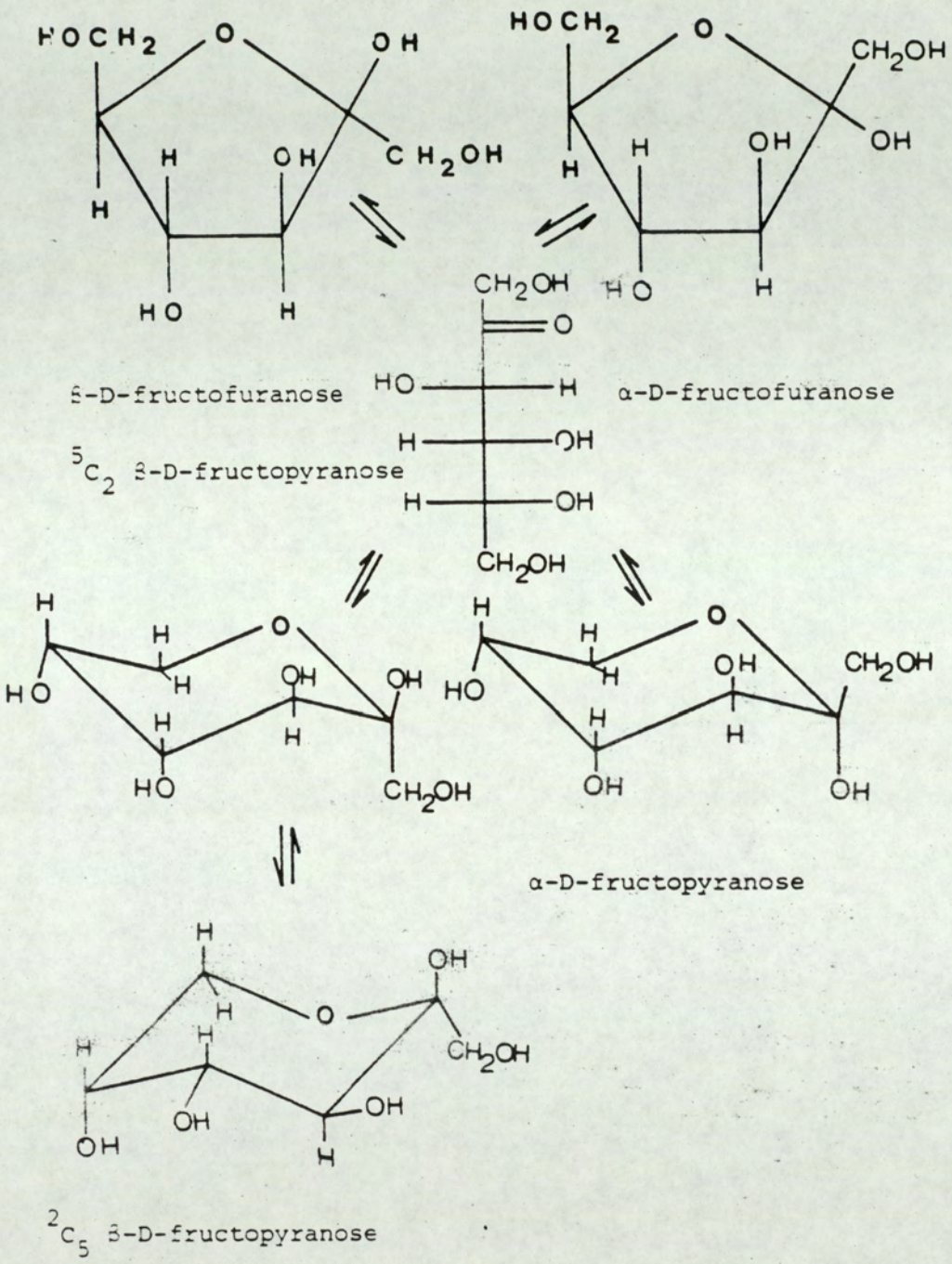
β-D-fructofuranose
α-D-fructofuranose
$^{5}C_{2}$ β-D-fructopyranose
α-D-fructopyranose
$^{2}C_{5}$ β-D-fructopyranose

hence only fructose forms the complex. This retards the fructose as it passes through the Ca^{2+} charged resin.

6.3.3 Packing Techniques

Good packing procedures in chromatographic columns is crucial to good performance. It is important that there are no spaces devoid of resin and that stratification does not occur, both of which can lead to poor flow distribution. The usual method of packing with synthetic ion exchange resins is to slurry pack them continuously.

This was difficult to achieve using the CCC equipment since excess water cannot be drained from the base of the chromatograph sufficiently quickly to pack the annulus continuously. Instead, volumes of approximately 2l of resin were poured into the annular space incrementally. After each portion of resin was added the equipment was tapped with a piece of wood to ensure that no air spaces had been produced and so that the packing was levelled ready for the next portion of resin. Excess water was syphoned from the top of the chromatograph.

6.4 Unpacking and Repacking

Several months of using the resin caused drastic increases in the pressure drop through the packing. The packing had become more compressed and fines and debris had accumulated within the spaces between the particles. Backwashing using this equipment was not readily

possible due to the large number of outlets beneath the chromatograph. it was necessary therefore to repack with fresh resin. The arrangement shown in Figure 6.4 was used for this. Resin and water as a slurry was drawn through an 8mm diameter polypropylene tube (A) due to the vacuum created by water passing through the 12mm diameter stainless steel pipe.

As an alternative to repacking compressed air at (20-40 psi) was applied via a distribution system of PTFE tubes to 20 outlets from the chromatograph. This was carried out for approximately four hours and had the effect of disturbing heavily compressed regions of the packing which had developed. Fines and debris were also brought to the surface where they were removed by syphoning. The position of the PTFE tubes was altered to ensure that all parts of the packing had received attention. Compressed air has the advantage over backwashing with water in that flooding could not occur. This had the effect of reducing the pressure drop through the packing, allowing higher eluent flowrates to be used.

6.5 Void fraction determination

An important part of modelling and evaluating the equipment involves determination of the voidage, ε

$$\varepsilon = \frac{\text{Volume of voids (l)}}{\text{Volume of bed (l)}}$$

Figure 6.4 Resin Removal

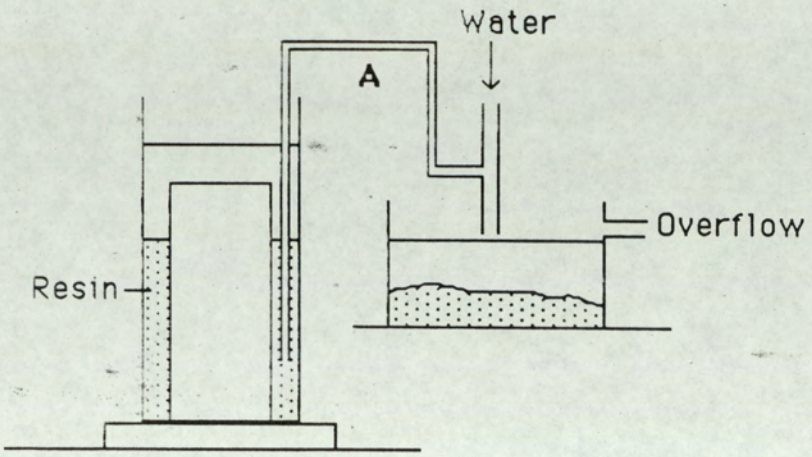

Figure 6.5 The Osmotic Effect of Molasses on the Duolite Resin.

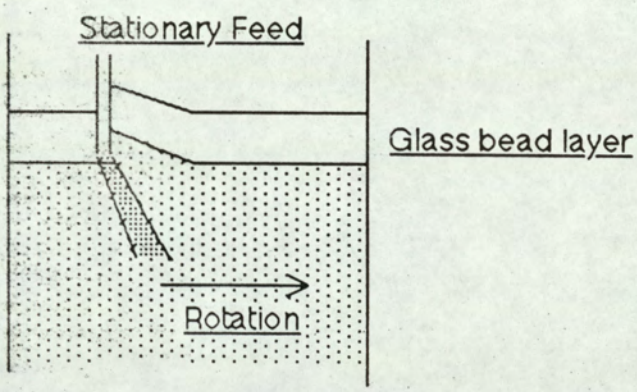

Determination of the void fraction was carried out using a 2% w/v solution of blue dextran 2000 as feed. Blue dextran 2000 has an average molecular mass of 2,000,000 and as such is totally excluded from the resin pores. Blue dextran therefore passes through the resin at the same velocity as the eluent and it is therefore possible to calculate the volume of voids and hence the voidage. The conditions used were:

Eluent flowrate = 7.5 l h^{-1}

Feed flowrate (Blue dextran solution) = 60cm^3 h^{-1}

Rotational speed = 144 deg h^{-1}

The Blue dextran band can be observed through the glass column, however a refractometer was connected on-line to the chromatograph in order to determine the exact exit position, $\bar{\theta}_D$.

The exit position, $\bar{\theta}_D$, of blue dextran was found to be 95° from the feed entry point. From this it is possible to calculate the voidage, ε from equation 2.28.

$$\bar{\theta}_D = \frac{\omega_L}{V} [\varepsilon + (1 - \varepsilon) K] \qquad \text{..... 2.29}$$

Since blue dextran is totally excluded from the resin pores the distribution coefficient, K for dextran is 0. This gives:

$$\varepsilon = \frac{\bar{\theta}_D V}{\omega L} = 0.34$$

6.6 Flow Distribution

Another important check which had to be carried out was a determination of the constancy of flow throughout the annulus. This was carried out at an overall flowrate of 12 lh^{-1}. The following procedure was carried out:

1 All exit pipes from the chromatograph were pulled tightly to ensure that no water remained in these and that they all drained properly.

2 Fifty dry, empty sample bottles (150cm^3) were positioned in the collecting tank as quickly as possible to avoid differences in volume due to the time taken to position the bottles.

3 The annulus was kept stationary and after 30 minutes each sample bottle was withdrawn.

4 Each sample bottle was then weighed.

5 The experiment was repeated with the annulus rotating at 2 revolutions per hour, for 30 minutes this was necessary to determine whether the packing or the outlet pipes were responsible for any variations in flow. If the outlet pipes were responsible for flow problems, then upon rotating the equipment similar variations in flow would show up to when the annulus was stationary.

The results are shown in Tables 6.2 and 6.3. The experiment was carried out after the compressed air had been applied to the underside of the chromatograph to "clean up" the resin.

Tables 6.2 and 6.3 show up a certain amount of variation in the liquid flow rates through different parts of the annulus. Some of the samples collected which had low volumes in both the rotational test and the static test were traced to blockages within the sample collecting ring. After cleaning these obstructions greater volumes could be collected at these positions. Some of the discrepancies in the static test could not be explained easily. Because two outlet holes in the baseplate drain into one collection hole, it may have been possible for three outlets to be draining into one collection hole and only one outlet to be draining into the adjacent collection hole. The results show that there is perhaps room for improvement here. It was considered however that the liquid distribution was sufficiently good as to give reasonable results but future improvements may be possible.

Table 6.2 - Flow distribution in the CCC stationary

Exit position	Mass of water (g)	Exit position	Mass of water (g)
1	108	26	144
2	79	27	108
3	134	28	98
4	121	29	111
5	69	30	69
6	117	31	112
7	135	32	112
8	107	33	140
9	122	34	144
10	133	35	121
11	101	36	122
12	87	37	117
13	139	38	81
14	110	39	94
15	124	40	83
16	103	41	139
17	137	42	140
18	140	43	137
19	106	44	106
20	85	45	120
21	57	46	126
22	136	47	109
23	135	48	140
24	120	49	139
25	103	50	83

Table 6.3 - Flow distribution (rotational)

Exit position	Mass of water (g)	Exit position	Mass of water (g)
1	121	26	104
2	142	27	140
3	134	28	131
4	112	29	137
5	96	30	100
6	98	31	97
7	99	32	136
8	94	33	140
9	134	34	91
10	149	35	120
11	101	36	121
12	103	37	121
13	105	38	117
14	122	39	116
15	122	40	140
16	120	41	132
17	134	42	116
18	140	43	117
19	99	44	107
20	107	45	100
21	144	46	140
22	111	47	131
23	96	48	126
24	122	49	121
25	122	50	127

6.7 Air in the packing

It was found to be very difficult to prevent the water in the annular chromatograph from draining away while the equipment was not in use. This was due to the large number of outlets beneath the annulus. Initially attempts were made to block each hole with small rubber bungs. This was found to be extremely time-consuming and not very successful since the chances of one bung escaping was very high. It was decided therefore that a liquid level controller should be installed in the headspace above the annulus so that as water escaped from the equipment this would be detected by the electrical controller and the eluent pump would be switched on to refill the chromatograph to its original level. This had the added advantage of ensuring that water in the chromatograph was never completely stagnant, keeping down the growth of micro-organisms and flushing out any sugar etc which may have remained in the apparatus.

Occasionally however the liquid level controller did not function as it should and the liquid level dropped below the upper surface of the ion exchange resin. This had the effect of drawing air into the spaces between the resin particles. Upon rectifying the problem with the controller and refilling with water the bubbles of air remained trapped. Air trapped in chromatographic columns causes channelling of solutes which can spoil a separation and so a method had to be found of removing this trapped air. Heating water to high temperatures, ie. above 80°C causes

degassing to occur as air dissolved in the water form bubbles and rise to the surface. If water which had been heated to approximately 80°C was pumped through the aerated packing, the air bubbles could be seen to dissolve in the water. After 24 hours at a flowrate of greater than 6 l h^{-1} the air bubbles could be seen to have dissolved back into the degassed water completely giving an air free bed.

Duolite C211/2558 Na^+ Form Ion-Exchange Resin

The Duolite resin has a mean aperture of 420μm with 70% minimum within 370-470μm (ie. ± 12% of mean aperture) and 98% minimum within 315-550μm. This is a typical industrial scale chromatographic resin and as such may not be perfect for the CCC equipment. This type of resin has however, been used successfully for the separation of sucrose from non-sugars in molasses in conventional columns.

The Duolite resin differs not only in terms of the size of the particles compared to the Purolite resin, it is also only 5.5% cross-linked with DVB. This means that the resin is more porous which improves the separation of the sucrose from the non-sugars but has the disadvantages of shrinking under conditions of high sugar or salt concentrations due to osmotic effects. It is also able to withstand less pressure. The particle sizes are larger however reducing the pressure drop through the bed length and hence allowing higher overall throughputs.

The separation of sucrose from other components in molasses is carried out partly by ion exclusion. The sucrose passing through the resin is delayed on the column owing to diffusion in and out of the resin pores. The ionic material is excluded from entering the resin beads due to what is known as the Donnan membrane effect, the charge on the resin beads having a repellent effect on passing ions. Other charged molecules and large molecules such as the colour bodies because of size effects are eluted before the sucrose.

The Duolite resin was used in the Na^+ form, since this has been shown by British Sugar Research to give better separation of the ionic components from the sucrose (67). In the Ca^{2+} form there is no apparent separation at all between the two components. During experiments using molasses some exchange occurs between the K^+ ions in the feed and the Na^+ ions on the resin. This has been shown when the effluent produced during an experiment is analysed for Na^+ ions.

Quantities of Na^+ ions produced are greater than expected and quantities of K^+ are reduced. British Sugar experiments with the Duolite resin have shown, however that K^+ ions on the resin behave in exactly the same way as the Na^+ ions, giving very similar separations.

After several months of running the apparatus with molasses, two samples of resin were obtained from the top and the bottom of the annulus. Analysis was carried out to determine the concentrations of sodium, potassium and calcium on the resin. Table 6.4 lists these.

Table 6.4 - Cation Concentrations

Resin	Sodium meq cm^{-3}	%	Potassium meq cm^{-3}	%	Calcium meq cm^{-3}	%
Top	0.46	32	0.97	67	0.02	1
Bottom	0.43	30	0.82	57	0.19	13

Table 6.4 shows the extent of ion exchange on the Duolite resin, with the K^+ concentrations being greater than the Na^+ concentrations. The Ca^{2+} concentration at the top of the bed is not really significant, however at the bottom of the resin it is fairly high and indicates a need for periodic regeneration with sodium chloride.

A wet sieve analysis was carried out on the same resin samples which indicated that 99% of the particles were between 420μm and 500μm diameter. The number of broken beads present was measured and found to be less than 1% of the total number, this is not excessive as new, unused resins quite often have the same proportion of broken beads.

6.8 Osmotic Effects.

Because of the nature of the Duolite resin and its lower cross-linkage, water can pass in and out of the resin pores according to the external environment. In highly concentrated solutions water passes out of the beads by osmosis causing the beads to shrink. When the highly concentrated solution is removed and replaced by water the beads return to their normal size as water passes back inside again. Upon regenerating the Duolite resin with sodium chloride solution (1.7M) in the chromatograph an approximate decrease of 10cm was noted in the height of the packing, indicating a shrinkage of 7%. After passing deionised water through the packing a slow return to be original height was noted.

Another effect which was noted whilst the molasses experiments were being carried out was a drop in the height of the packing through which the feed nozzle had just passed through. Figure 6.5 shows what happened. This created a wave effect as the annulus rotated past the feed point. This created a few problems in that occasionally the packing would drop to such an extent that the feed nozzle became clear of the top of the glass bead layer causing molasses to be distributed across the entire surface of the resin. To overcome this a larger quantity of glass beads was introduced. An adjustable feed nozzle has now been incorporated into the design with the facility of vertical movement.

Void Fraction

The void fraction was determined in a similar manner to that described for the Purolite resin using Blue dextran solution. A value of ε = 0.40 was obtained.

CHAPTER SEVEN

EXPERIMENTAL RESULTS AND DISCUSSION

7.1 Introduction to Results

Four main types of separation have been carried out in order to assess the potential and diversity of the CCC equipment. These were:

(1) Separations of glucose and fructose mixtures

(2) Separations of glucose, fructose and sucrose mixtures

(3) The separation of glucose, fructose and non-sugars in inverted beet molasses

(4) The separation of sucrose from non-sugars in beet molasses.

A number of experimental runs have been carried out under a variety of operating conditions and considerable valuable information has been obtained from these experiments. The work carried out, however, due to limitations imposed by time and mechanical breakdowns does not represent a comprehensive study for each feedstock used. It is instead intended as a starting point for initial insight into how the equipment behaves, what the operating problems are and how to obtain the best possible results from the equipment. Many of the results obtained have been incorporated into a computer simulation program which can predict the behaviour of the equipment under different circumstances, (see Chapter

8).

7.2 The Separation of Glucose from Fructose using the CCC Equipment

Several runs were carried out using glucose and fructose mixtures in order that a comparison could be made directly of the performance of this equipment against that of the SCCR equipment. These separations were carried out using Purolite PCR 833 ion-exchange resin (as described in Chapter 6).This resin was charged in its calcium form and is an exact equivalent of the Zerolit 225 SRC14 resin used in the SCCR equipment(68)

Product samples produced during experimental runs were analysed using HPLC equipment. A chromatogram was produced from the sugar concentrations obtained using the analytical data.(Figure 7.1)

A series of experiments were carried out to assess the effects of altering certain key operating parameters on the separation. The effects of varying the feed flowrate and the rotational speed were considered to be of greatest importance and hence emphasis was made on the investigation of the effects of these parameters on the separation.

7.2.1 The effect of feed flowrate on the separation of glucose from sucrose on the CCC

Seven experimental runs were carried out to test the effect of feed flowrate on the separation of glucose from fructose whilst maintaining constant eluent flowrate, rotational speed, feed concentration and temperature. A feed sugar concentration of 50g/100 cm^3 was used

Figure 7.1 Chromatogram for experiment

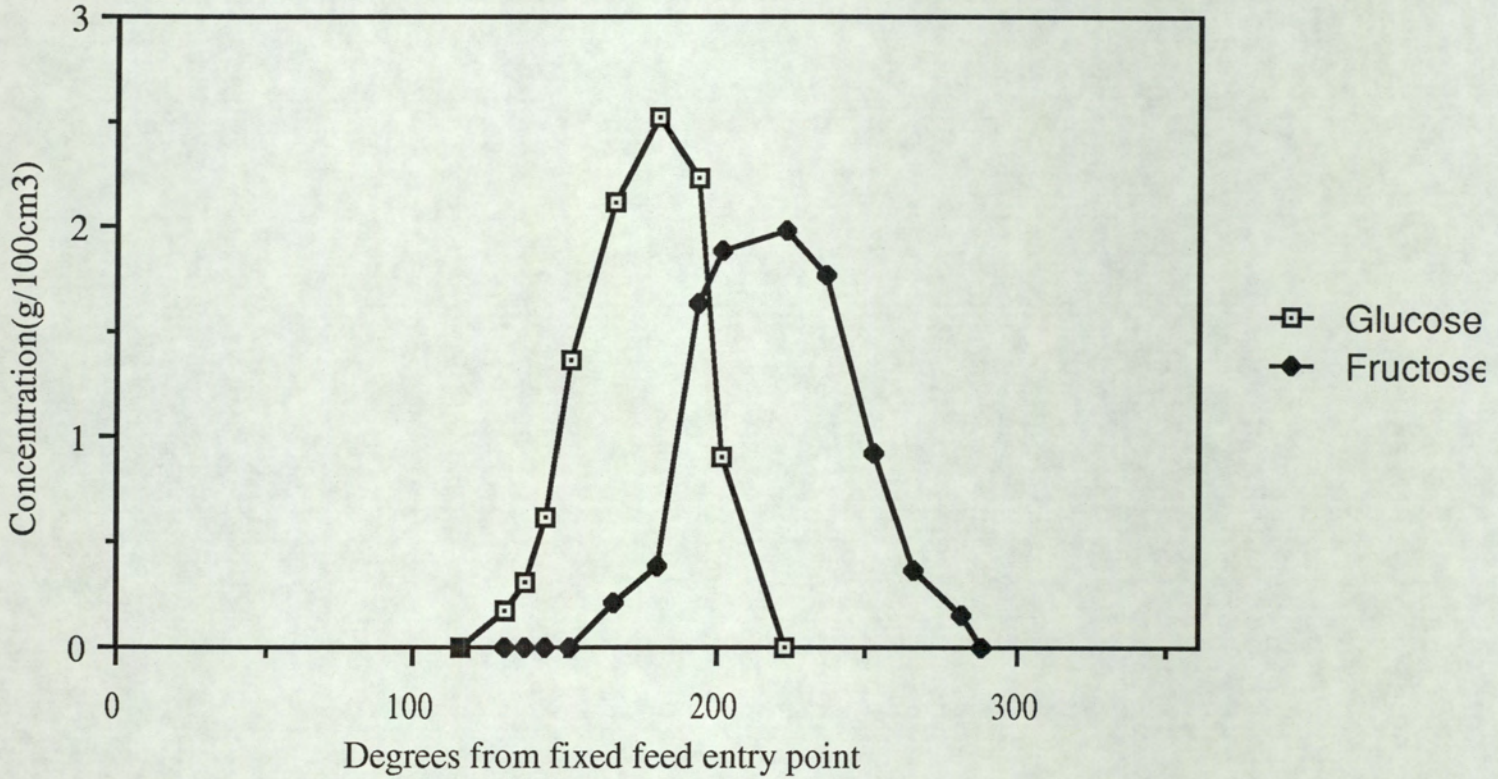

(25g/100cm^3 glucose concentration, 25g/100cm^3 fructose concentration). A temperature of 20°C was maintained throughout the equipment.

From the chromatograms obtained for each experimental run specific measurements can be made which help to quantify the separation.

The distance from zero, ie. the feed point, to the maximum of the peak in degrees is designated, $\bar{\theta}$. Drawing tangents to the curves on both sides of the peak maximum and extending them to the baseline gives the baseline bandwidth, W, (Figure 7.2). These two sets of values allow a comparison to be made of the degree of separation from experiment to experiment. This was achieved by calculating the resolution as defined in equation 2.31. Other conditions for these experiments were: eluent flowrate of 12 lh^{-1}, rotational speed of 220 deg h^{-1}.

$$R_S = \frac{(\bar{\theta}_y - \bar{\theta}_x)}{Y_2 (W_x - W_y)} \qquad \text{..... 2.32}$$

Figure 7.2 Chromatogram

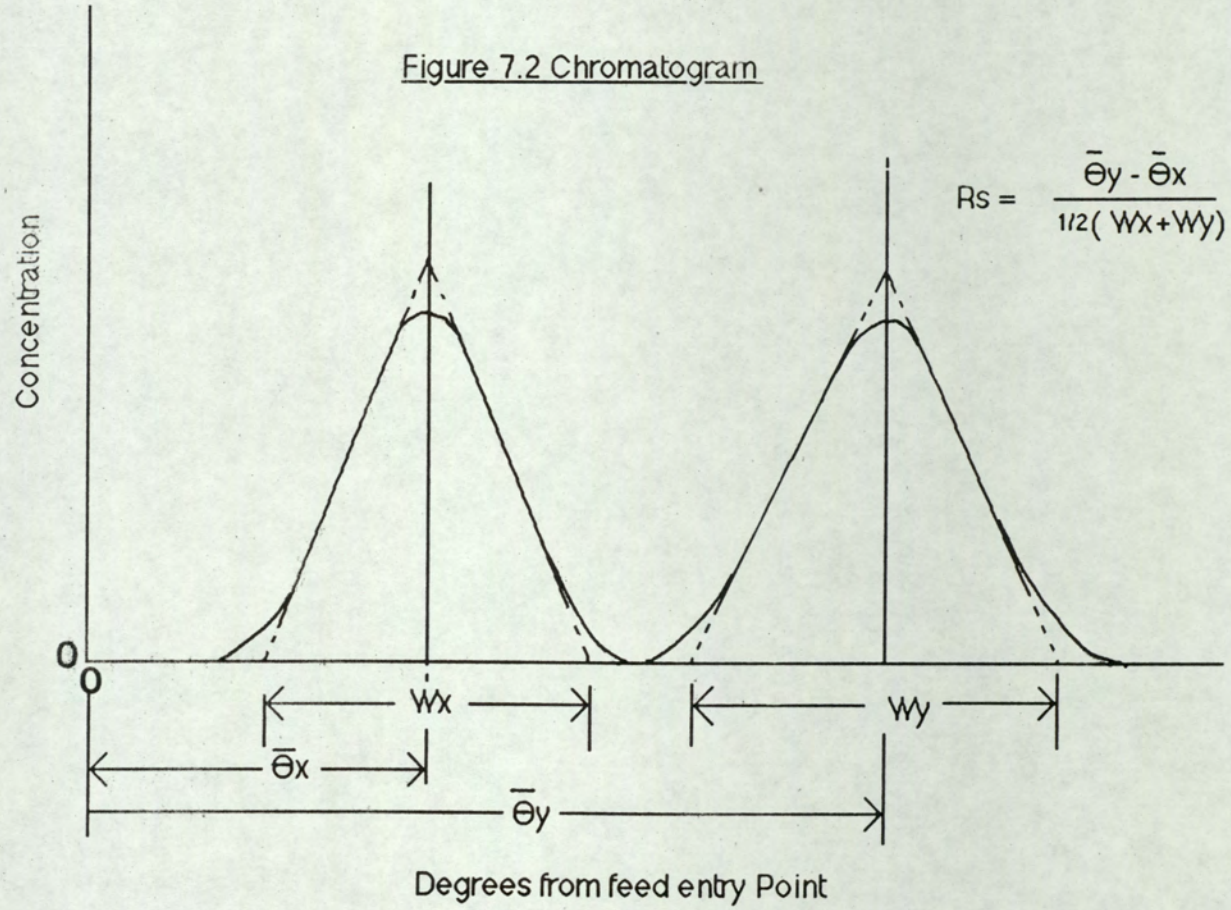

7.2.1 The Effect of Feed Flowrate on the Exit Band Position of the Glucose and Fructose Bands

Table 7.1

Run	Feed flowrate/ $cm^3\ h^{-1}$	$\bar{\theta}_G$ degrees	$\bar{\theta}_F$
1/GF	50	165	208
2/GF	100	167	210
3/GF	150	165	205
4/GF	200	164	216
5/GF	250	171	217
6/FG	300	186	225
7/GF	350	170	216

Table 7.1 and Figure 7.3 shows that as feed flowrate is increased there appears to be little variation in the exit position of the glucose and fructose bands. This is predicted by the plate theory. This suggests that the distribution coefficients, K_G and K_F for glucose and fructose are unaffected by increasing feed flowrate since K is calculated from the eluent velocity, the rotational speed, the bed length, and the void fraction which remain constant throughout all the experiments; and the peak position.

It is clear from Table 7.1 that the peak band position for fructose is always greater than that for glucose. This is due to the greater affinity of the fructose for the resin. As described previously, fructose forms a weak complex with the Ca^{2+} ions on the ion exchange resin. From the average exit position for glucose and fructose, the distribution coefficient, K for each

Figure 7.3 The effect of feed flowrate on the exit position of glucose and fructose

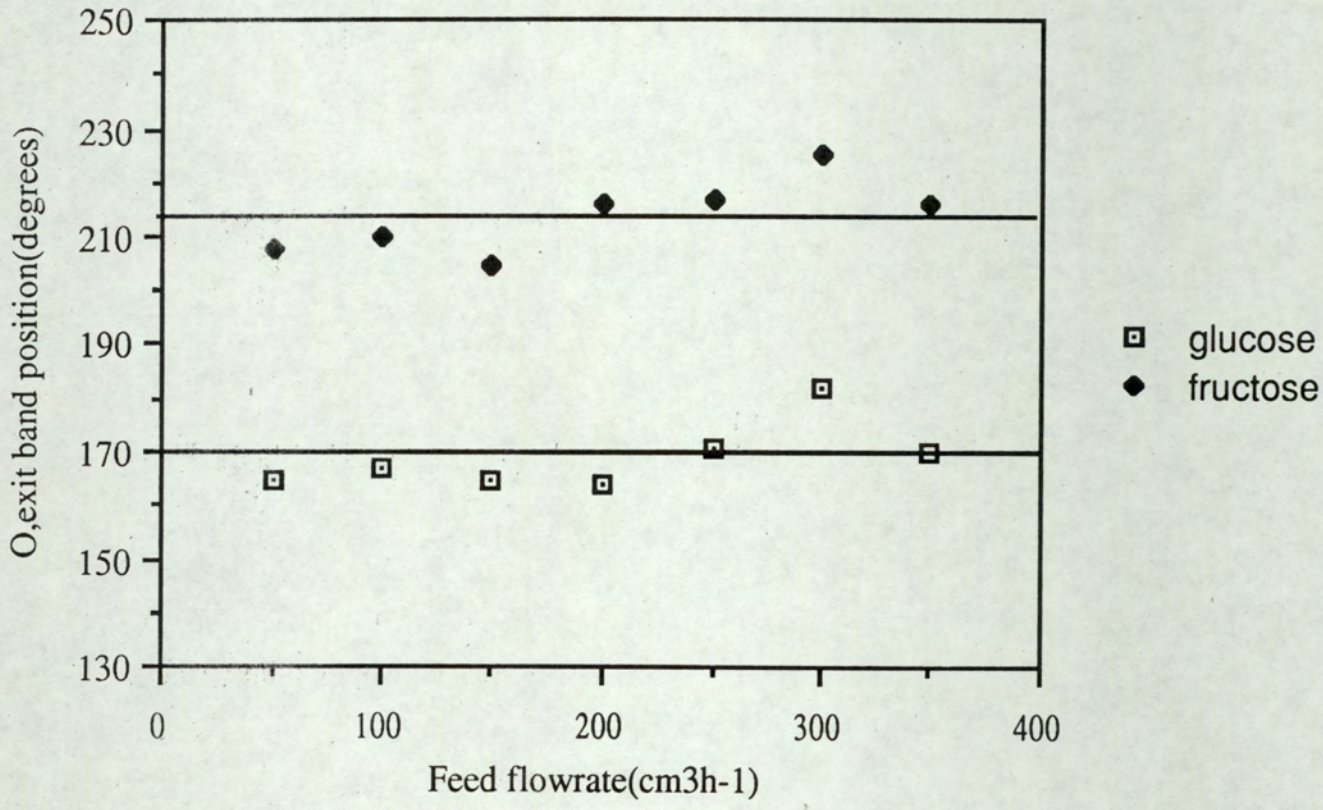

solute can be calculated using equation 2.29.

$$K = \left[\left(\frac{\bar{\theta}V}{\omega L}\right) - \varepsilon\right] \Big/ (1 - \varepsilon) \qquad \text{..... 2.30}$$

where

$\bar{\theta}$ = band peak position (degrees)

V = eluent superficial velocity (cm h^{-1})

L = bed length (cm)

ε = void fraction

ω = rotational spee (deg h^{-1})

Average $\bar{\theta}$ value for glucose = 170°

Average $\bar{\theta}$ value for fructose = 213°

$$K_G = \left[\frac{170 \times 113}{220 \times 135}\right] - 0.34 \Big/ 1 - 0.34$$

$$= 0.46$$

$$K_F = \left[\frac{213 \times 113}{220 \times 135}\right] - 0.34 \Big/ 1 - 0.34$$

$$= 0.71$$

7.2.1.2 The effect of increasing feed flowrate on band spreading in the CCC using Glucose and Fructose as feed

Table 7.2

Run No	Feed flowrate $cm^3 h^{-1}$	W_G (degrees)	W_F
1/GF	50	42	54
2/GF	100	53	66
3/GF	150	65	76
4/GF	200	89	104
5/GF	250	101	126
6/GF	300	150	189
7/GF	350	167	216

Figure 7.4 shows that as feed flowrate was increased the exit bandwidth increased. This is to be expected since the initial feed bandwidth also increases as the feed flowrate is increased. Using equation 2.35 the calculated initial bandwidth at 50 $cm^3 h^{-1}$, feed flowrate is 1.50 degrees and at 350 cm^3h^{-1} feed flowrate is 10.2 degrees. The increase in bandwidth greatly exceeds that predicted by the plate theory. The plate theory does not however take into account axial dispersion experienced in annular chromatography or non-uniformity of the packing at different parts of the annulus both of which could be contributory factors in the increased band spreading as feed rate is increased. Another possible cause of increased band spreading is radial dispersion at the exit points due to "hold-up" of solutes at the base of the annulus.

Figure 7.4 The effect of feed flowrate on the exit bandwidths of glucose and fructose

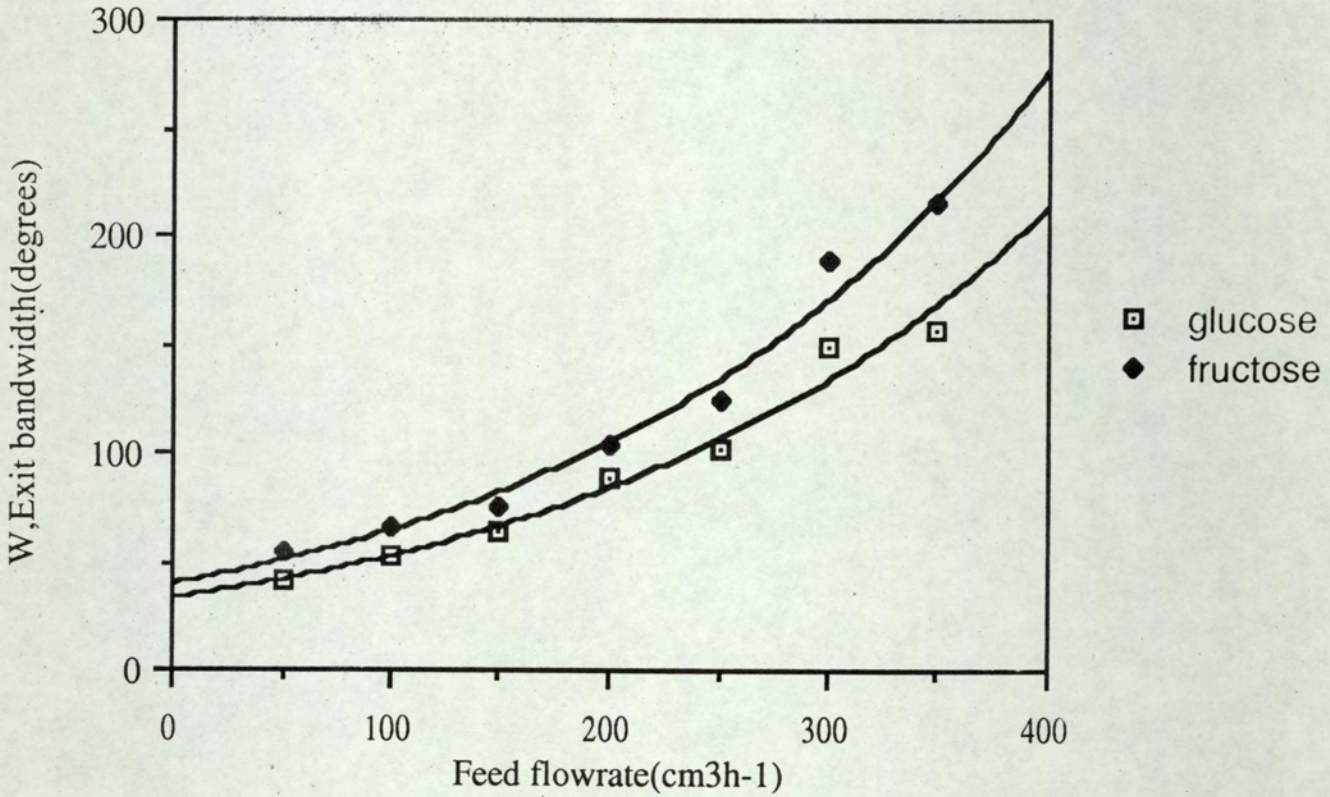

The shapes of the curves for glucose and fructose appear to be very similar, both rising exponentially. The fructose bandwidth is always greater than that of the glucose. This is almost certainly due to the fructose being the more highly retained solute. The greater the retention time for a solute the greater the opportunity for dispersion and therefore the greater the band spreading.The curves intersect the Y axis at approximately 40 degrees approximately 40 degrees.This appears to be a minimum value no matter how small the feed flowrate is.An additional point has not been put at the origin as the other points fit the curves so well.

7.2.1.3 The Effect of Feed flowrate on the Height Equivalent to a Theoretical Plate

Table 7.3

Run No	Feed flowrate ($cm^3 h^{-1}$)	Average No of theoretical plates	Average height equivalent to a theoretical plate (cm)
1/GF	50	250	0.54
2/GF	100	160	0.84
3/GF	150	110	1.23
4/GF	200	61.8	2.18
5/GF	250	45.5	3.00
6/GF	300	23.6	5.72
7/GF	350	20.7	6.52

The height equivalent to a theoretical plate or number of theoretical plates in a column is a measure of that columns efficiency.Equation 2.34 defines the number of theoretical plates.

the number of theoretical plates.

$$N = \frac{16\bar{\theta}^2}{W^2 - W_o^2} \qquad \text{..... 2.34}$$

The height equivalent to a theoretical plate is obtained by dividing the bed length by the number of plates.

$$H = L/N \qquad \text{..... 7.1}$$

where

H = height

L = bed length

N = number of theoretical plates

The effect of feed rate on average theoretical plate height is shown in Figure 7.5. Over the feed range studied a 13-fold increase in plate height occurred. This result is unexpected since the plate theory predicts only a slight increase in plate height due to the increase in total flowrate as the feed rate is increased. This clearly shows that plate theory cannot adequately account for bandspreading in the CCC.

Figure 7.5 The effect of feed flowrate on the height eq. to a theoretical plate.

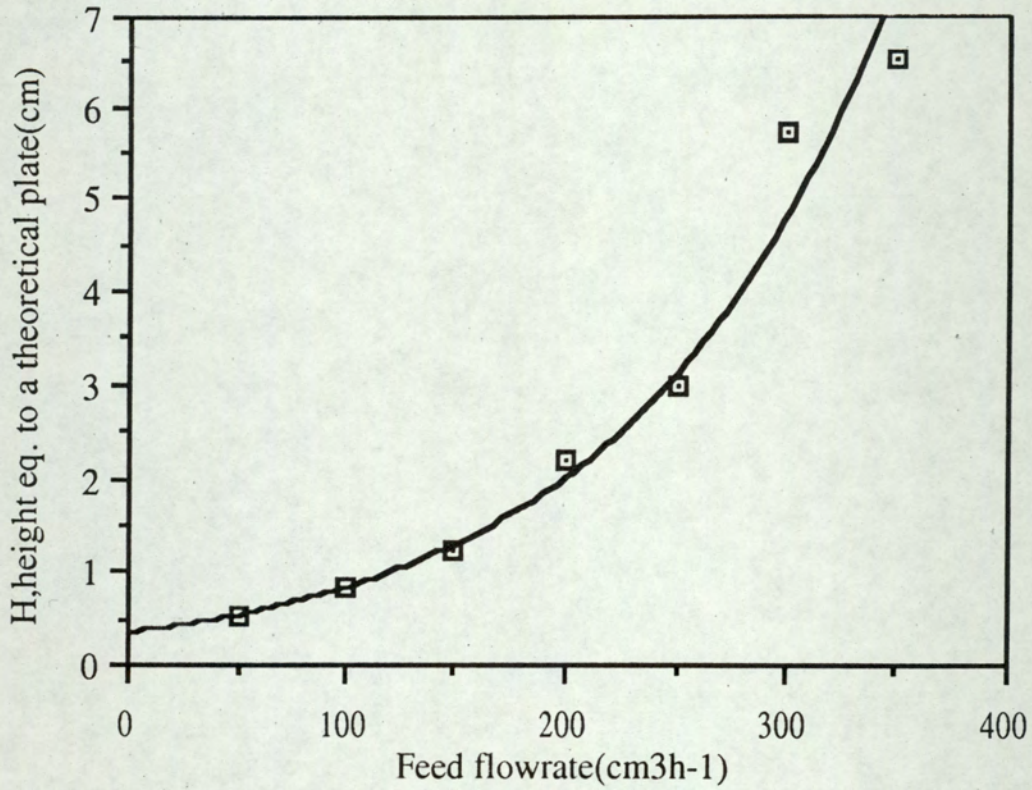

7.2.1.4 The Effect of increasing feed flowrate on dilution in the CCC

Table 7.4

Run No	Feed flowrate $cm^3\ h^{-1}$	Average dilution factor, D_f
1/GF	50	32.0
2/GF	100	19.9
3/GF	150	16.0
4/GF	200	16.4
5/GF	250	15.6
6/GF	300	19.2
7/GF	250	18.7

Dilution factor has been discussed in Chapter 2 and is a measure of the change in concentration of a particular solute from the point of entry into the annulus to the outlet. It is calculated by dividing the initial feed bandwidth, which can be calculated from feed flowrate and the eluent flowrate into the exit bandwidth, equation 2.32.

$$W_o = 360\ Q_f/(Q_f + Q_E) \qquad \text{..... 2.35}$$

Q_f = feed flowrate ($cm^3\ h^{-1}$)

Q_E = eluent flowrate ($cm^3 h^{-1}$)

W_o = initial feed bandwidth (deg)

$$D_f = \frac{W}{W_o} \qquad \text{..... 2.33}$$

Table 7.4 and Figure 7.6 show that as feed flowrate is increased keeping other factors constant there is initially, from 50 cm^3h^{-1} feed rate to 150 cm^3h^{-1} feed rate a substantial decrease in the dilution factor, ie. more concentrated products. At a feed rate of greater than 150 cm^3h^{-1} some fluctuation in the dilution factor occurs, but the overall effect is that the dilution factor appears to level off at approximately 17. Increasing the feed flowrate above 150cm^3h^{-1} in order to increase product concentrations is therefore pointless under these operating conditions. It is useful to discover this limit on dilution factor if a specific product concentration is required. The limit will obviously vary as the other operating parameters are changed however.

7.2.1.5 The effect of feed flowrate on resolution

Table 7.5

Run No	Feed flowrate (cm^3h^{-1})	Resolution
1/GF	50	0.89
2/GF	100	0.72
3/GF	150	0.56
4/GF	200	0.53
5/GF	250	0.41
6/GF	300	0.23
7/GF	350	0.25

Resolution is defined by equation 2.32.

Figure 7.6 The effect of feed flowrate on the dilution factor,Df

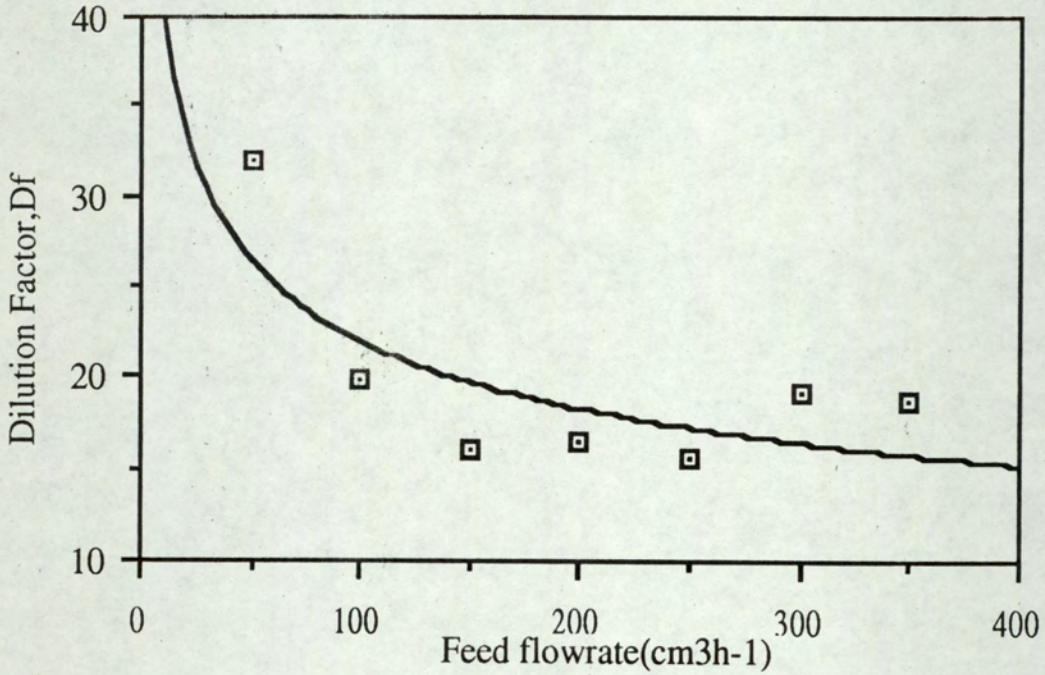

$$R_S = \frac{\bar{\theta}_y - \bar{\theta}_x}{1/2\,(W_x + W_y)} \qquad \text{..... 2.32}$$

Since resolution depends upon the peak band position, θ which has been shown to remain fairly constant and the exit bandwidths, which have been shown to increase with increasing feed rate, it follows that as feed rate is increased resolution decreases. The relationship between feed rate and resolution appears to be a linear one (Figure 7.7). Using this set of conditions there seems to be a limit to resolution of close to 1 no matter how small the feed flowrate. The graph also indicates a feed flowrate of approximately 450 cm^3h^{-1} at which the resolution is zero, ie. glucose and fructose peaks are completely overlapping and no separation is possible.

7.2.2 The effect of rotational speed on the separation of glucose from fructose on the CCC

Five experimental runs were carried out to determine the effect of increasing the rotational speed on the separation of glucose and fructose.

A constant eluent flowrate of 12 lh^{-1}, feed flowrate of 120 $cm^3\,h^{-1}$, feed concentration of 50g/100cm^3 (25g/100cm^3 glucose, 25g/100 cm^3 fructose) and a temperature of 20°C were the conditions used.

7.2.2.1 The effect of rotational speed on the exit position of glucose and fructose

Table 7.6 and Figure 7.8 show the effect on the position of the band as it exits the annulus from the feed entry position in degrees.

Figure 7.7 The effect of feed flowrate on resolution

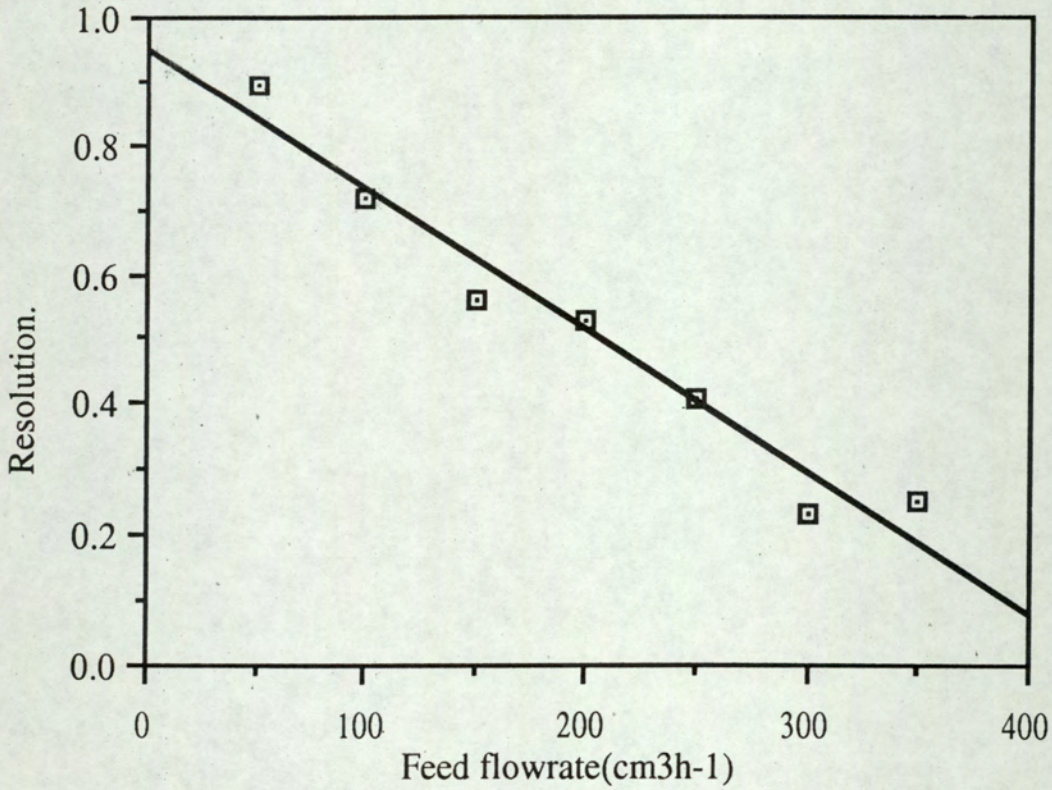

Figure 7.8 The effect of rotational speed on the exit posion of glucose and fructose

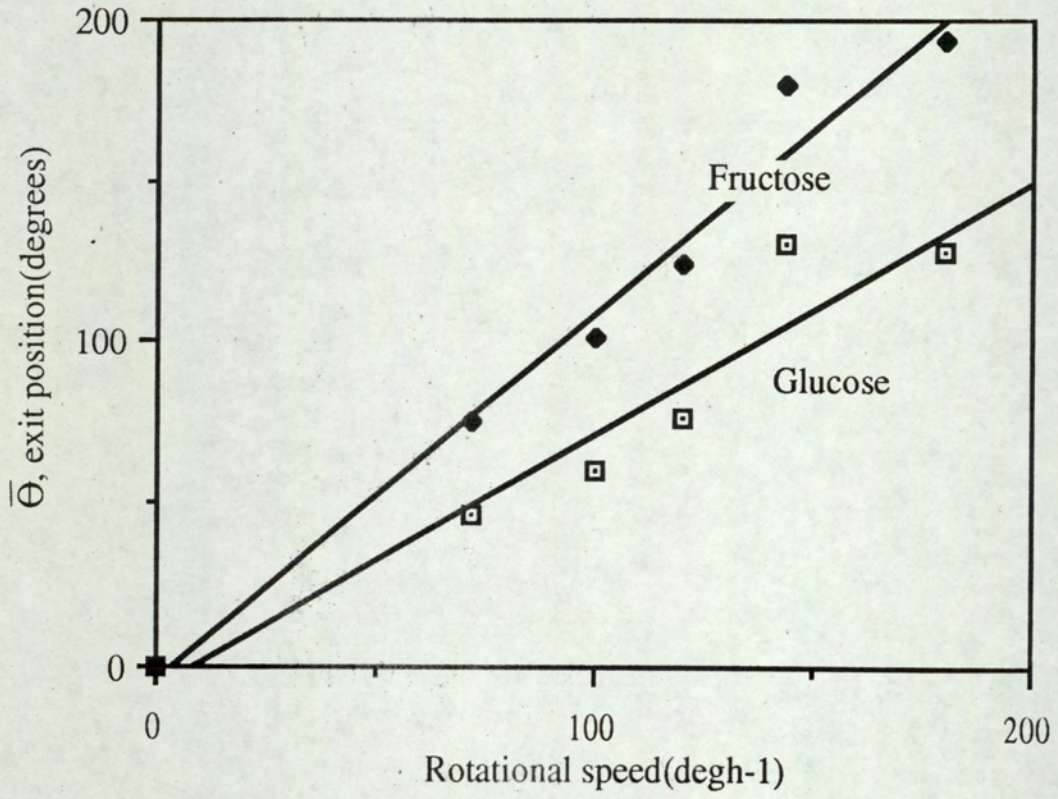

Table 7.6

Run	Rotational speed(deg h^{-1})	Exit band position (degrees) $\bar{\theta}_G$	$\bar{\theta}_F$
8/GF	72	46	76
9/GF	100	60	102
10/GF	120	77	125
11/GF	144	131	180
12/GF	180	128	194

The graph shows two straight lines which appear to pass through the origin. This is predictable from the theory since $\bar{\theta}$, is according to equation 2.29 directly proportional to the rotational speed, ω.

The slope of the glucose line is smaller than that of the fructose. This is again due to the greater retention of fructose within the resin. It is a reflection of the differences in distribution coefficient between the glucose and the fructose. The graph also tends to indicate that the distribution coefficient of each sugar is unaffected by rotational speed since for both glucose and fructose a linear line is obtained through the points. If the slope of each line is calculated then distribution coefficients of 0.41 for glucose and 0.82 for fructose can be obtained; these values are approximately the same as those obtained for the feed rate runs. It should be possible therefore using these distribution values to calculate an

approximate position for the glucose and the fructose bands under any experimental operating conditions at this temperature, using this resin and the feed concentration mentioned above.

7.2.2.2 The effect of rotational speed on bandspreading in the CCC

Table 7.7

Run	Rotational speed(deg h^{-1})	Exit bandwidth(degrees) W_G	W_F
8/GF	72	51	61
9/GF	100	57	68
10/GF	120	62	76
11/GF	144	75	96
12/GF	180	83	96

Table 7.7 and Figure 7.9 show the effect of rotational speed on the exit bandwidths. It is noted that the bandwidths increase as the speed is increased. The curves that have been drawn can only be regarded as approximate due to the limited number of points.

It does appear however that the increase in bandwidth with rotational speed is non-linear. If equations 2.28 and 7.1 are substituted into equation 2.34 then upon rearrangement, equation 7.2 can be obtained as follows:

$$W^2 = W_o^2 + 16\left[\frac{\omega}{v}\right]^2 HL\,[\varepsilon + (1 - \varepsilon)\,K]^2 \qquad \ldots\ldots 7.2$$

Figure 7.9 The effect of rotational speed on the exit bandwidth of glucose and fructose

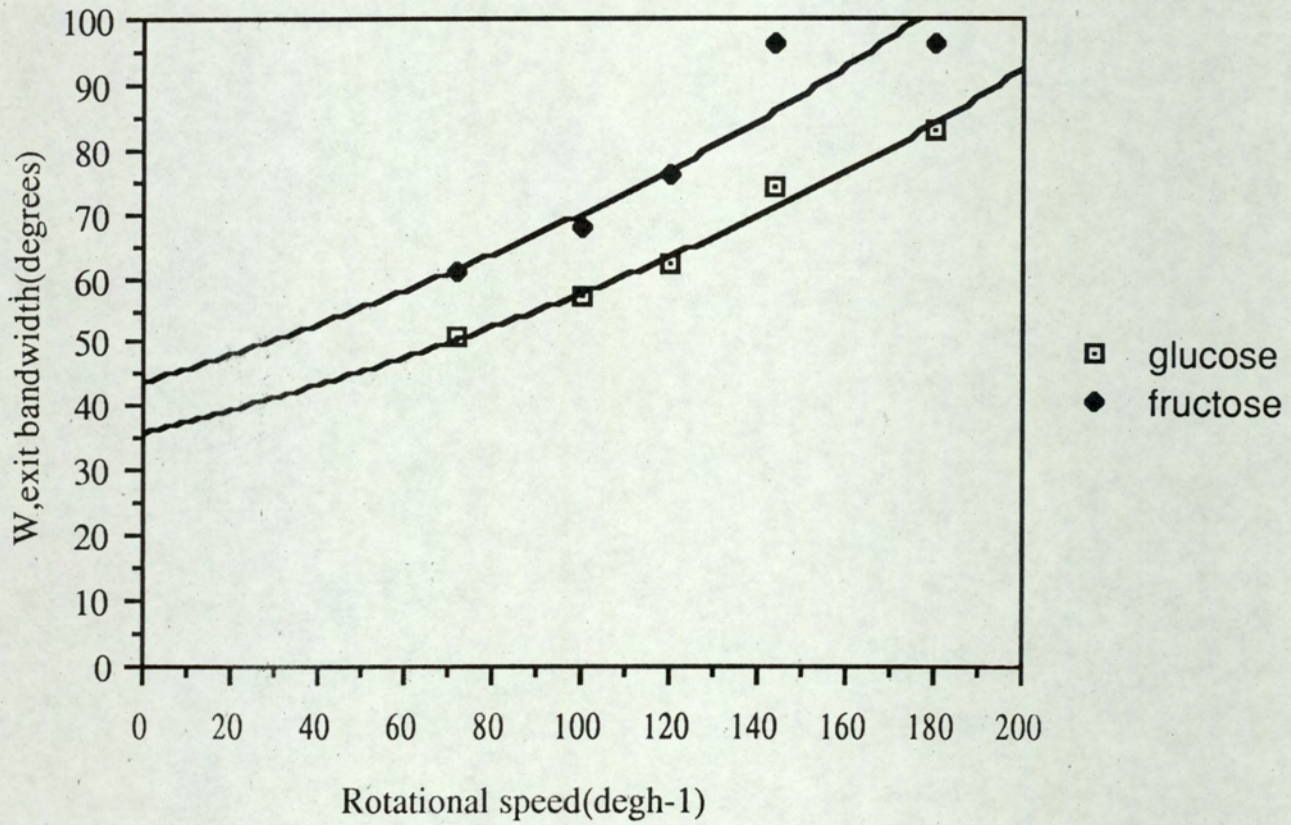

This equation allows the plate theory to be used to predict exit bandwidth; the exit bandwidth curve should intersect the ordinate at a value for the initial bandwidth at zero rotation rate. This is not the case however, as the calculated initial bandwidth for these runs should be 3.6 degrees. The curves would appear to intersect the ordinate at approximately 45° for glucose and 58° for fructose. This again shows that band spreading is much greater than is predicted by the plate theory.

7.2.2.3 The effect of rotational speed on the number of theoretical plates and the height equivalent to a theoretical plate using glucose and fructose

Table 7.8

Run	Rotational speed (deg h^{-1})	Average No of plates	Average H (cm)
8/GF	72	18	7.5
9/GF	100	21	6.4
10/GF	120	29	4.7
11/GF	144	51	2.6
12/GF	180	48	2.8

Table 7.8 and Figure 7.10 show the effect of rotational speed on the height equivalent to a theoretical plate. It can be seen that as the rotational speed is increased the number of theoretical plates increases and therefore the height equivalent to a theoretical plate decreases. The number of plates is directly related to the efficiency of the separation and therefore greater efficiency is accomplished at higher rotational rates. The number of plates appears to start levelling off at high rotation rates however.

Figure 7.10 The Effect of Rotational Speed on the Height Equivalent to a Theoretical Plate

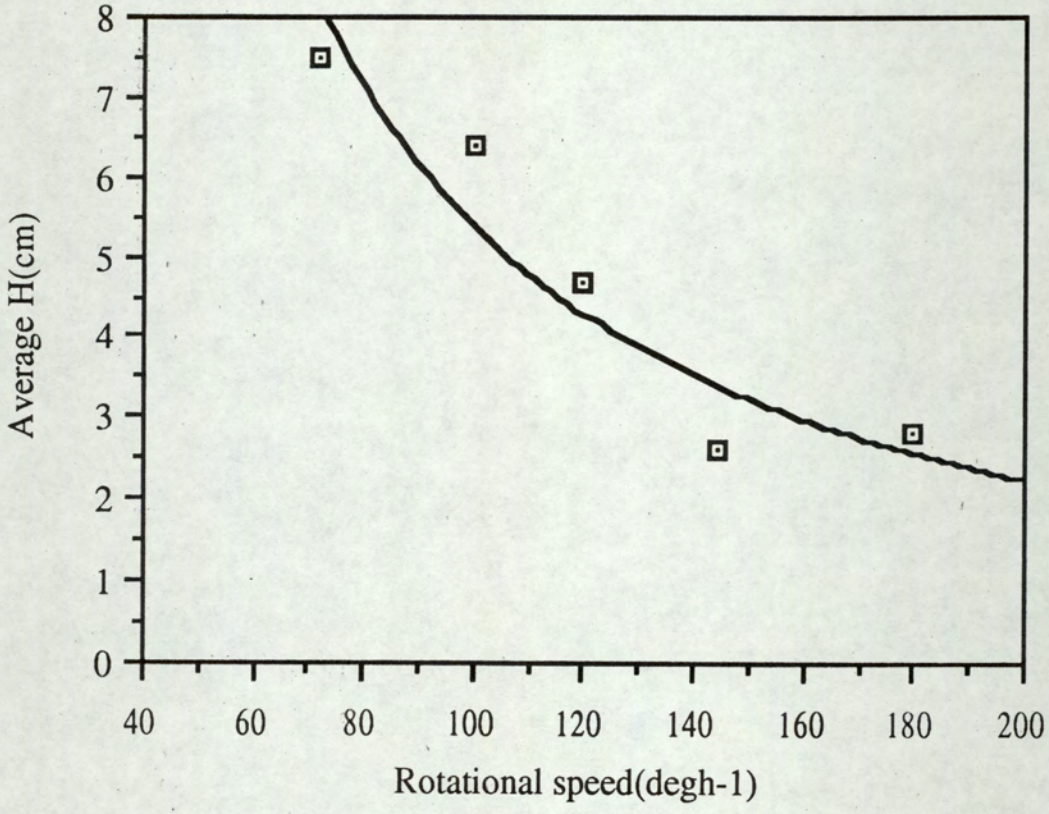

The increase in efficiency at higher rotation rates can be explained by the decrease in bed loading which occurs. Bed loading decreases from 1.66cm^3/deg at 72 $degh^{-1}$ rotational speed to 0.66 cm^3/deg at 180°h^{-1} rotational speed.

7.2.2.4 The effect of rotational speed on the resolution using glucose and fructose

Table 7.9

Run	Rotational speed/deg h^{-1}	Resolution
8/GF	72	0.53
9/GF	100	0.67
10/GF	120	0.69
11/GF	144	0.61
12/GF	180	0.74

Table 7.9 and Figure 7.11 show an increase in the resolution between the glucose and the fructose peaks as the rotational speed is increased with a levelling off of the resolution at higher rotation rates. This can be explained by considering the two parameters which affect the resolution; the peak band position, θ and the exit bandwidth, W (equation 2.32). As the rotational speed is increased, θ, the peak position increases proportionally; the exit bandwidths do not increase by the same amount. This is probably due to reduced bed loading, ie. less feed is introduced to each sector of the packing. Glucose and fructose have identical molecular sizes and hence resolution depends entirely on the retention of the

Figure 7.11 The effect of rotational speed on the resolution of glucose and fructose

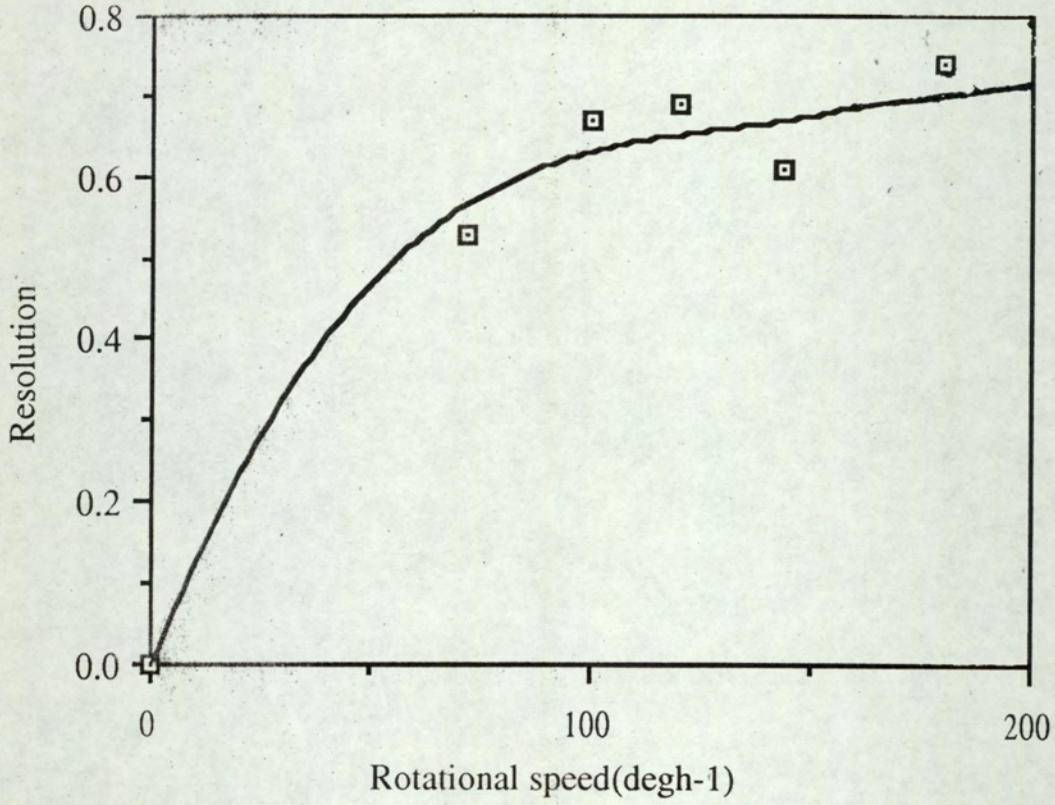

fructose. Fructose complexes with the Ca^{2+} ions present and the rate of formation of the complex must depend on the number of free Ca^{2+} ions on the resin. If there is a high fructose, concentration in the vicinity, which would be the case at low rotational speeds then the rate of fructose complex formation will not be as great as at low fructose concentrations.

7.2.2.5 The effect of rotational speed on the dilution of sugars leaving the annulus

The calculated initial feed bandwidth depends on the feed flowrate and the eluent flowrate:

$$W_0 = 360\ Q_f/(Q_f + Q_E) \qquad \text{..... 2.35}$$

In this case the calculated initial feed bandwidth is:

$$360 \times 120/(120 + 12000) = 3.56^\circ$$

Therefore the dilution factor, D_f is proportional to the exit bandwidth since Q_f and Q_E, the feed flowrate and the eluent flowrate are constant. Figure 7.12 shows that although resolution is improved as rotational speed is increased dilution also increases. It appears that doubling the rotational speed causes the bulk product concentration to be approximately halved. This is an important factor since diluted products

Figure 7.12 The effect of rotational speed on the dilution of glucose and fructose

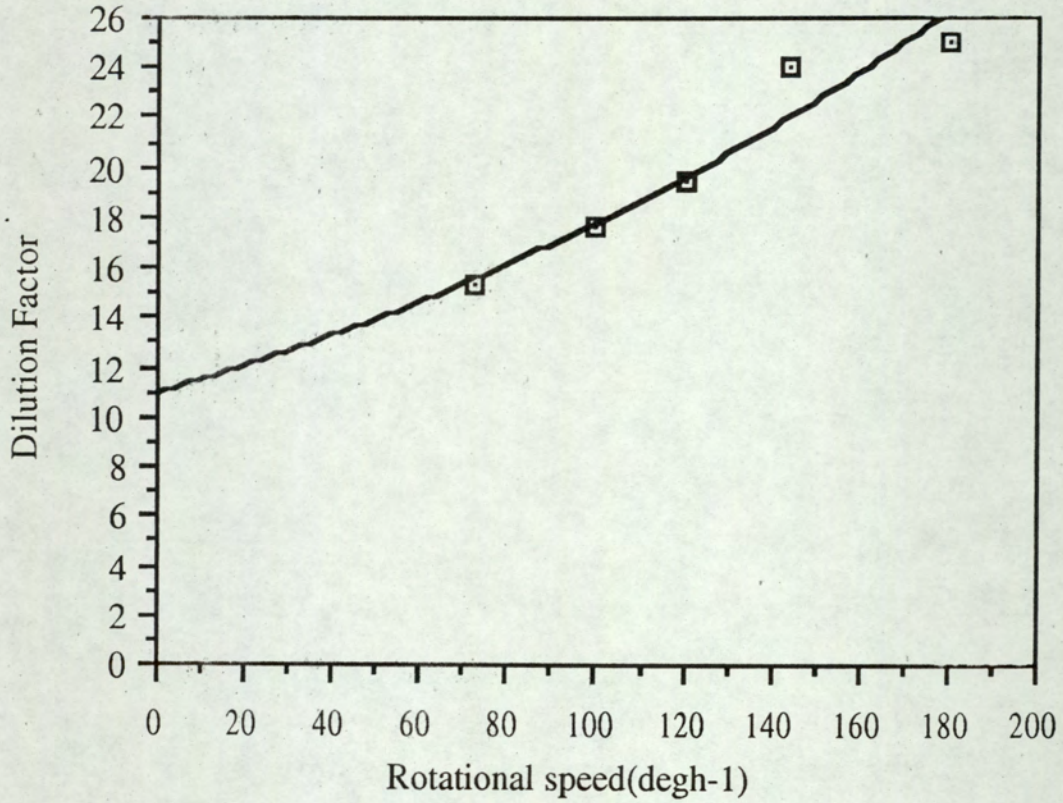

require greater energy costs to evaporate off the extra water. On the one hand increasing rotational speed causes improved resolution, however greater dilution occurs at high rotation rates.

7.2.3 The effect of eluent flowrate on the separation of glucose and fructose

Two experimental runs were used to show the effect of eluent flowrate on the separation. These were run 11/GF carried out with an eluent flowrate of 12 lh^{-1}, feed flowrate of 120cm^3h^{-1}, a rotational speed of 144 deg h^{-1} and a temperature of 20°C. Run 13/GF was carried out under identical conditions except for an eluent flowrate of 7.5 lh^{-1}.

Figures 7.13 and 7.14 show the chromatograms for these two runs.

Table 7.10

Run	Eluent flowrate/ $l\,h^{-1}$	$\bar{\theta}_G$	$\bar{\theta}_F$	W_G	W_F	R_S
11/GF	12	131	180	75	96	0.61
13/GF	7.5	232	288	72	79.2	0.71

Figure 7.13 Chromatogram experiment 11/GF

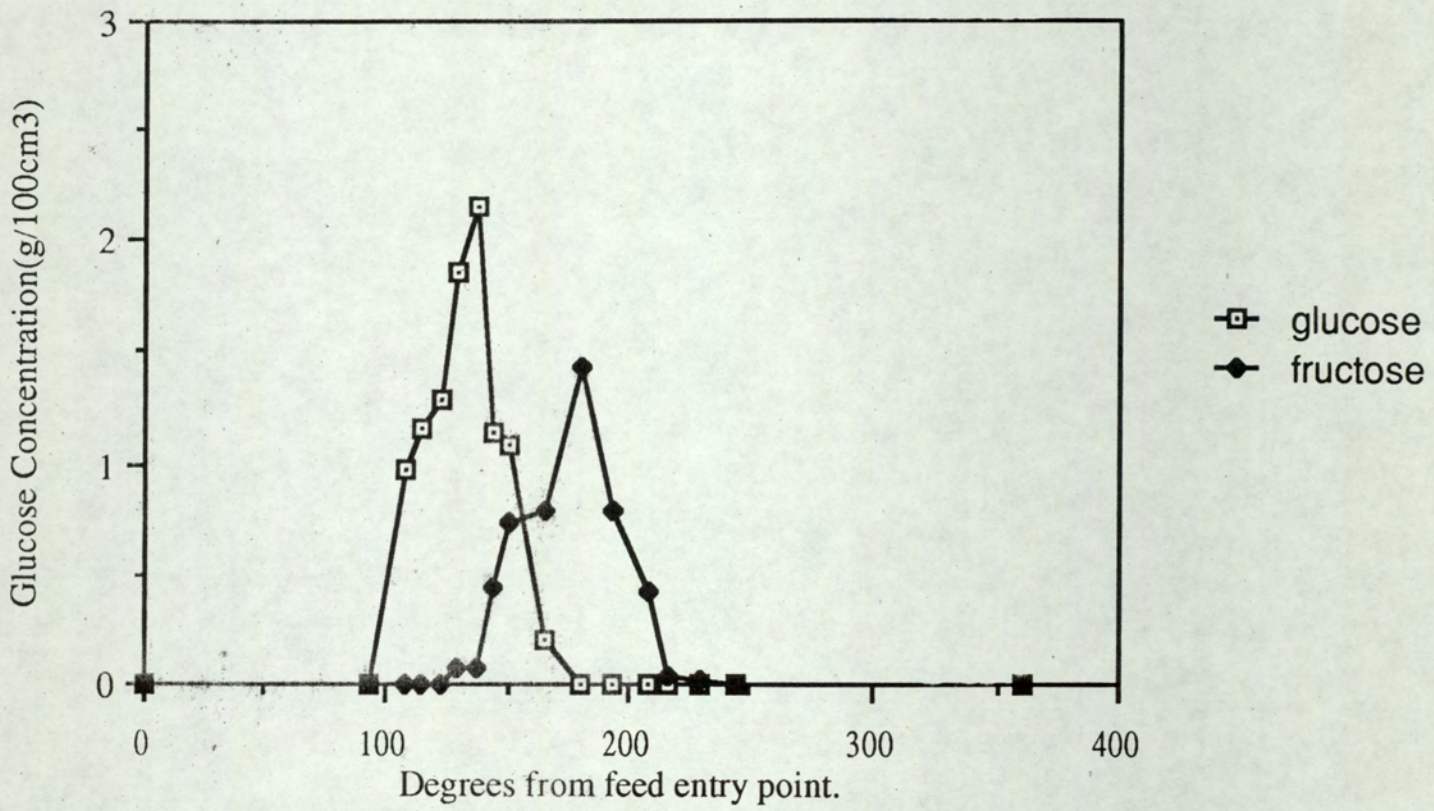

Figure 7.14 Chromatogram for experiment 13/GF

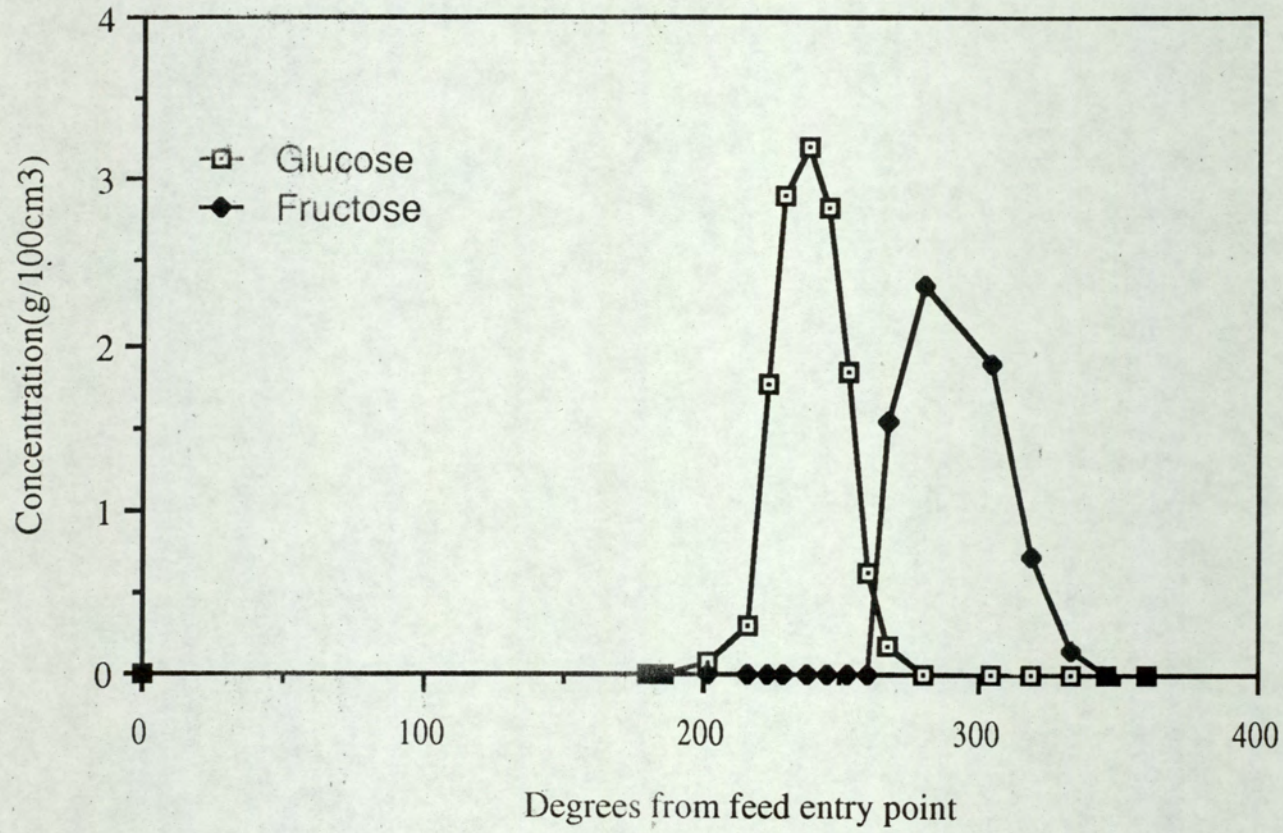

Table 7.10 shows the effect of reducing eluent flowrate from 12 lh^{-1} to 7.5 lh^{-1}. The first point to note is that the peak band positions are greater at lower eluent flowrates. This can be predicted by the theory, since a solute travelling down the column at a slower rate and rotated at the same speed will inevitably exit the annulus at a greater angle from the feed entry point. Exit bandwidths for the two runs show a decrease as the eluent flowrate is reduced, although only a small one. This decrease in exit bandwidth and the increase in resolution from 0.61 to 0.71 indicates that some efficiency is lost as the eluent flowrate is increased. This is predictable since if the sugars move through the packing at a slower rate, as controlled by the eluent flowrate then there is greater opportunity for interaction of the fructose with the ion-exchange resin. From the results obtained the dilution factor using an eluent flowrate of 7.5 lh^{-1} is 13.3 and using an eluent flowrate of 12 lh^{-1} it is 22.6.

7.2.4 A method of increasing the total throughput in the CCC using glucose and fructose

Using the plate theory it should be possible to increase the overall throughput by increasing the feed flowrate, the eluent flowrate and the rotational speed in proportion to each other. Two experimental runs were carried out, see Table 7.11. An eluent flowrate of 22.5 litres h^{-1} was almost the maximum achievable at the time without exceeding the safe pressure limit for the glass column. Run 15 G/F was carried out at three times the rotational speed, eluent flowrate and feed flowrate as run 14 G/F.

Figures 7.15 and 7.16 are the chromatograms for these runs.

Table 7.11

Run	Feed flowrate $cm^3\ h^{-1}$	Eluent flowrate $l\ h^{-1}$	Rotational speed $deg\ h^{-1}$
14 G/F	120	7.5	98
15 G/F	348	22.5	295

A feed flowrate of 348 cm^3h^{-1} was used as opposed to 360 cm^3h^{-1} since the output limit of the feed pump had been reached; however this represents a difference in relative feed flowrate of only 3% and the results can be examined qualitatively quite well.

Table 7.12 shows the effect of tripling the operating parameters on the exit band position, the exit bandwidth and the resolution. The results for the two runs are quite similar with a slight loss in resolution and a slight increase in dilution at the higher level.

Table 7.12 - Results for increasing Q_f, Q_E and W

Run	θ_G	θ_F	W_G	W_F	R_S	D_F (average)
	degrees		degrees			
14/GF	161	203	72	76	0.58	13.2
15/GF	145	195	79	116	0.50	17.8

The exit band positions are smaller at the higher level

Figure 7.15 Chromatogram for experiment 14/GF

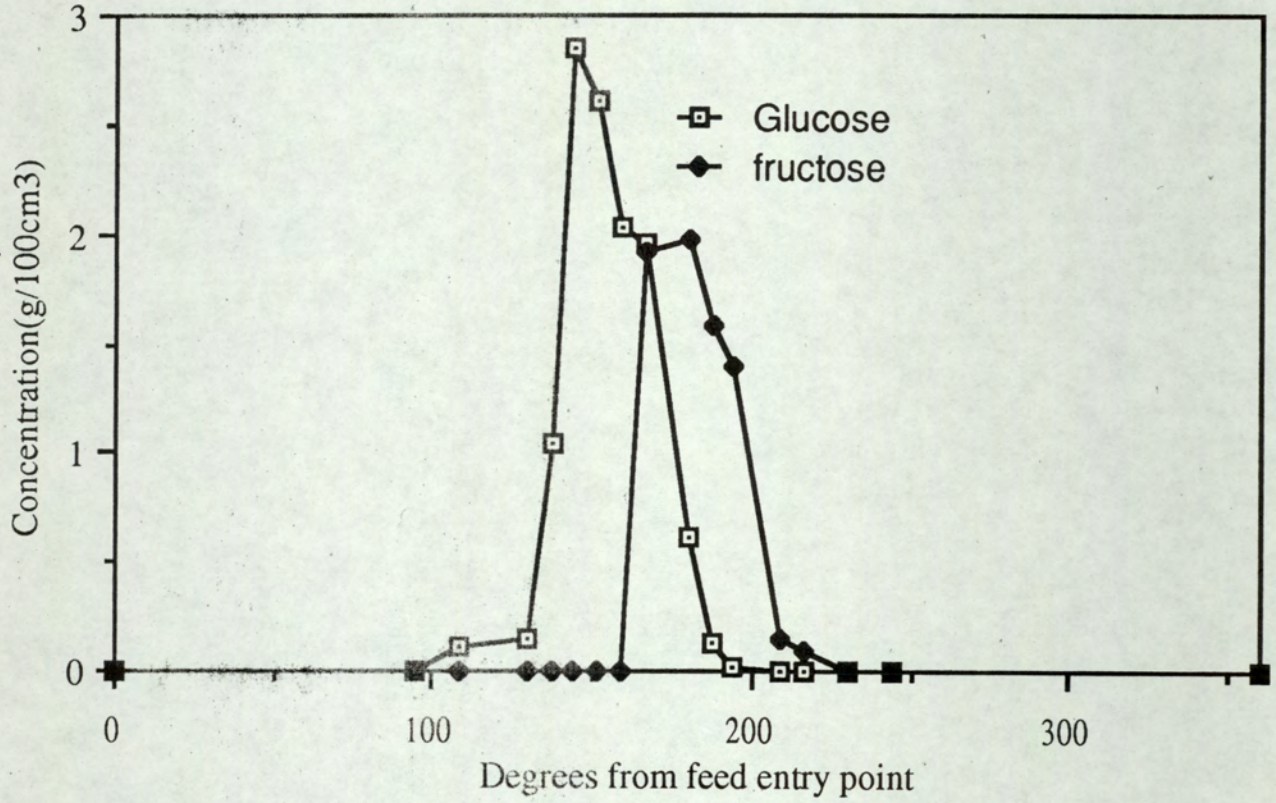

Figure 7.16 Chromatogram for experiment 15/GF

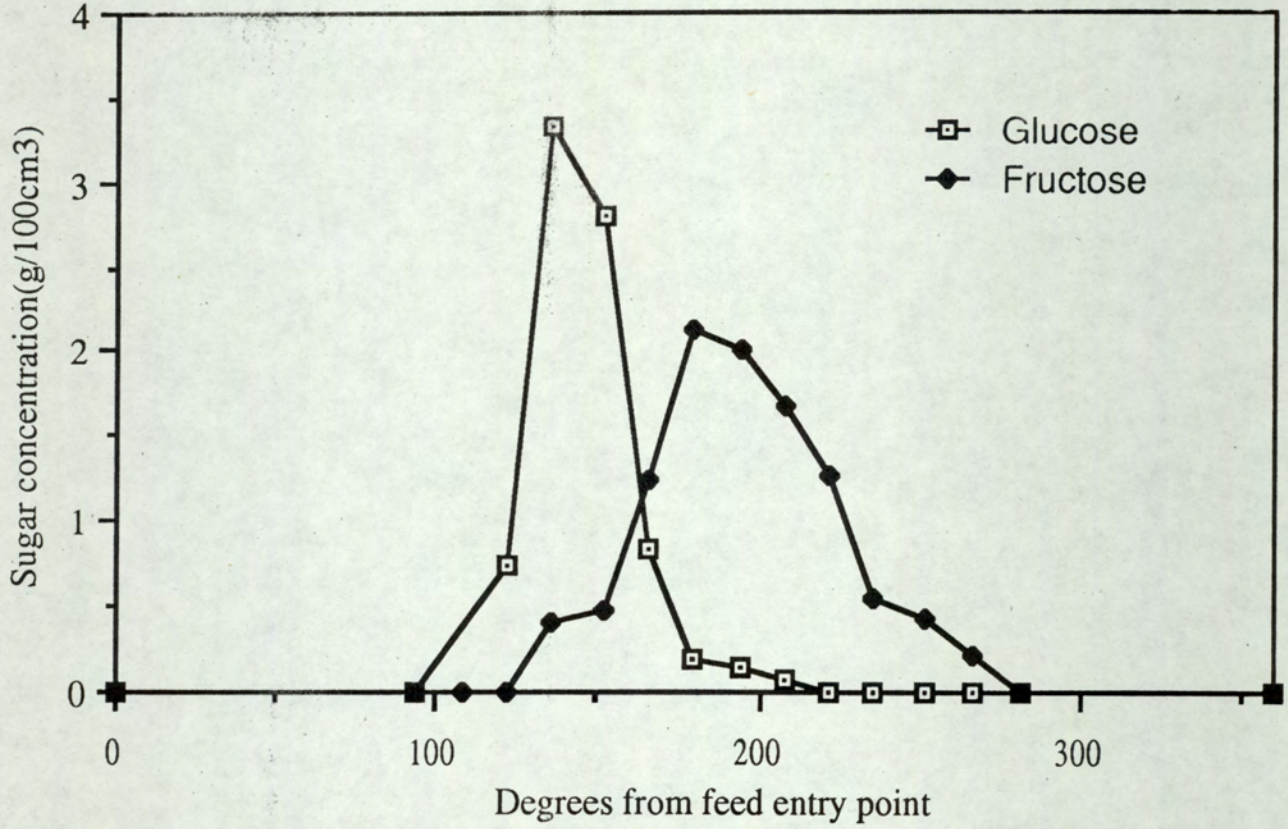

indicating less interaction with the resin, ie. less diffusion in or out of the pores. This is expected since the sugars are remaining in the column for shorter periods of time. Exit bandwidths are increased, in the case of fructose the increase is considerable, approximately 50%. This increase in the exit bandwidths and decrease in the exit band positions signifies a decrease in the number of theoretical places, N. Hence at high eluent flowrates the efficiency is reduced. It appears, however that large increases in throughput can be made using this method without a serious effect on the separation.

7.2.5 High Throughput Experimental Run

Experimental run 16/GF was carried out at a feed flowrate of 480 $cm^3\ h^{-1}$, eluent flowrate of 22.5 $l h^{-1}$ and a rotational speed of 295 deg h^{-1}. Feed flowrate has been increased by 132 $cm^3\ h^{-1}$ over run 15/GF by addition of an extra pumphead to the feed pump. Figure 7.17 shows the chromatogram for this run.

Table 7.13 - High throughput glucose-fructose separation

$\bar{\theta}_G$	$\bar{\theta}_F$	W_G	W_F	R_S	D_f
139	180	91	110	0.35	13.4

These results show a slight reduction in the peak band positions,

Figure 7.17 Chromatogram for experiment 16/GF

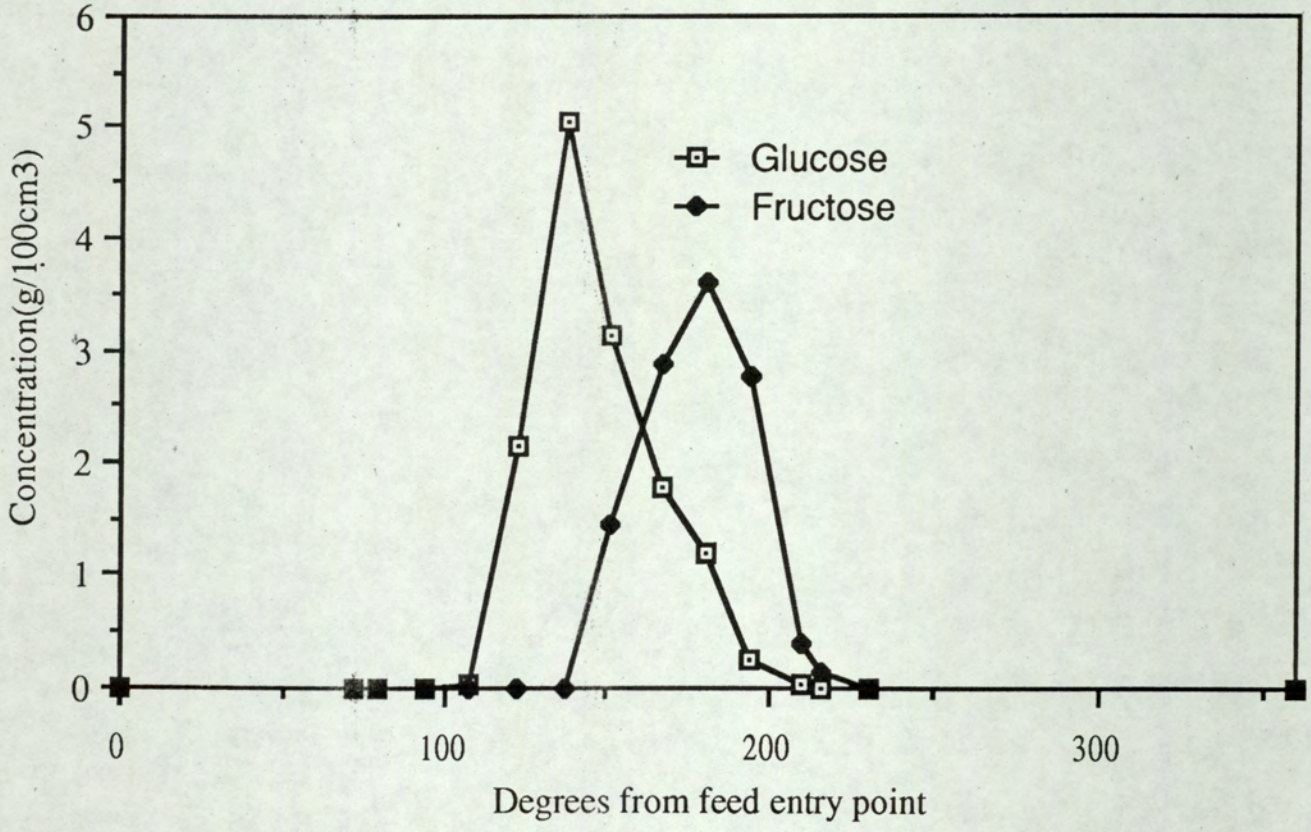

indicating a reduced distribution coefficient value, probably due to overloading of the resin. The exit bandwidths for glucose has increased, whereas that for fructose has been reduced by a few degrees. The decrease in the fructose bandwidth is unexpected and can only be explained by changes in the resin bed. Run 16/GF was carried out two days after the liquid level in the apparatus had dropped allowing air bubbles to enter the packing. Run 15/GF was carried out only one day after this took place. The air bubbles appeared to have gone completely after one day but some may have remained. Air bubbles in chromatographic packing can cause "channelling" to occur. This may be responsible for the small change which occurred in the exit bandwidths.

The total angle over which all the products exit the annulus can be calculated from the following equation:

$$\emptyset = W_G + W_F - (\tilde{\theta}_F - \bar{\theta}_G) \qquad \text{..... 7.3}$$

In the case of run 16/GF this angle is approximately 150°. It is therefore possible to increase throughput by using another feed entry point 180° from the first one without overlapping between the two groups of peaks. This is a useful method of increasing throughput since there is less dilution than if one feed point is used in conjunction with a greater rotational speed. To calculate actual yields and purities of products obtained, areas under the curves were determined. From this and the eluent flowrate the

mass of sugar leaving the annulus between any two points can be estimated. In the case of run 16/GF a yield of 47% of 100% pure glucose at a concentration of 0.03g cm^{-3} (3% w/v) and a yield of 43% of 95% pure fructose at a concentration of 0.024g cm^{3} (2.4% w/v) can be obtained. If the purity required is not so high then yields can be greatly increased. It is also feasible under the conditions utilised in run 16/GF to have three feed nozzles placed at 120° intervals. There would be some overlapping of the edge of the fructose band but this is useful since it removes the low concentration fructose. If the fraction between 94° and 137° is removed with its two equivalent fractions at the 120° intervals a yield of 84% glucose at a concentration of 0.048g cm^{-3} (4.8% w/v) and 90% purity can be obtained. This is equivalent to 302g h^{-1} 90% pure glucose in total. If the fraction between 158° and 210° and its equivalents is removed then a yield of 67% fructose at a concentration of 0.026g cm^{-3} (2.6% w/v) and 90% purity can be removed. This gives a total fructose throughput of 241g h^{-1}. This leaves the region between 137° and 158° which could be recycled. This fraction contains 25% of the total glucose and fructose used.

7.3 The Separation of Glucose, Fructose and Sucrose in the CCC Equipment

To show that the continuous circular chromatograph is capable of resolving multicomponent mixtures, a feed solution consisting of equal quantities of sucrose, glucose and fructose and total concentrations of 0.5g cm^{-3} was used. Seven runs were carried out in this series. Table 7.14

shows the operating conditions used during these experiments. All runs were carried out at a temperature of 20°C. Before commencing these runs the ion exchange resin was "regenerated" using a $100gl^{-1}$ solution of $Ca(No_3)$ solution as described in Chapter 4. The experiments were carried out to investigate the effect of increasing feed flowrate on this separation; runs 1/SGF and 2/SGF and runs 3/SGF and 4/SGF, the effect of eluent flowrate on the separation; runs 1/SGF and 3/SGF and runs 2/SGF and 4/SGF, the effect of increasing rotational speed; runs 1/SGF and 5/SGF and runs 4/SGF and 6/SGF. Experiment 7/SGF is a high throughput run in whch the feed flowrate, the rotational speed and the eluent flowrate used are a multiple of those used for run 1/SGF, ie. feed rate, rotational speed and eluent flowrate have been increased by 2.9 times.

Table 7.14 - Operating conditions for glucose, fructose and sucrose separations

Run	Feed flowrate ($cm^3 h^{-1}$)	Eluent flowrate ($l h^{-1}$)	Rotational speed ($deg h^{-1}$)
1/SGF	60	12	144
2/SGF	120	12	144
3/SGF	60	7.5	144
4/SGF	120	7.5	144
5/SGF	60	7.5	108
6/SGF	120	7.5	300
7/SGF	350	35	420

7.3.1 $\bar{\theta}$, The exit band position for sucrose, glucose and fructose separations

In all the experiments carried out in this series the three sugars exit the annulus in the same sequence. Sucrose always appears at smaller angles from the feed entry point, glucose appears at greater angles than sucrose and fructose exits at the largest angle from the feed point. Figure 7.18 shows a typical chromatogram for the separation of glucose, fructose and sucrose. This shows that the sucrose travels through the chromatographic packing at a faster rate than the glucose and the fructose. This effect is due to the size of the sucrose molecule. The molecular weight and molecular size of sucrose is approximately twice that of glucose and hence penetration of the resin pores by sucrose is less likely based on the size exclusion effect. Table 7.15 shows $\bar{\theta}$ values for sucrose, glucose and fructose for the seven experiments.

Table 7.15

Run	Q_F	Q_E	W	$\bar{\theta}_S$	$\bar{\theta}_G$	$\bar{\theta}_F$
1/SGF	60	12	144	75	126	190
2/SGF	120	12	144	65	110	181
3/SGF	60	7.5	144	100	171	255
4/SGF	120	7.5	144	146	196	252
5/SGF	60	7.5	108	92	141	212
6/SGF	120	7.5	300	280	358	499
7/SGF	350	35	420	74	112	179

Q_F = feed flowrate($cm^3\ h^{-1}$)

Figure 7.18 Chromatogram for experiment 2/SGF

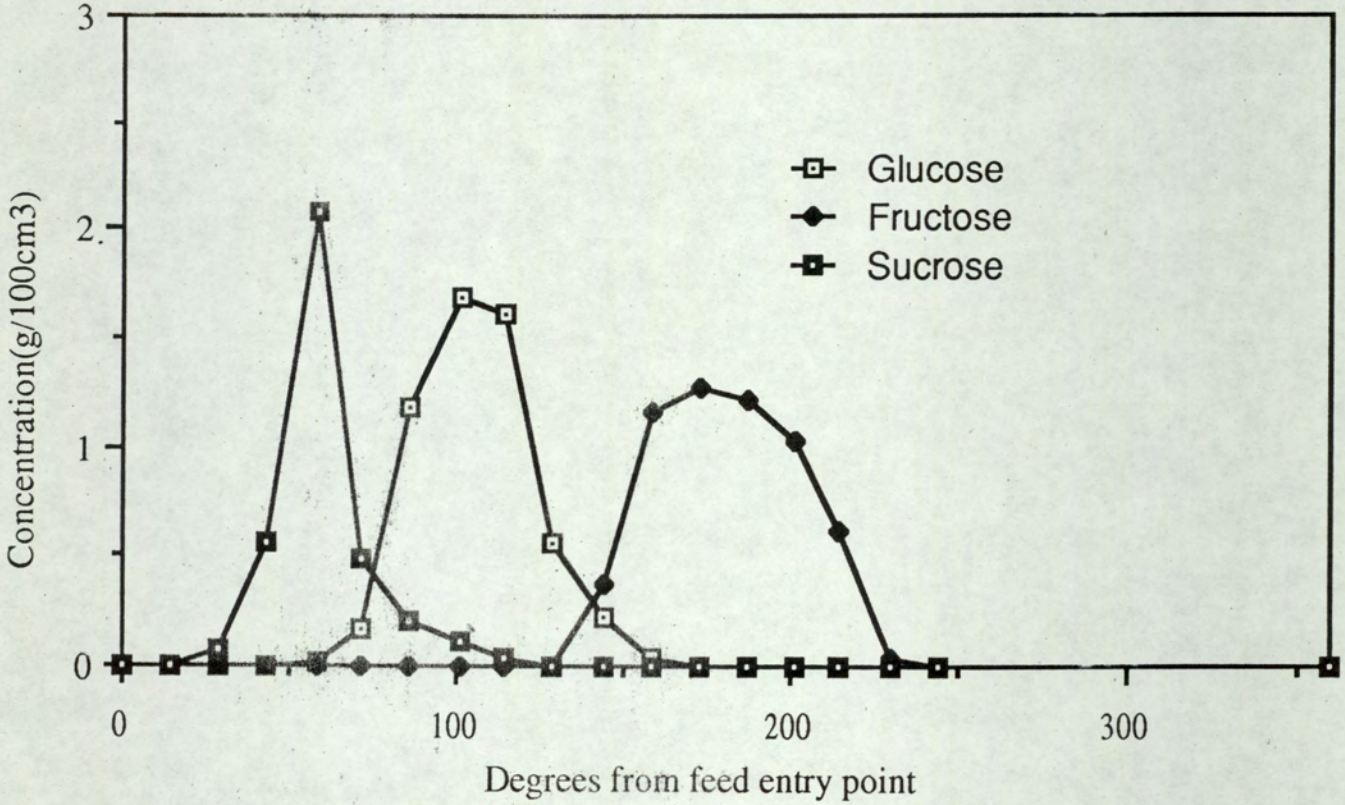

Q_E = eluent flowrate l h^{-1}

W = rotational speed deg h^{-1}

$\bar{\theta}_S$ = sucrose exit peak position/degrees

$\bar{\theta}_G$ = glucose exit peak position/degrees

$\bar{\theta}_F$ = fructose exit peak position/degrees

All values of these positions are calculated from estimated bandwidths. The peak maximum was taken at the midpoint of the bandwidths.

Table 7.15 provides four items of information and confirms the results obtained using the glucose/fructose feedstock runs. These are:

1 Sucrose exits the annulus at smaller angles to the feed entry point than glucose and fructose.

2 As the feed flowrate is increased keeping other factors constant there is no appreciable change in the peak exit position, $\bar{\theta}$.

3 As the eluent flowrate is increased keeping other factors constant then $\bar{\theta}$ decreases.

4 As the rotational speed is increased keeping other parameters

constant then $\bar{\theta}$ increases.

Using equation 2.30 for these runs an average for the K value, or distribution coefficient can be calculated for each solute. These averages are:

$K_{sucrose} = 0.13$

$K_{glucose} = 0.48$

$K_{fructose} = 0.92$

The values obtained for the glucose and fructose experiments were 0.46 and 0.71 respectively. The distribution coefficient for glucose has hardly changed, that for fructose has increased noticably indicating greater retention of the fructose. An explanation for this is that the fructose concentration in the feed during these runs was 16.6g/100cm^3, during the glucose and fructose experiments the fructose concentration was 25g/100cm^3. This reduction in concentration may have allowed greater interaction with the packing. $K_{sucrose}$ is much smaller than $K_{glucose}$ indicating the extent that this sugar enters the resin pores.

7.3.2 W, The exit bandwidth for sucrose, glucose and fructose separations

Table 7.16

Run	Q_F	Q_E	W	W_S	W_G	W_F
1/SGF	60	12	144	54	90	99
2/SGF	120	12	144	72	94	105
3/SGF	60	7.5	144	81	72	117
4/SGF	120	7.5	144	90	92	120
5/SGF	60	7.5	108	85	87	109
6/SGF	120	7.5	300	121	144	152
7/SGF	350	35	420	75	89	110

The first point to note from the results in Table 7.15 is that for each experiment the bandwidth for sucrose, W_S is always smaller than for glucose and fructose. This is due to the smaller retention time of sucrose within the packing and consequently, the less diffusion which can occur.

Secondly, as the feed rate is increased, there is an increase in the exit bandwidth as discussed for the glucose and fructose runs (runs 1/SGF to 4/SGF).

There appears to be some variation in the effect of eluent flowrate on the exit bandwidths. The overall tendency is for a small increase in bandwidth as the eluent velocity is reduced from 12 lh^{-1} to 7.5 lh^{-1}; this can be explained by the increase in the initial feed bandwidth, see equation 2.35. This contradicts the results from the glucose and fructose runs where a slight decrease was noted as the eluent flowrate was reduced. If the results for runs 1/SGF to 4/SGF are examined, the glucose

bands do actually reduce in size as the eluent rate is reduced; however for sucrose and fructose an increase of approximately 20% is noted.

Experiment 3/SGF and 5/SGF shows little change in exit bandwidth when rotational speed is decreased from 144 $degh^{-1}$ to 108 $degh^{-1}$. Experiment 4/SGF and 6/SGF show that as rotational speed is increased from 144 $degh^{-1}$ to 300 $degh^{-1}$ maintaining the other operating conditions constant then an increase in bandwidth is noted of approximately 50%. This effect was noticed with the glucose/fructose separations.

7.3.3 R_S. The resolution between peaks in the separation of glucose, fructose and sucrose

Here an average value for the resolution or degree of separation has been calculated from the resolution between sucrose and glucose, and the resolution between glucose and fructose.

Table 7.17 gives the following information.

1 Runs 1/SGF to 4/SGF show that as the feed flowrate is increased the average resolution is reduced.

2 Runs 1/SGF to 4/SGF also show that as the eluent flowrate is increased from 7.5 l h^{-1} to 12 l h^{-1} the resolution between the peaks decreases.

Table 7.7 - Resolution values for sucrose/glucose.fructose experiments

Run	Q_f	Q_E	W	Average R_S
1/SGF	60	12	144	0.71
2/SGF	120	12	144	0.54
3/SGF	60	7.5	144	0.93
4/SGF	120	7.5	144	0.56
5/SGF	60	7.5	108	0.57
6/SGF	120	7.5	300	0.60
7/SGF	350	35	420	0.46

3 The results show that as rotational speed increases then resolution increases.

4 The resolution for experiment 7/SGF is smaller than for experiment 2/SGF in which the operating conditions are approximately one third of those in 7/SGF, ie. bed loading is identical. This is probably an effect of the very high eluent rate, 35 l h^{-1}. The peak positions for this run are closer together and the bandwidths are greater. Experiment 7/SGF has the three bands exiting the annulus between 30° and 260° (Figure 7.19) however at the edge of the fructose band between 220° and 260° the amount of fructose is small. It should be possible in this case to use two feed entry points 180° apart and obtain reasonably pure products with a total throughput of 350g h^{-1}.

Figure 7.19 The Enzyme Inversion of Sucrose

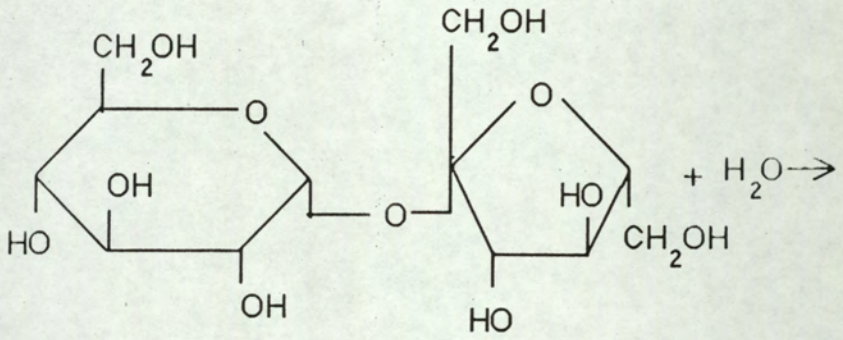

Glucose

+

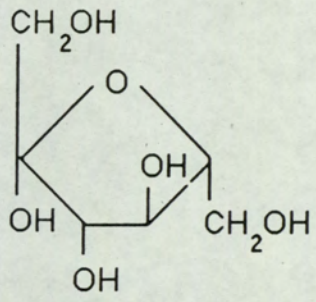

Fructose

Figure 7.19 Chromatogram for experiment 7/SGF

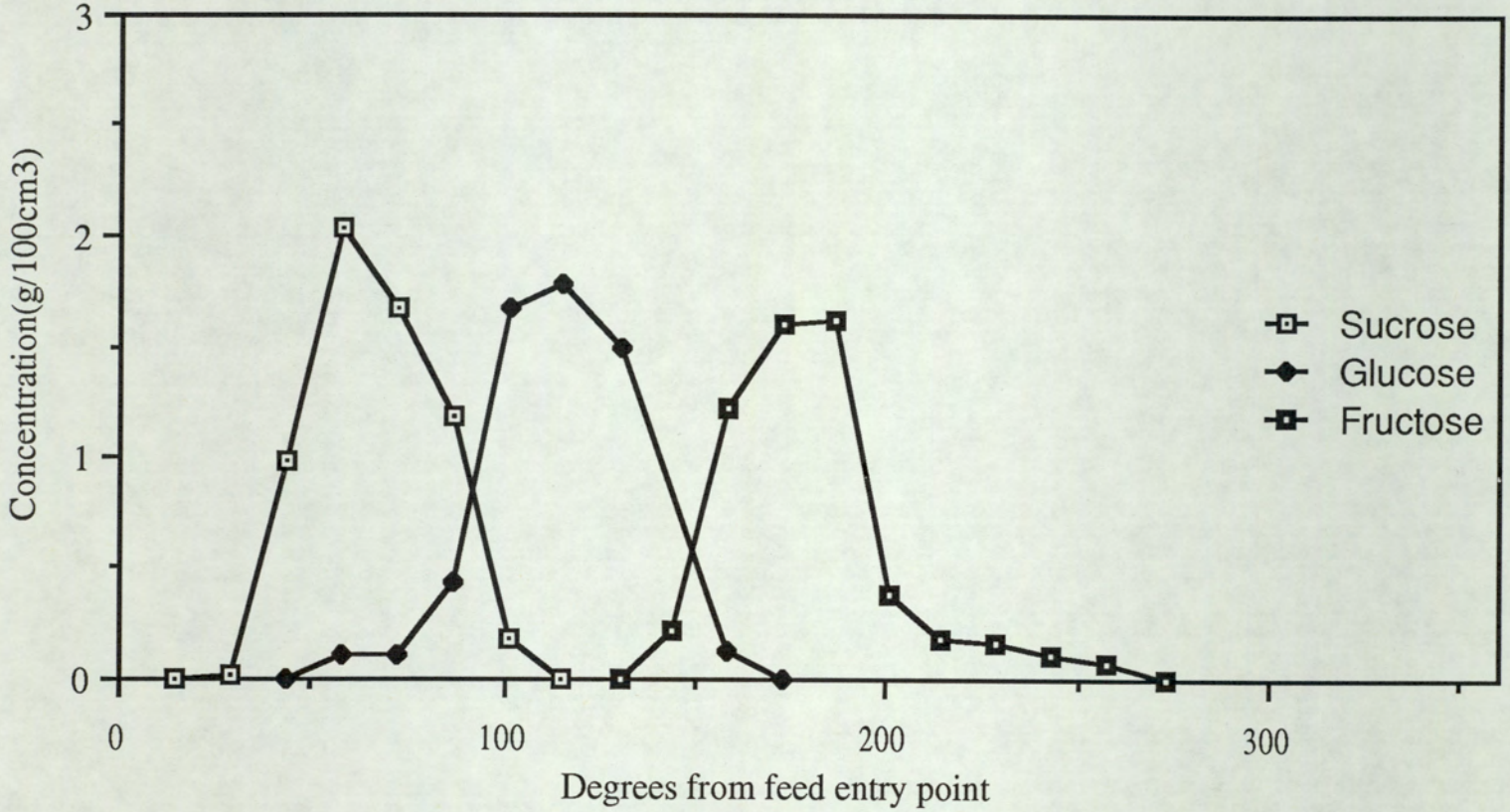

7.3.4 Experiment 8/SGF

Since one of the primary aims of this work was to attempt to remove sucrose from beet sugar molasses which has one component, ie. the sucrose in very high concentration compared to the other components, it was decided to carry out an experiment using a feedstock consisting of 80% w/w sucrose (dry), 10% w/w glucose (dry) and 10% w/w fructose (dry). Experimental conditions were as follows:

Feed flowrate	$60cm^3h^{-1}$
Eluent flowrate	$7.5\ l\ h^{-1}$
Rotational speed	$144\ deg\ h^{-1}$
Temperature	20°C
Feed concentration	$0.5g\ cm^{-3}$, 50% w/v (total)

The exit positions and bandwidths were as follows:

Run 8/SGF

$\bar{\theta}_S = 147^\circ$

$\bar{\theta}_G = 193^\circ$

$\bar{\theta}_F = 241^\circ$

$W_S = 66^\circ$

$W_G = 25^\circ$

$W_F = 51^\circ$

$R_{S(Average)} = 1.12$

Figure 7.20 shows the chromatogram for this run. The lower concentration of glucose and fructose in this feed mixture has caused a reduction in the bandwidths and total product concentration for these sugars. The product concentration for sucrose is greater, however and the resolution between the peaks is good, almost a complete separation of the three bands has been achieved.

7.4 The separation of glucose, fructose and non-sugars in inverted beet sugar molasses

The inverted molasses solutions used for these experiments were supplied by British Sugar Research Laboratories. Inverted molasses was obtained by treating molasses with a solution of yeast invertase or B.fructosidase on enzyme which converts sucrose into the glucose-fructose mixture, commonly known as invert sugar. This reaction is shown as in Figure 7.21 was carried out at 35°C and a pH of 4-5.

Figure 7.20 Chromatogram for experiment 8/SGF

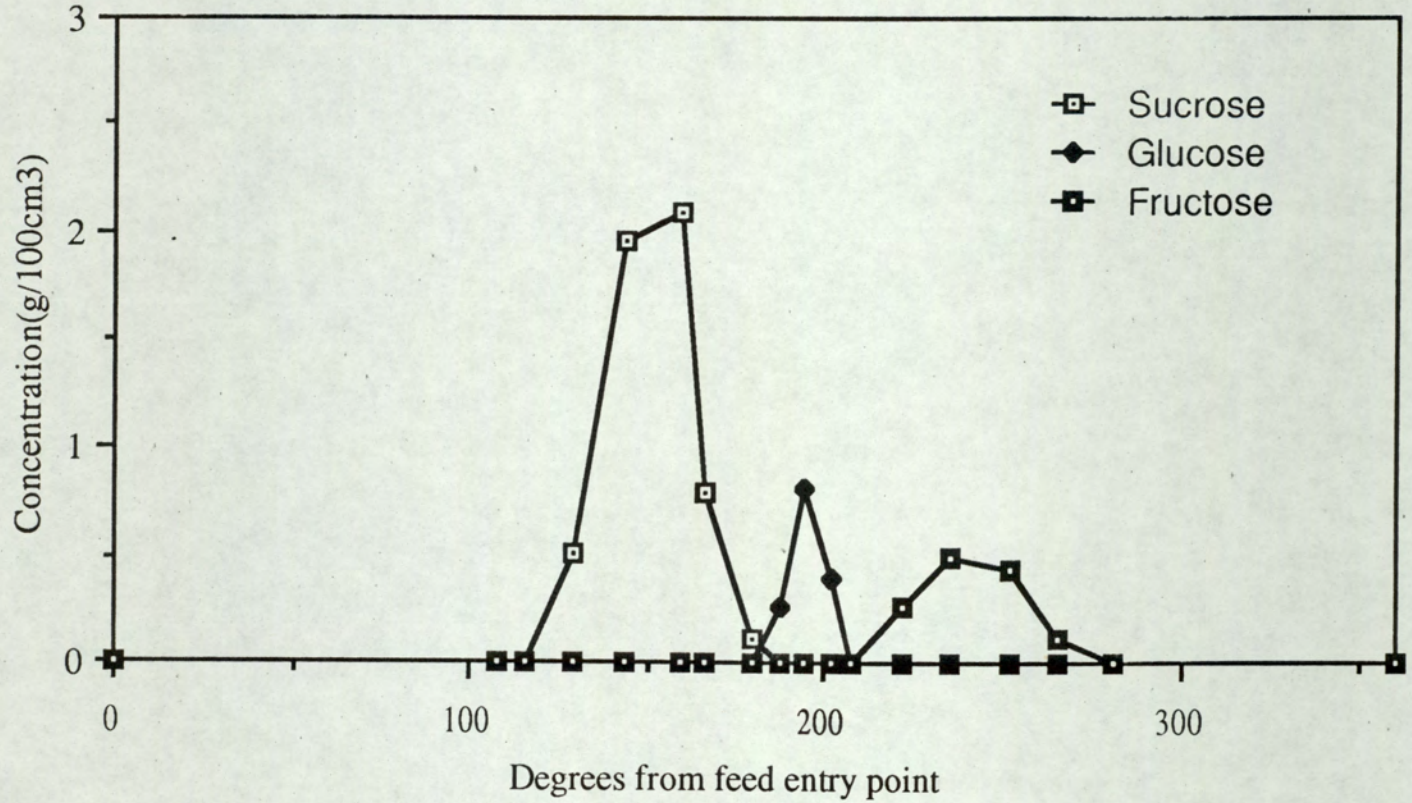

The purpose of the few experiments carried out using this feedstock was to show the capability of the annular chromatograph for the separation of non-synthetic feedstocks and compare the results with runs using the synthetic glucose and fructose feed.

Using synthetic sugar solutions the problems of bacterial and fungal growth within the annulus and ancillary equipment is not great. After each experiment care was taken to flush the feed container and feed entry pipe thoroughly with deionised water. The eluent pump was then used to pump deionised water through the chromatograph for several hours to ensure removal of all sugar from the packing and outlet pipes. Upon using the inverted molasses solution however, the problems of microbial growth escalated dramatically. This is because molasses contain many nutrients, minerals and vitamins as well as the sugar which provide many micro-organisms with an almost perfect growing medium. If molasses is kept in concentrated form (approximately 75% w/w total solids), then the high omotic pressure of this solution prevents bacteria and fungus from surviving. As soon as the solution is diluted, however, air-born spores etc enter these solutions and begin to multiply. In the case of the CCC this created two problems, the first problem being the formation of small black dots approximately 1-2mm diameter appearing on the resin, a sure indication of the growth of micro-organisms. The effect of this is that inevitably some of the sugar in the solutions entering the packing will be metabolised by these species altering the overall composition of the

inverted molasses. The second problem created was that the tubes leading into the collection tank were becoming heavily blocked with black mould growths. In order to give good drainage these tubes were made from fairly large diameter (10mm) PVC tubing since there are 50 of these tubes on the apparatus then the products leaving the annulus can take several minutes to pass through the tubes aggravating the problem.

A solution of sodium azide ($2.0 \times 10^{-4} g\ cm^{-3}$) was prepared in the eluent tank and the feed container after each run. This was pumped through for approximately four hours. Sodium azide is commonly used as a sterilising agent and is highly poisonous. Using high concentrations of sodium azide could have caused some replacement of the calcium ions on the resin by sodium ions. This did appear to arrest the contamination and as a precaution the exit pipes were replaced with new ones.

Attempts to run the CCC using 50% w/v, ($0.5 g cm^{-3}$) sugar concentration in the molasses as a feedstock were found to be impossible under the conditions and temperatures used. The viscosity of this feed solution is very high and upon entering the glass beads on the surface of the resin the molasses tended to accumulate near the top of the annulus and then move very slowly through the resin in a very broad band to begin with at a shallow angle to the surface. Some 20-30cm below the upper surface the gradient of the band changed to a steeper one as dilution reduced the viscosity of the solution. At 40% w/v glucose and fructose in the molasses the situation improved but was still unsatisfactory, the same

problems occurring as with the 50% w/v solution but to a lesser extent. At a feed sugar concentration of 30% w/v the feed solution did not accumulate at the top of the annulus, and the bands produced seemed to have no gradient change. At 30% w/v therefore the molasses appeared to have a uniform velocity through the ion exchange resin. To save great complication on attempting to model the molasses experiments and because at high concentration there appeared to be very little resolution, indicating using the on-line monitoring techniques, it was decided to abandon attempts to use anything greater than 30% w/v sugars in the feed solution. Five experimental runs were caried out using inverted molasses as feed; these are shown in Table 7.18.

Table 7.18 - Inverted molasses experiments

Run	Feed conc ($\times 10^2 g cm^{-3}$)	Feed flow-rate ($cm^3 h^{-1}$)	Eluent flowrate ($l h^{-1}$)	Rotational speed ($deg\ h^{-1}$)	Temp (°C)
1-IM	30	120	12	144	20
2-IM	30	120	12	144	20
3-IM	30	120	75	144	40
4-IM	30	120	75	144	40

Experiments 1/IM and 3/IM were caried out first. After these two runs the pressure within the apparatus exceeded 940 kPa (14 psi) at an eluent flowrate of 12 l h^{-1}. This was thought to be due partly to the

microbial growth discussed previously and partly due to the packing becoming more compressed with continued use. Attempting to backwash the resin would be very difficult because of the number of outlets from the chromatograph. A solution to this problem was found involving firstly removing the glass beads from the upper surface of the resin by syponing them out as a slurry. A length of flexible polypropylene tubing, 4mm diameter carrying compressed air was then introduced into the packing in order to agitate and bring any fires or debris to the surface. The resin was kept covered by water during this operation and from time to time this water was syphoned off and replaced with fresh deionised water. During this procedure it was noticed that certain regions of the packing had become excessively compacted and proved very difficult to break down with the compressed air. Other regions of the packing appeared to be quite mobile, however. After agitation the two experiments 2/IM and 4/IM were carried out to compare results before and after the treatment. Analysis for these runs was confined to HPLC analysis on the glucose and fructose present. Results are shown in Table 7.19.

Table 7.19 - Results for inverted molasses runs

Run	$\bar{\theta}_G$	$\bar{\theta}_F$	W_G	W_F	R_S
1/IM	151	188	72	92	0.37
2/IM	160	209	95	145	0.38
3/IM	234	268	77	79	0.36
4/IM	228	259	84	79	0.38

If run 1/IM is compared to run 11/GF (see Table 7.10) which was carried out under the same eluent flowrate, feed flowrate and rotational speed using synthetic feed. Exit bandwidths are similar. Exit positions for glucose and fructose in the molasses runs are further from the feed entry point, this indicates that the distribution coefficients have increased; this may be due to the lower sugar concentration in the molasses solution, ie. $300gl^{-1}$ as opoosed to $500gl^{-1}$. Barker and Thawait (62) have shown that distribution coefficients of glucose and fructose increase as the sugar concentration increases. Resolution between the glucose and the fructose is smaller using the inverted molasses since the band positions are also fewer degrees apart. Using a synthetic 30% w/v feed concentration an increase in resolution would be expected. However using molasses there are many other compounds present which may interfere with the separation. The presence of fairly high concentrations of sodium and potassium ions, both cations cause displacement of the calcium on the resin in the region of separation. A calcium charged resin is essential for the separation of gluocse and fructose hence any exchange of calcium is bound to reduce resolution. After the resin had been "cleaned up" using the compressed air there was found to be little change in θ values for glucose and fructose and an increase in the bandwidths for glucose and fructose. The increase in exit bandwidth was probably due to some air remaining in the packing after agitation causing a little "channelling" to occur. This may be one disadvantage of using compressed air, however in both cases the

resolution had been improved.

The effect of reducing eluent flowrate can be noted when comparing experiment 1/IM and 3/IM, 2/IM and 4/IM. Firstly the exit band positions are greater at 7.5 l h^{-1} eluent flowrate than at 12 l h^{-1} as predicted by the plate theory. The exit bandwidths for glucose and fructose decrease or increase very slightly with reduced eluent flowrate. Since the initial bandwidth is increased at smaller eluent flowrates from equation 2.35 then also there is less dilution without loss of resolution.

Experiment 5-IM was carried out at a feed flowrate of 120 cm^3 h^{-1} eluent flowrate of 12 l h^{-1} and rotational speed of 144° h^{-1} using the same feed concentration as for experiments 1-SM to 4-SM. The resin had been regenerated prior to this using a solution of calcium nitrate ($100gl^{-1}$) as described in Chapter 6.

The bandwidth for the conductivity peak is very difficult to estimate due to the long tail-off of the band. The results here show the advantage of regenerating; the resolution is almost doubled, the fructose is much more highly retained within the pores of the resin having a greater θ value by approximately 60° whilst the glucose remains at approximately the same point. Exit bandwidths are slightly greater than those for run 2/IM as expected.

Figure 5.5 shows a chromatogram from experiment 5-IM and Table 7.20 shows the detailed analysis carried out by British Sugar on experiment 5-IM. Figure 5.5 shows the conductivity peak which indicates

the position that the ionic components leaving the annulus. This was obtained using the in-line monitoring technique using a conductivity cell and meter as described in Chapter 5. The chromatogram shows that the bulk of the ionic fraction in the inverted molasses exits the annulus at a smaller $\bar{\theta}$ value than the glucose and the fructose indicating little retention within the resin; traces of conductivity run through the glucose and the fructose bands, the concentration of ions decreasing the further away from the feed entry point it is.

The major part of the ionic fraction exits at the beginning of the glucose peak because the charge on the ion exchange resin repels the ions keeping them in solution and preventing them from entering the pores, this is an ion exclusion effect. The long tail-off of this band shows that there is some ion exchange or interaction with the resin.

Also indicated on the chromatogram is the position of betaine. Betaine or trimethylglycine is a low molecular weight nitrogen compound. It is approximately 5% of the dry substance in molasses. Betaine exits the annulus at a large angle from the feed entry point, in this case it is approximately 360°. The small size of the betaine molecule is probably reponsible for its high retention within the packing.

7.5 The separation of sucrose from the non-sugars in beet molasses

7.5.1 Introduction

Molasses is a complex mixture of carbohydrates, amino acids, salts, organic acids etc. Sucrose comprises approximately 60-65% of the dry weight. This sucrose cannot be crystallised due to the high mineral content which keeps the sucrose in solution. Chromatography offers a good method of purifying the sucrose allowing crystallisation to become possible.

In 1963 Stark (70) described the use of ion exclusion for the separation of molasses. Molasses solutions of 40° Brix* were applied to columns of 50-100 mesh Dowex 50W resin in the K^+ form at 25°C and 90°C. At 25°C separation of sucrose from reducing sugars was obtained, but not from ionic impurities. At 90°C large proportions of the chloride ash, colour and nitrogen compounds appeared in the effluent before the sucrose, whereas reducing sugars and some other nitrogen compounds appeared later. Stark investigated the influences of temperature, degree of cross-linking, flow rates and recycling. Sugino and Takahishi (71) and Takahashi and Takikawa (72) described the purification and decolourisation of beet molasses by ion exclusion and showed that the separation was improved at smaller feed volume, lower feed concentration and higher temperature. An apparent purity of 90 and a sucrose recovery of 90% were obtained under optimum conditions. Recycling was found to improve the separation and increase the sucrose concentration.

* Brix is defined as the percentage sugar by weight.

Schneider and Mekule (73) in various patents discussed the removal of solids from the molasses and dilution to 40-60° Bx and if necessary the removal of alkaline earth metals prior to separation. After this pretreatment the molasses was passed at 86°C through a sulphonated cationic resin in the Na^+ form, cross-linked with 4-5% divinylbenzene. Elution was carried out with hot water and the eluent divided into several fractions of purity 84-91. The lowest purity fractions from the effluent were concentrated from 10% w/w to 70% w/w and used to regenerate the resin, which had become progressively loaded with Ca^{2+} and Mg^{2+} ions.

Munir et al (74,75,76) devised a process whereby cane or beet molasses at 40-60° Bx and 50-99°C was passed at a rate of 2-6cm min^{-1} over a cationic resin in the Ca^{2+} form. For molasses at a purity of 60-70 it was found that the amount of molasses treated corresponds to 17-19g sugar/l resin; for purities of less than 60 it corresponds to 10-14g non-sugars/l resin. Use of this process enabled a recovery of 96% sugar from molasses at a purity of 91 and its dry substance content was 9.5-10.5%. After evaporation and crysztallization 8.5% of molasses sugar was recovered in crystalline form. Frequent regeneration of the resin with calcium chloride solution was required to replace any calcium ions displaced due to the high sodium and potassium content in molasses.

Hongisto et al (77,78,79,80,81) working for the Finnish Sugar Company have described in a number of papers, a commercial scale

process for the desugarisation of beet molasses and cane molasses by ion-exchange chromatography. Owing to the differences in composition between the beet molasses and the cane molasses, the latter required additional pre-treatment involving the precipitation of Ca^{2+} together with some of the turbidity by adding phosphoric acid and removing the precipitate in a decanter centrifuge; residual Ca^{2+} ions were removed by ion exchange.

Sayana, Okawa et al (82,83) in Japan have carried out much work in the field of the chromatographic separation of molasses constituents. The recovery of sucrose, betaine, inositol, nucleic acids and related substances, raffinose and adenosine have all been accomplished using various operating conditions.

Sucrose recovery was carried out using Dowex 50WX4, resin in the Na+ form, 50-100µm. A feed concentration of 30° Brix was used. Approximately 2 tonnes of sugar per m^3 of resin could be treated per day to give sucrose solutions of 87.5% purity.

The desugarisation of molasses using ion exclusion chromatography has been carried out by several workers in Czechoslovakia (84), Italy (85) and Poland (86).

7.5.2 Experimental

A study of the effects of feed flowrate and the effect of rotational speed has been carried out using molasses. The molasses which was

used had been supplied by British Sugar in its undiluted, untreated form; approximately 75° Bx. Prior to each experimental run the molasses was analysed using HPLC and diluted such that the sucrose concentration was 0.30g cm^{-3} (30% w/v). This solution was used as feed and discarded at the end of each run. Analysis was carried out using HPLC, conductivity measurements and refractive dry substance (RDS) measurements on individual product samples. This allowed chromatograms to be produced which showed the position of the sucrose, the ionic fraction, the position of the betaine peak and an approximate value of the total solids in each sample from the RDS measurement. At low concentrations RDS measurements are not very accurate especially since the dry substance content is calculated using the refractive index of sucrose solutions which may vary from that of other components present in the product creating errors. A good estimate of the degree of separation can be obtained from the resolution between the sucrose peak and the conductivity peak.

$$R_S = \frac{\bar{\theta}_S - \bar{\theta}_C}{1/2\,(W_S + W_C)}$$

where

$\bar{\theta}_S$ = sucrose peak band position in degrees

$\bar{\theta}_C$ = conductivity peak band position in degrees

W_S = sucrose exit bandwidth in degrees

W_C = conductivity peak exit bandwidths in degrees

After removal of the Purolite PCR 833 ion exchange resin and repacking with Duolite C211/2558 sodium form resin a solution of sodium chloride (1.7M) was allowed to pass through the packing at a flowrate of $6lh^{-1}$ for 10 hours. This regeneration was necessary to ensure that the resin was completely in its sodium form. During this procedure a decrease in the height of the packing of approximately 10cm was noted. Deionised water was then allowed to pass through the resin. This led to expansion of the packing back to its original height. This drop in the packing height was due to the high salt concentration creating an osmotic effect which caused water to leave the resin particles, shrinking the particles to a smaller size. The shrinkage in the presence of high salt concentrations is greater using this resin because the cross-linkage is only 5.5% compared to 8% with the PCR 833 resin. The greater the cross linkage the greater the mechanical strength of the resin and hence the greater the resistance to shrinkage.

7.5.3 The effect of feed flowrate on the separation of sucrose in beet molasses

Five experimental runs have been carried out to test the effect of feed flowrate on the separation of sucrose molasses. Table 7.21 shows the conditions used during these experiments.

Table 7.21

Run	Feed flowrate (cm^3h^{-1})	Eluent flowrate ($l h^{-1}$)	Rotational speed ($deg h^{-1}$)	Temperature °C
1-SM	40	6	96	20°C
2-SM	60	6	96	20°C
3-SM	70	6	96	20°C
4-SM	80	6	96	20°C
5-SM	100	6	96	20°C

7.5.3.1 The effect of feed flowrate on the exit band position for sucrose, betaine and the ionic fraction in molasses

Run	Feed flowrate cm^3h^{-1}	$\bar{\theta}_C$ degrees	$\bar{\theta}_S$ degrees	$\bar{\theta}_B$ degrees
1-SM	40	114	180	252
2-SM	60	128	173	280
3-SM	70	148	187	259
4-SM	80	155	217	260
5-SM	100	124	173	261

$\bar{\theta}_C$ = exit band position for the ionic fraction (deg)

$\bar{\theta}_S$ = exit band position for sucrose (deg)

$\bar{\theta}_B$ = exit band position for betaine (deg)

Figure 7.22 shows graphically the effect of feed flowrate on exit band position for sucrose, ionics and betaine and it appears that feed flowrate has little effect on the band position of each peak. The first peak to appear is the ionic peak. This is made up of a number of ions each contributing to the overall peak. This explains the lack of symmetry for this peak. The ionic peak appears early due to its low retention within the packing. The change which resides on the resin particles has a repellent effect on cations passing through it. There is also some exchange with K^+ ions, this is however a fast process and K^+ ions remaining on the resin have been shown not to affect the separation.

Figure 7.22 shows that as with the synthetic feed solution the feed flowrate does not appear to have a significant effect on the exit band position. The mean $\bar{\theta}$ value obtained from these experiments for sucrose is 186°, using equation 2.29 and the calculated value of the voidage of 0.40 a distribution coefficient for sucrose of 0.67 is derived. For the ionic fraction values of θ are difficult to obtain accurately since this band is composed of many different components each appearing at slightly different angles from the feed point. It was also noted that on each of the chromatograms produced from these experiments a small peak just before the main peak showed up. From Table 7.22 this small initial peak appears to be due to Na^+ ions.

An estimate of the mean $\bar{\theta}$ value for the ionic fraction can be obtained if the small peak which always appears before the main part of the

Figure 7.22 The Effect of Feed Flowrate on the Exit positions of Sucrose,Ionics and Betaine

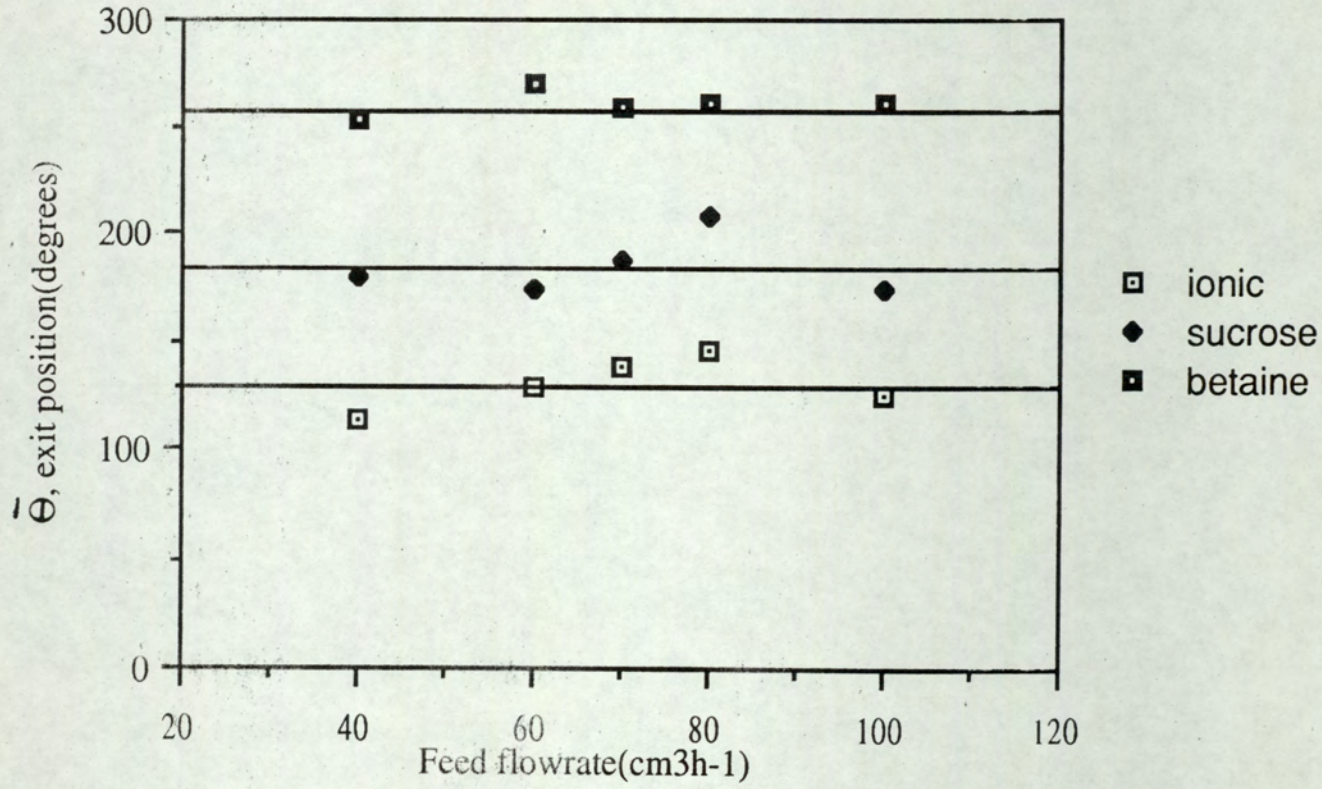

peak is ignored. In this case a $\bar{\theta}$ value of 133° is obtained which gives a distribution coefficient for the ions of approximately 0.28. For betaine the mean θ value of 262° is obtained giving a distribution coefficient of 1.21. The mean distribution coefficient for sucrose is 0.67. Obviously there are many other components in the molasses however the majority are present in very small quantities. Using HPLC analysis it is difficult to identify these components due to the quantities of the other components in molasses. Some of these components are hidden by the large sucrose peak. Many are difficult to identify due to the proximity of other component peaks. Since the extraction of sucrose is of greatest interest in this project it was decided to concentrate on the three fractions sucrose, ionic components and betaine in this study.

Sucrose and other sugars are more highly retained than the majority of the ionic components. Sugars have no charge and hence are not repelled by the resin particles. The Duolite C211/2558 resin is quite porous and it is this which is instrumental in the separation; sucrose molecules pass easily in and out of the pores of the resin retarding its progress through the chromatograph.

Betaine is a small uncharged molecule, this allows very easy penetration of the pores and hence even slower movement through the packing; hence betaine appears at large angles to the feed entry point. One experimental run was analysed by British Sugar, see Figure 5.4 and Table 7.22 to show detail of the position of specific ions and the the position of the

colour during the separation.

Table 7.22 shows the position of maximum colour is at the exact point of the position of maximum conductivity and falls off as the conductivity decreases. This is a useful phenomenon since purification of the sucrose requires not only removal of ions but also of colour. The colour bodies are organic molecules mainly and not ionic in nature. From the results obtained all of the ions which were tested appeared at the same positions including the anions.

7.5.3.2 The effect of feed flowrate on bandspreading using sucrose molasses as feed

Table 7.23

Run	Feed flowrate ($cm^3 h^{-1}$)	W_C	W_S (degrees)	W_B
1-SM	40	43	49	46
2-SM	60	46	51	49
3-SM	70	57	68	75
4-SM	80	49	98	61
5-SM	100	70	104	73

The results expressed in Table 7.23 and Figure 7.22 show four features which have been noted with previous experiments.

1 As the feed flowrate increases for each component in the feed the bandwidths increase.

2 For each component there appears to be a minimum value for the exit bandwidths of approximately 40°. This suggests that since feed flowrate has little or no effect on the exit band position then reducing feed rates below certain values does not improve the resolution

3 The increase in exit bandwidth appears to be exponential.

4 Overall sucrose has the largest bandwidth followed by betaine followed by the conductivity peak.

7.5.3.3 <u>The effect of feed flowrate on the number of theoretical plates for sucrose in the CCC equipment</u>

A logarithmic curve has been fitted to the points of the graph since at zero bandwidth, ie. zero flowrate there must be an infinite number of theoretical plates. From the points on the graph it can be seen that the number of plates decreases as the feed flowrate is increased. The number of plates is a measure of the efficiency of the separation, hence reduction in efficiency occurs as the feed flowrate is increased. A similar effect has been noted with the synthetic feed experiments, however in the case of molasses the reduction in efficiency with feed flowrate is not so marked. Figure 7.23 shows the curve.

Figure 7.23 The effect of feed flowrate on the Average Number of theoretical plates(molasses)

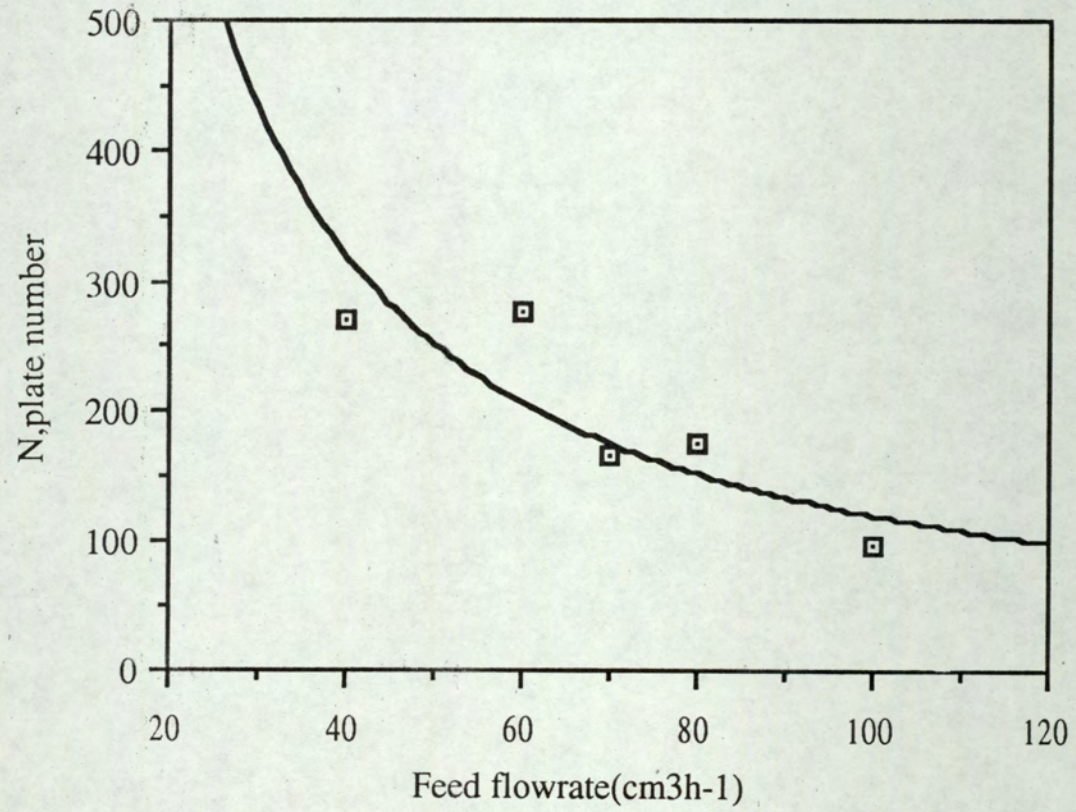

7.5.4 The effect of rotational speed on the separation of sucrose from beet molasses

7.5.4.1 The effect of rotational speed on the exit position of sucrose, ionic and betaine peaks

Table 7.24

Run	Rotational speed (deg h^{-1})	$\bar{\theta}_C$	$\bar{\theta}_S$ (degrees)	$\bar{\theta}_B$
6-SM	50	75	100	158
2-SM	96	128	173	280
7-SM	120	150	214	338
8-SM	144	200	291	472
9-SM	180	279	358	500

Figure 7.24 shows a clear linear relationship between the exit band position for each component in molasses and the rotational speed. Determination of distribution coefficients using the slope of the lines θ/ω gives values as follows:

$K_C = 0.31$

$K_S = 0.67$

$K_B = 1.35$

Figure 7.24 The effect of rotational speed on the Exit positions of sucrose,ions and betaine.

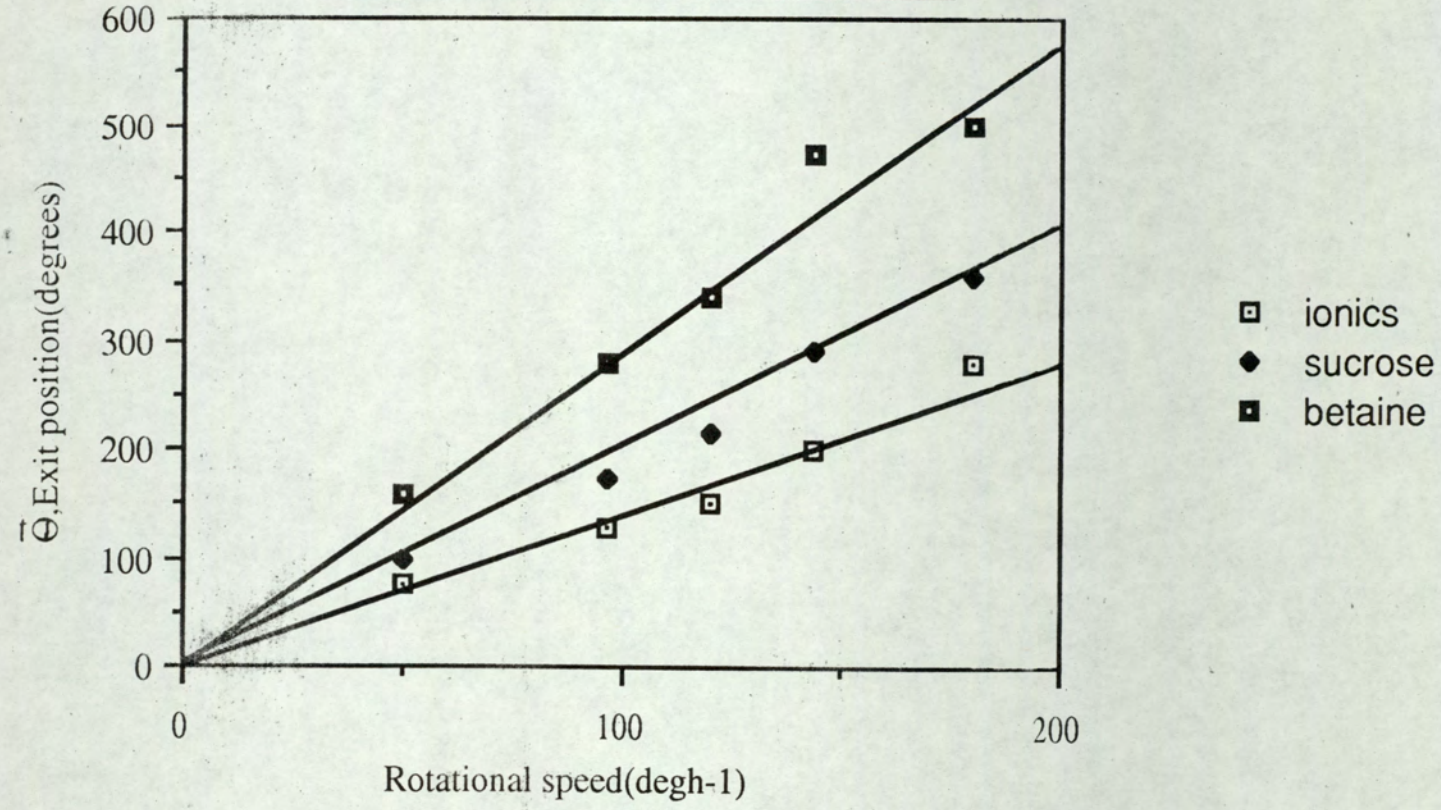

These distribution coefficients show good agreement with K values obtained from the feed rate experiments and provides more evidence that if the distribution coefficient is known then it is possible to predict the $\bar{\theta}$ value for given solutes under other operating conditions.

7.5.4.2 The effect of rotational speed on the exit bandwidth of sucrose, betaine and ionic non-sugars

Table 7.25

Run No	Rotational speed (deg h^{-1})	W_C (deg)	W_S (deg)	W_B (deg)
6-SM	50	51	66	39
2-SM	96	57	61	74
7-SM	120	55	97.5	103
8-SM	144	60	93	116
9-SM	180	72	120	133

As the rotational speed is increased the exit bandwidths increase. Each band in this case appears to have its own rate of increase as the rotation rate is increased. The exit bandwidth for betaine is greater than the bandwidth of the other two components except at the lowest rotational speed of 50 deg h^{-1}. The rate of increase of the betaine band width is greater than that of the other components. The sucrose bandwidth is in each case greater than that of the ionic peak. The bandwidth for sucrose appears to increase at a greater rate than that of the ionic peak as

Figure 7.25 The effect of rotational speed on the Exit bandwidths of sucrose,ions and betaine

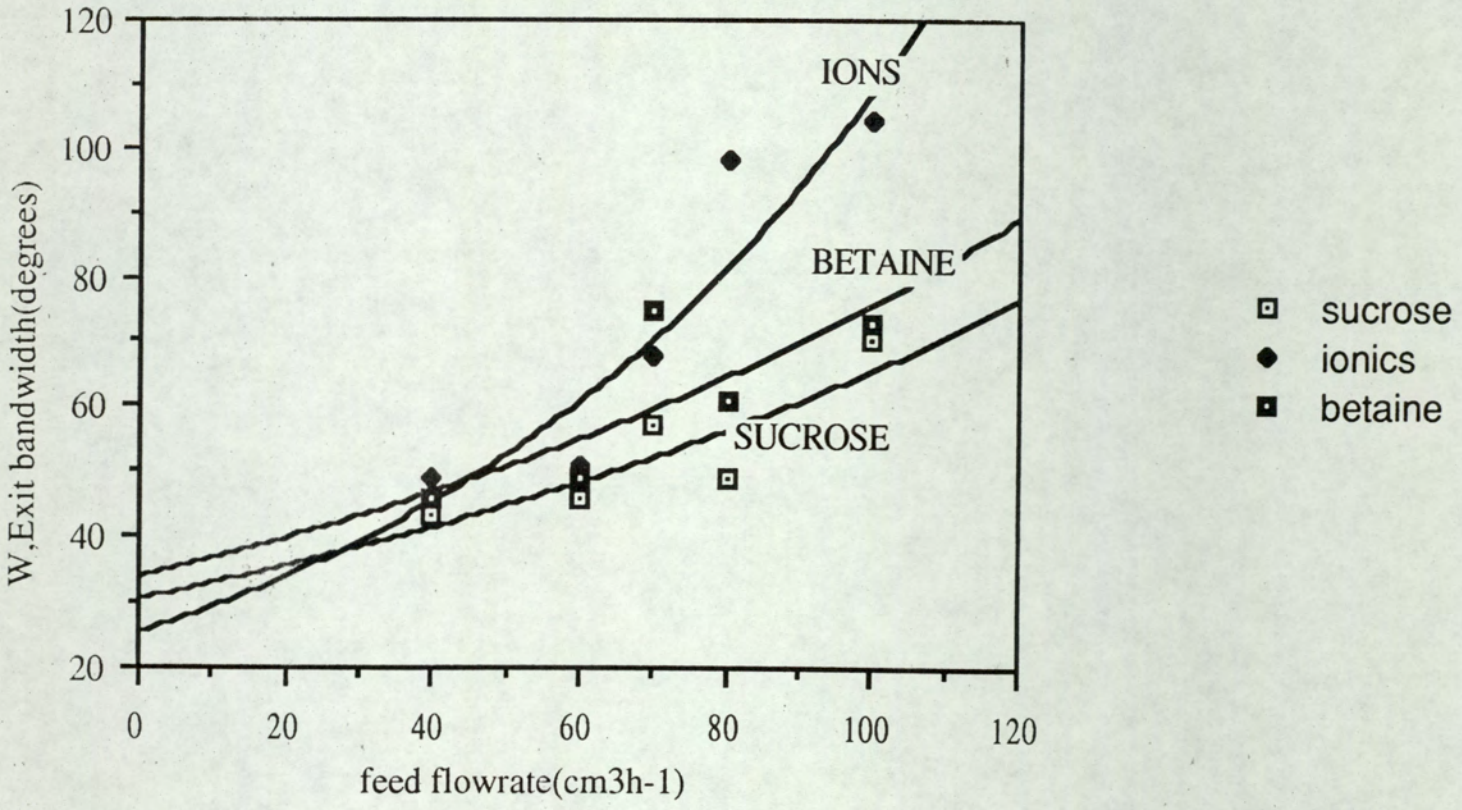

the rotation rate is increased. It has been noted previously in this chapter that the bandwidth is influenced by the angle which the exiting band is from the feed entry point or alternatively the retention time of that solute within the packing. Therefore sucrose which stays in the annulus longer than the ionic components gives peaks which are wider than the ionic peaks. Betaine however has a very long retention time and hence the peaks for betaine are usually wider than the peaks for sucrose under the same conditions of rotational speed etc. Peak bandwidths have also been shown to be affected by the relative quantities of components in the feed mixture; if a component is present in low concentration then a smaller bandwidth is expected than if the component is present at high concentrations. Since the ionic peak consists of many components each appearing at slightly different regions of the annulus it is difficult to apply this relationship. Examination of the relative sizes of the betaine peak and the sucrose peak reveals that the betaine is on average 5% wider than the sucrose peak. This is despite the fact that betaine is present in molasses only as approximately 5% of the dry matter compared to approximately 60-65% for sucrose. This reveals that the retention time of a solute within the CCC packing or the distribution coefficient of a solute has a much greater effect on the bandwidth than the concentration of that solute within the feed mixture.

7.5.4.3 Effect of rotational speed on the resolution between the sucrose and the ionic fraction peaks using molasses

Table 7.26

Run No	Rotational speed (deg h^{-1})	Resolution
6-SM	50	0.42
2-SM	96	0.74
7-SM	120	0.84
8-SM	144	1.05
9-SM	180	0.94

Figure 7.26 shows as with previous experiments that the resolution between two peaks increases as the rotational speed is increased due to reduced bed loading. There appears to be a levelling off of the resolution as the rotational speed is increased above approximately 144° as noted with the glucose/fructose experiments. This effect has been noted by Begovich (61) and shows that there is an optimum rotation rate below which the resolution between components decreases due to increased bed loading, whilst above this rate the column is not being fully utilised. The other consideration here is whether or not the solutes exit the column within one resolution. For experiment 8-SM all the components do leave the annulus within 360°; however in experiment 9-SM there is overlap between the betaine peak and the conductivity peak (see Figures 7.27 and 5.4). This may be a useful technique for grouping together all the non-sugars in one region and all the sucrose in another but since the

Figure 7.26 The effect of Rotational Speed on the Resolution of Sucrose and Ions

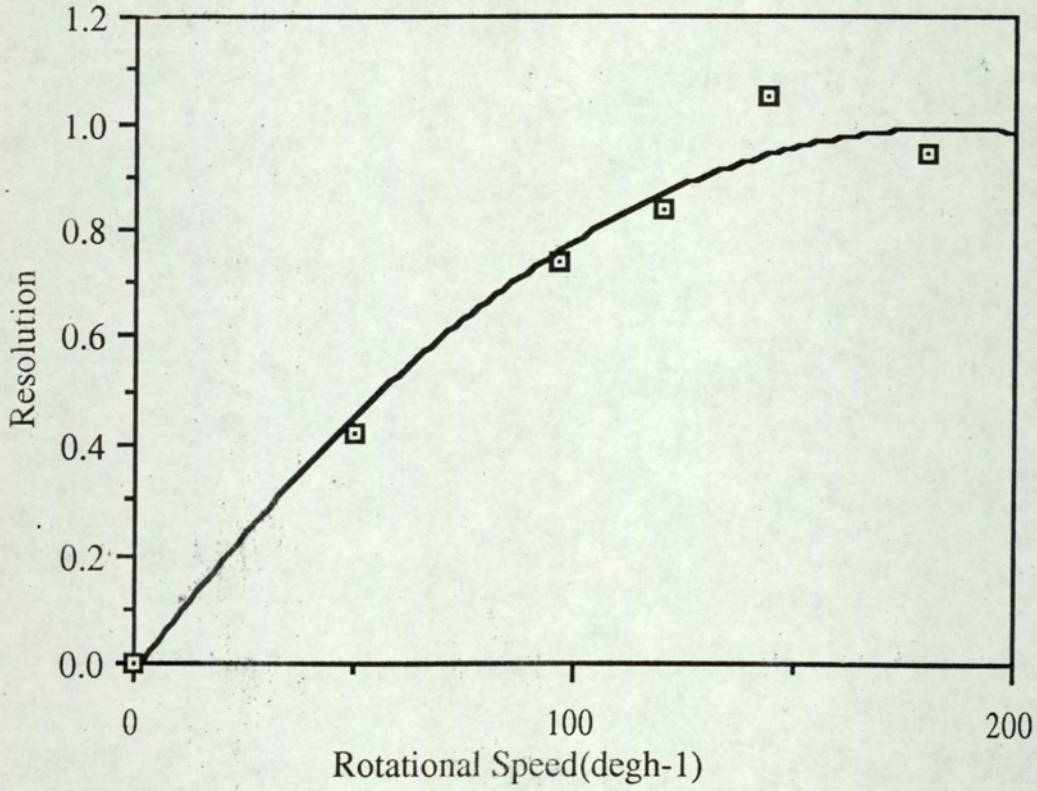

Figure 7.27 Chromatogram for experiment 9-SM

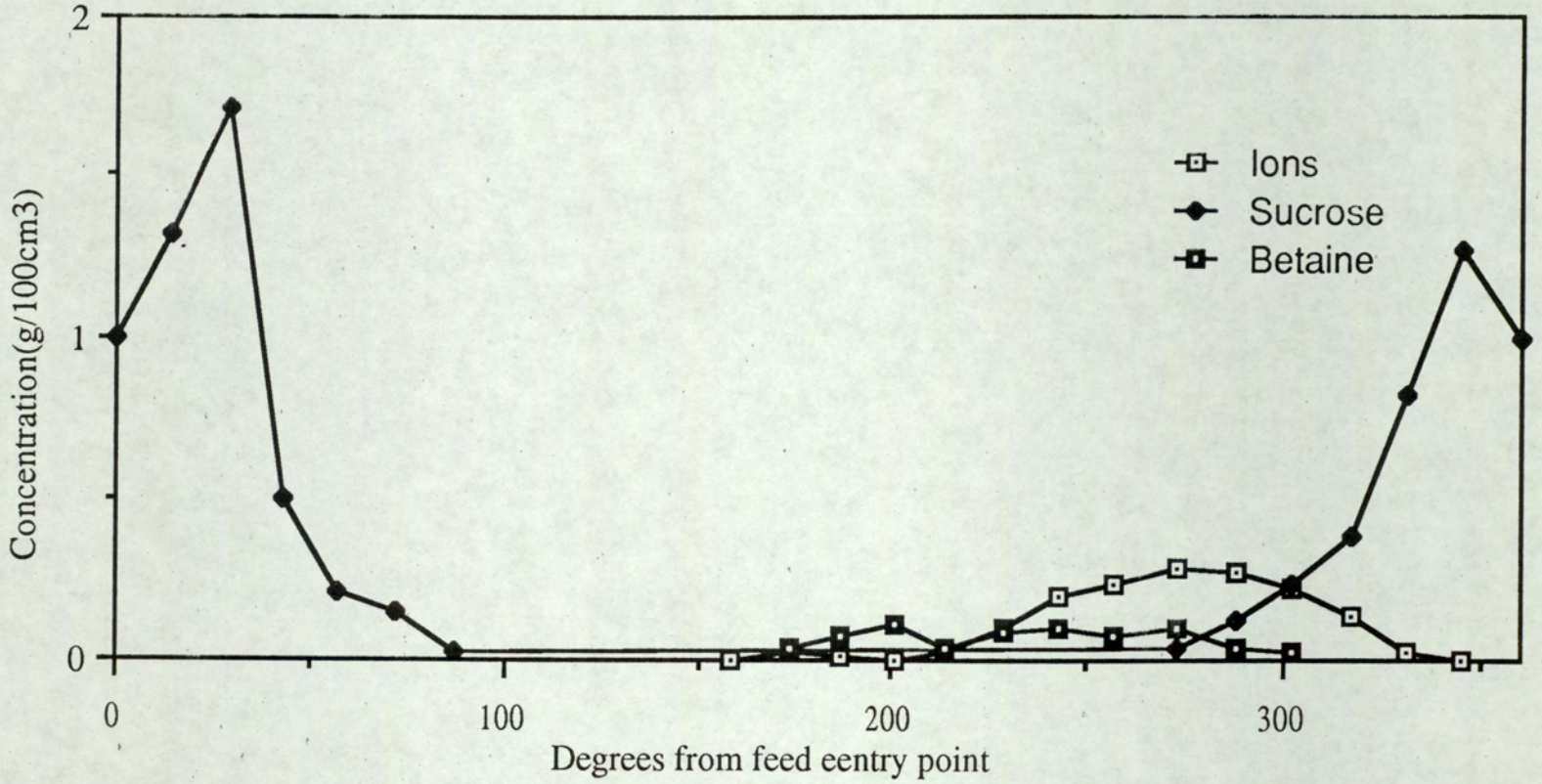

resolution between the sucrose peak and the ionic peak has not increased there is no advantage to be gained by this. The bandwidths and hence the dilutions also increase between 144 deg h^{-1} and 180 deg h^{-1} rotation rates.

CHAPTER EIGHT

COMPUTER SIMULATION OF THE CONTINUOUS CIRCULAR CHROMATOGRAPH

8.1 Plate Theory

Modelling of this type of equipment requires a prediction of the exit position of solute bands, $\bar{\theta}$. The results from the synthetic bands, θ and of solute bandwidths at the exit, W. The results from the synthetic feed experiments and the molasses runs have shown that it is possible to make a good prediction of the exit position of the solute peak using the plate theory equation:

$$\bar{\theta} = \frac{\omega L}{V} [\varepsilon + (1 - \varepsilon) K] \qquad \text{..... 2.28}$$

Provided the distirbution coefficient, K, the voidage of the resin being used ε, and the experimental operating conditions are known, equation 2.28 gives a good indication of the band position. The distribution coefficients may be determined by carrying out experiments on a conventional batch column or by carrying out experiments on the annular chromatograph. Predictions of $\bar{\theta}$ can be made since it has been shown that when the feed flowrate is altered, provided other conditions are kept constant, the position of the band changes very little. It has also been shown that the exit position of a solute band in degrees is directly proportional to the rotational speed

provided other factors are kept constant for a given solute. Predictions of θ can be made using equation 2.29.

Predicting the exit bandwidth is more difficult however. From the plate theory the following expression can be obtained:

$$W = \sqrt{W_o^2 + 16(\omega/L)^2 HL [\varepsilon + (1 - \varepsilon) K]^2} \quad \text{..... 8.1}$$

If the results 1-GF to 7-GF are examained (Table 7.1) the distribution coefficients remain almost constant as shown by the θ values. However, as the exit bandwidths increase and the height equivalent to a theoretical plate, H remains constant the bandwidths would increase to a much smaller extent than actually occurs (Table 7.2). If H is calculated for run 1/GF a value of 0.54cm can be obtained; if this remained constant then the increase in exit bandwidth would be due to the increases in the initial feed bandwidth, W_o, only. If all the bandwidths are calculated using this H value then the difference between the exit bandwidth at 50cm^3 h^{-1} feedrate and 350cm^3 h^{-1} feed rate would only be approximately 0.1 degrees when in fact there was a four-fold increase in bandwidth.

The effect of rotational speed on the exit bandwidth is also difficult to predict. If results for experiments 8-GF to 12-GF are examined; a value for H of 7.5cm is obtained using equation 8.1 for run 8/GF at 72 deg h^{-1} rotational speed, at 180 deg h^{-1} rotational speed (run 12/GF) the average

exit bandwidth would, according to the plate theory be 140°, in fact the average bandwidth is 90°. Using the plate theory the bandwidth is overpredicted by almost 60%.

8.2 Differential Model

The equation which results from a mass balance on a differential element in a conventional chromatographic column was given previously as:

$$\frac{\partial c}{\partial t} + \left(\frac{1-\varepsilon}{\varepsilon}\right)\frac{\partial n}{\partial t} = D_z\frac{\partial^2 c}{\partial z^2} - \frac{V}{\varepsilon}\frac{\partial c}{\partial z} \qquad \text{..... 2.27}$$

Equation 2.27 assumes a constant eluent velocity and negligible radial variations in velocity or concentration.

Lapidus and Amundson (7) obtained an analytical solution to equation 2.27 using the equilibrium relationship of the following form:

$$n = k_0 + k_1 C \qquad \text{..... 8.2}$$

Houghton (87) obtained an analytical solution when a non-linear isotherm of the following polynomial form was used:

$$n = k_0 + k_1 C + k_2 C^2 \qquad \text{..... 8.3}$$

He further defined a measure of the nonlinearity of the isotherm, I, given by:

$$\lambda_c = 2k_2/\varepsilon\ (1 + k_1)/\varepsilon \qquad \text{..... 8.4}$$

To solve equation 2.27 using the isotherm, 8.2, Houghton had to assume that the absolute value of λc was much less than one. This solution is therefore limited to cases where the solute concentration is low or the adsorption isotherm is linear. No consideration is given to interactions between solutes in multicomponent systems.

The analytical solution of Houghton has been incorporated into a computer program "CHROMA", which can be found in Appendix A.

Nonlinear langmuir competitive solute resin binding isotherms common to many separations were used to determine k_1 values. These isotherms relate to the liquid and solid phase solutes as follows:

$$n_1 = \frac{N_c\, k_{Li}\, C_i}{1 + \sum_{j=1}^{p} k_{Lj} C_j} \qquad \text{..... 8.5}$$

where

n_i = solute i concentration in the solid phase (mol l^{-1})

c_i = solute i concentration in the liquid phase (mol l^{-1})

N_c = Langmuir isotherm parameter (l mol^{-1})

ρ = number of solutes

The subscript i refers to the i^{th} solute. Figure 8.1 shows a typical plot of this isotherm.

k_1 values were obtained by fitting the Langmuir isotherm to the polynomial isotherm to the polynomial isotherm. Specifically the equation to be fitted was:

$$n = k_o + (1 - \varepsilon) N_c k_L c + k_2 C^2 \qquad \text{..... 8.5}$$

If k_o and k_2 are assumed to be zero this gives:

$$n = (1 - \varepsilon) N_c k_L C \qquad \text{..... 8.6}$$

The $(1 - \varepsilon)$ term serves to convert the amount of solute adsorbed per unit volume of sorbent, as given in this work, to the amount of solute adsorbed per unit volume of bed, as given by Houghton. $N_c k_L$ is used to approximate k_1 as shown in Figure 8.1.

Figure 8.I

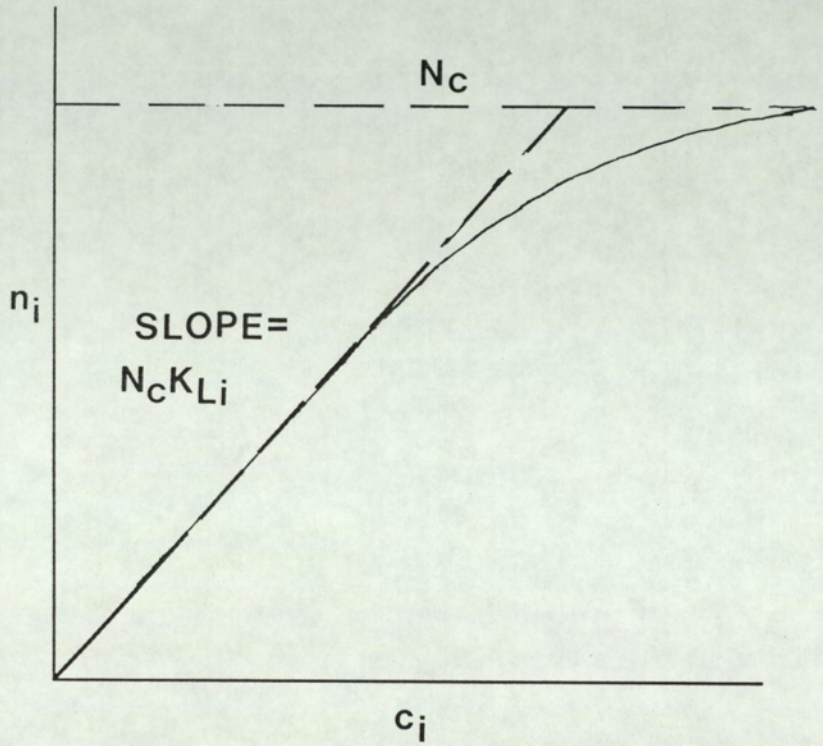

Langmuir Isotherm

A simulation of the results from the sucrose molasses experiments 1-SM to 9-SM was carried out using the program "CHROMA" (Appendix A) for the ionic fraction and the sucrose. The dispersion coefficient, D_z used in the model essentially incorporates a number of factors including the effects of dispersion, mass transfer resistance and end effects and was obtained for each experiment such that the bandwidth of the two solute peaks obtained matched the experimental results. This dispersion term determines the size of the bandwidth given by the computer. Table 8.1 shows that there is considerable variation in the dispersion value. Using an average dispersion value to model the experiments is one possibility, however this does not give very satisfactory results.

Results 1/GF to 12/GF were examined in order to find dispersion coefficients which matched the bandwidths obtained experimentally, Table 8.2 shows this. A large variation in dispersion coefficient exists. It was at this point that a relationship was discovered between the D_z term and the amount of bed loading.

Table 8.1 - Dispersion coefficients for molasses runs

Experiment	Experimentally obtained		Computer calculated Dz	
	W_c bandwidth(deg)	W_s	Ionic	Sucrose
1-SM	43	49	1.2	0.79
2-SM	46	51	1.2	0.79
3-SM	57	68	1.5	1.30
4-SM	49	98	2.7	3.0
5-SM	70	104	5.0	4.5
6-SM	51	66	1.2	0.79
7-SM	55	98	1.2	1.80
8-SM	60	93	1.0	1.10
9-SM	72	120	0.7	1.10

Table 8.2 - Dispersion coefficients for glucose/fructose experiments

Experiment	Experimentally obtained Exit bandwidths (degrees)		Computer calculated Diffusivity coefficients	
	W_G	W_F	Glucose	Fructose
1-GF	48	62	1.0	1.0
2-GF	53	66	1.9	1.9
3-GF	65	76	4.3	4.3
4-GF	89	104	7.6	7.6
5-GF	101	126	12.0	12.0
6-GF	150	189	17.6	17.6
7-GF	167	216	21.4	21.4
8-GF	51	61	12	12
9-GF	57	68	10	10
10-GF	62	76	8.0	8.0
11-GF	75	96	7	7
12-GF	83	96	6	6

Tables 8.3 and 8.4 show for each experiment the diffusivity coefficient and the amount of bed loading. Bed loading is directly proportional to feed flowrate and indirectly proportional to rotational speed.

$$\text{Bed loading} = \frac{Q_f}{\omega} \quad (cm^3\ min^{-1}\ deg^{-1})$$

where ω = rotational speed (deg min^{-1})

Initially the dispersion coefficients for glucose and fructose were taken to be the same for each experiment. The experimental results shown this to be an accurate assumption. To determine if a relationship existed between the bed loading and the diffusivity coefficient two graphs were plotted, one for the molasses runs and one for the glucose and fructose runs, see Figures 8.2 and 8.3. Both gave an approximate linear plot having correlation coefficients of 0.90 in each case. If the diffusivity coefficient is assumed to be proportional to the bed loading then a good fit of experimental results and computer calculated results is obtained. The slope of each graph was measured and this number was multiplied by the bed loading to give the predicted dispersion coefficient, D_z. The dispersion coefficients and the k_1 values were fed into the computer program along with the rotational speed, feed flowrate and eluent flowrate, the feed concentrations and the number of components. A print-out was then obtained of the exit positions, $\bar{\theta}$, the bandwidth, W and the resolution value for each experiment.

Table 8.3 - The variation in the computer calculated dispersion coefficient with bed loading for sucrose molasses experiments

Experiment	Q_f ($cm^3 min^{-1}$)	Q_E ($cm^3 min^{-1}$)	ω (deg^{-1})	Bed loading ($cm^3 min^{-1} deg^{-1}$)	Calculated average Dispersion coefficient ($cm^3\ min^{-1}$)
1-SM	0.67	100	96	0.42	1.0
2-SM	1.0	100	96	0.62	1.0
3-SM	1.167	100	96	0.73	1.4
4-SM	1.33	100	96	0.83	1.75
5-SM	1.67	100	96	1.04	2.85
6-SM	1.0	100	50	1.20	4.75
7-SM	1.0	100	120	0.50	1.50
8-SM	1.0	100	144	0.417	1.05
9-SM	1.0	100	180	0.33	0.90

Table 8.4 - The variation in the computer calculated dispersion coefficient with bed loading for the synthetic glucose, fructose feed runs

Experiment	Q_f ($cm^3\ min^{-1}$)	Q_E ($cm^3 min^{-1}$)	ω ($deg h^{-1}$)	Bed loading ($cm^3 min^{-1} deg^{-1}$)	Dispersion coefficient glucose & fructose ($cm^3 min^{-1}$)
1-GF	0.833	200	220	0.22	1.0
2-GF	1.667	200	220	0.45	1.9
3-GF	2.50	200	220	0.68	4.3
4-GF	3.33	200	220	0.91	7.6
5-GF	4.167	200	220	1.14	12
6-GF	5.0	200	220	1.36	17
7-GF	5.83	200	220	1.59	23
8-GF	2.0	200	72	1.667	12
9-GF	2.0	200	100	1.20	10
10-GF	2.0	200	120	1.00	8
11-GF	2.0	200	144	0.833	7
12-GF	2.0	200	180	0.667	6

Figure 8.2 Bed loading vs Dispersion Coefficint(molasses)

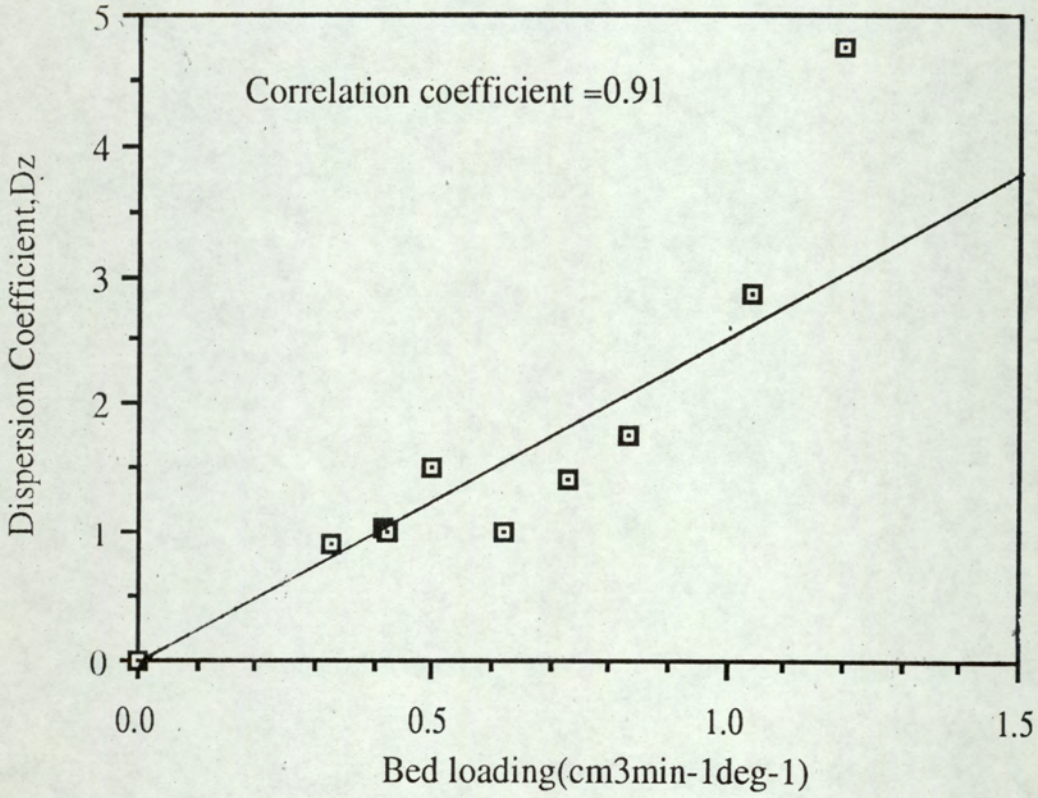

Figure 8.3 Bed loading vs dispersion(glucose/fructose

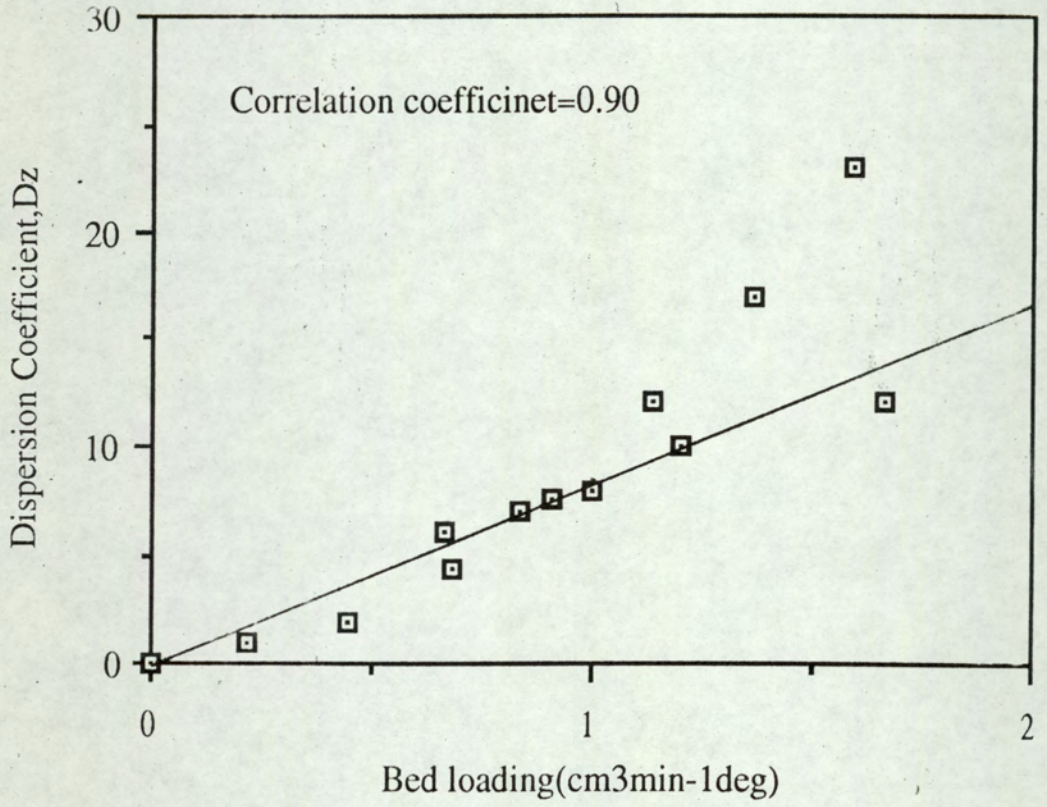

The throughput, purity and yield of each product was also calculated, see Figure 8.4. An extended version of this program was used to show visually how the experimental separation compares with the computer simulated separation, see Figure 8.5.

Table 8.5 shows how the experimental results compare with the computer calculated results for the glucose and fructose experiments using k_1 values of 0.30 and 0.48 for glucose and fructose respectively and D_z values obtained by multiplying the bed loading by 8.3. Overall the predictions achieved are very good especially when considering that it is difficult to accurately measure experimental exit bandwidths and exit positions. At high feed flowrates there is slight under-prediction of the bandwidths, ie. runs 6-GF and 7-GF and at low feed rates there is slight over-prediction of the bandwidths which may indicate the need for more complicated means of calculating the dispersion term, a great deal more data would be required to confirm this, however.

Table 8.6 shows how the experimental results compare with the computer calculated results for the sucrose molasses experiments. Using k_1 values of 0.18 and 0.40 for the ionic fraction and the sucrose respectively. D_z values were obtained by multiplying the bed loading by 2.5.

Figure 8.4
Computer Print-out

ROT	ANNULL	ANNULD	AR	EPS	QE	QF	M
220.00	135.00	29.700	107.5	0.34	200.00	4.16700	

FEED	CONC
0.2500	0.2500

DIFFYS	
12.0000	12.0000

K_2

0.000000E+00	0.0000000E+00

K1

0.4600	0.7100

COMPONENT	PEAK POS.	BANDWIDTH	PEAK CONC.	DF
1	164.0000	118.2383	2.47220100E-02	16.09229
2	210.0000	151.5168	1.92898474E-02	20.62151

RESOLUTION
0.3410501

THROGHPUT(G/MIN)	YIELD	SOLID CONC	PURITY
0.1514955	0.3153811	2.1205304E-02	0.8812720

RUN NUMBER
DATE

RUN CONDITIONS: 30% SUCROSE
FEED RATE: 60 $cm^3 h^{-1}$
ELUENT RATE: 6 ℓh^{-1}
ROTATIONAL SPEED: 50 $° h^{-1}$

KEY
EXPT
MODEL

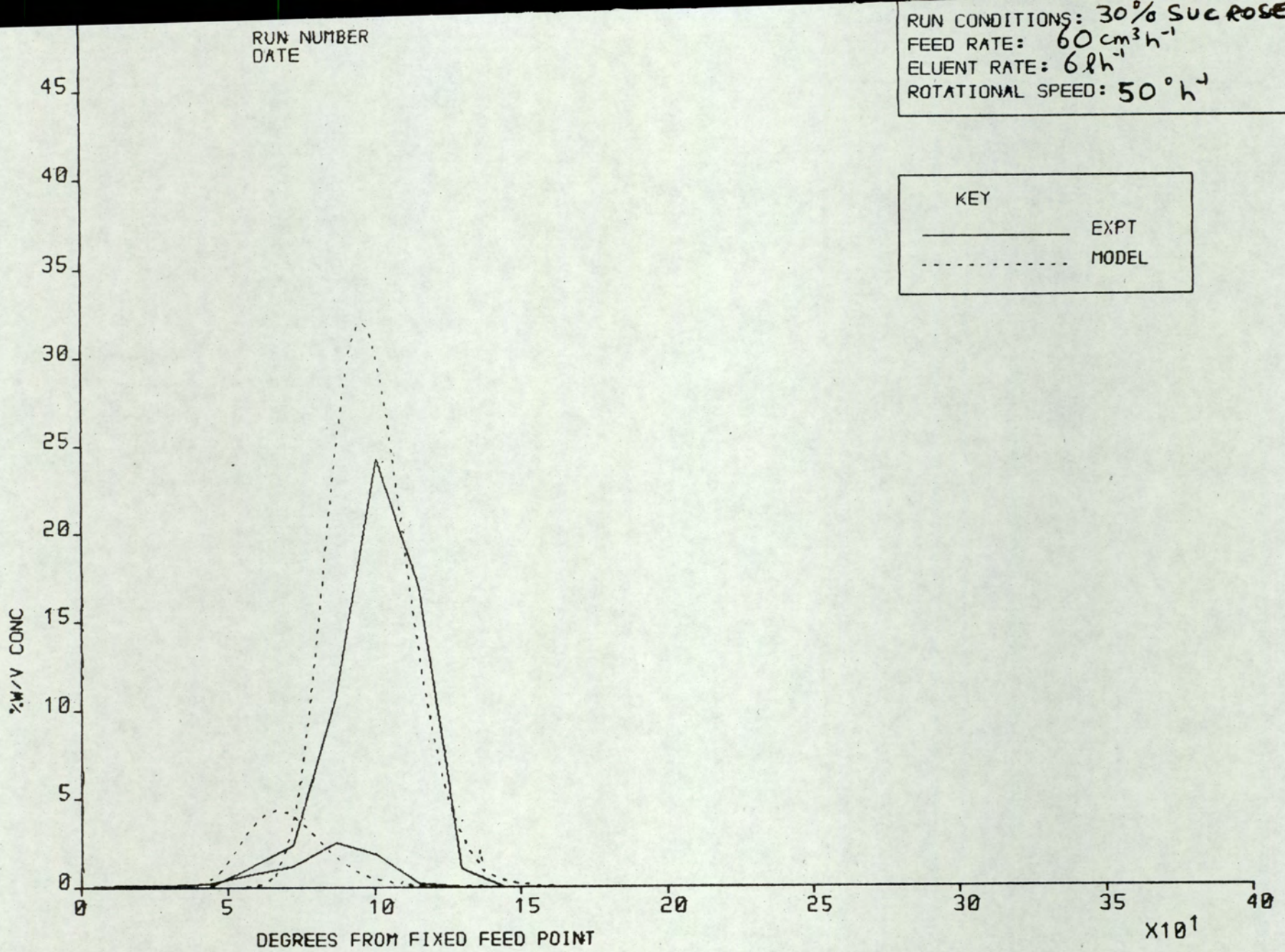

Table 8.5 - Comparison of computer calculated results with experimentally obtained results

Run	D_z	Experimental $\bar{\theta}_G$	Experimental $\bar{\theta}_F$	Computer calculated $\bar{\theta}_G$	Computer calculated $\bar{\theta}_F$	Experimental W_G	Experimental W_F	Computer calculated W_G	Computer calculated W_F	Resolution Exptl	Resolution Comp
1-GF	1.89	165	208	169	217	42	54	48	62	0.89	0.81
2-GF	3.79	167	210	168	215	53	66	67	86	0.72	0.65
3-GF	5.68	165	205	167	214	65	76	81	104	0.56	0.50
4-GF	7.58	164	216	166	212	89	104	94	121	0.53	0.42
5-GF	9.47	171	217	165	211	101	126	105	134	0.41	0.38
6-GF	11.4	186	225	164	210	150	189	115	147	0.23	0.35
7-GF	13.3	170	216	163	208	167	216	122	157	0.25	0.32
8-GF	13.9	46	76	44	73	51	61	42	56	0.53	0.38
9-GF	10.0	60	102	66	102	57	68	50	67	0.67	0.44
10-GF	8.3	77	125	88	122	62	76	52	73	0.69	0.54
11-GF	6.9	131	180	133	167	75	96	57	81	0.61	0.64
12-GF	5.5	128	194	128	184	83	96	62	89	0.74	0.73

Table 8.6 - Comparison of computer calculated results with experimentally obtained results

Run	D_z	Experimental $\bar{\theta}_C$	Experimental $\bar{\theta}_S$	Computer calculated $\bar{\theta}_C$	Computer calculated $\bar{\theta}_S$	Experimental W_C	Experimental W_S	Computer calculated W_C	Computer calculated W_S	Resolution Exptl	Resolution Comp
1-SM	0.84	114	180	133	183	43	49	39	53	1.43	1.1
2-SM	12.5	128	173	133	183	46	51	47	65	0.92	0.89
3-SM	1.45	148	187	132	182	57	68	51	70	0.62	0.83
4-SM	1.67	155	217	132	182	49	98	54	75	0.83	0.72
5-SM	209	124	173	132	182	70	104	62	87	0.65	0.69
6-SM	2.40	75	100	69	95	51	66	34	47	0.55	0.63
7-SM	1.00	150	214	166	229	55	98	52	74	0.16	1.00
8-SM	0.83	200	281	199	275	60	93	64	89	0.06	0.97
9-SM	0.67	279	358	249	344	72	120	69	96	0.96	1.14

The computer obtained data here is an even better match for the experimentally obtained results again with a slight under-prediction of the exit bandwidths at high bed-loading, ie. experiment 5-SM and 6-SM.

CHAPTER NINE

CONCLUSIONS

9.1 Separation of Carbohydrates

Four types of separation have been achieved using the CCC equipment all using deionized water as the mobile phase of eluent. These are;

1 The separation of glucose from fructose in a synthetic feed using Purolite PCR 838 ion exchange resin in the Ca^{2+} form.

2 The separation of sucrose, glucose and fructose in a synthetic feed using Purolite PCR 833 ion exchange resin in the Ca^{2+} form.

3 The separation of glucose, fructose, non-sugars and betaine in enzyme-inverted molasses using the previously mentioned resin.

4 The separation of sucrose, non-sugars and betaine in beet molasses using Duolite C211/2558 ion exchange resin in the Na^{+} form.

9.2 Trends

1 It has been found in all the separations that increasing the feed flowrate has little effect on $\bar{\theta}$, the peak position for a solute relative

to the fixed feed entry point provided all other conditions remain constant.

2 Increasing feed flowrate has been found to increase W, the solute exit bandwidth. The increase is exponential and is much greater than is predicted by the plate theory.

3 As a consequence of the increase in bandwidth, the number of theoretical plates, N is reduced as the feed flowrate is increased.

4 Increasing feed flowrate causes a decrease in the dilution experienced by a solute. However there appears to be a point beyond which increases in product concentration cannot be achieved.

5 Increasing feed flowrate causes a decrease in the resolution or degree of separation overall, ie. lower yields and/or purities of products are obtained.

6 Increasing the rotational speed causes a proportional increase in the $\bar{\theta}$ value.

7 Increasing the rotational speed causes an almost linear increase in the exit bandwidth, in this case however the plate theory underpredicts the increase in the exit bandwidth.

8 The height equivalent to a theoretical, H decreases with increasing rotational speed indicating higher efficiencies at greater rotational speeds.

9 Increasing the rotational speed caused an increase in the resolution as a result of reduced bed loading.

10 A decrease in product concentration results from an increase in the rotational speed.

11 Increasing eluent flowrate causes a decrease in the $\bar{\theta}$ value, a reduction in the resolution and an increase in the dilution of solutes passing through the chromatograph.

9.3 Glucose, Fructose Separations

It has been found possible to achieve a good separation of glucose from fructose using the CCC equipment with a 50g/100cm^3 total sugar concentration (25g/100cm^3 glucose; 25g/100cm^3 fructose). The glucose band always appears at smaller $\bar{\theta}$ values than the fructose band

and also has a smaller bandwidth than the fructose. A throughput of 300gh^{-1} glucose at 4.8% w/v concentration and 90% purity and a throughput of 240g h^{-1} fructose at 2.6% w/v concentration and 90% purity could be achieved using three feed entry points each supplying 480cm^3h^{-1} of feed at a rotational speed of 295 deg h^{-1} and an eluent flowrate of 22.5 l h^{-1}. The total throughput is 540g h^{-1} of sugar solids, which for the 9.5 litres of resin used with CCC equipment gives a specific throughput of 56.8 Kg m^{-3} resin h^{-1}. This throughput is superior to the 32.1 Kg m^{-3} h^{-1} throughput which has been achieved on the SCCR equipment (1), however the purity achieved on the CCC is slightly less and the product concentration is reduced considerably.

The major problem encountered with this separation technique using sugar solutions is that of dilution of the products. The desired throughputs can be achieved but product concentrations are usually quite low.

9.4 The separation of synthetic mixtures of sucrose, glucose and fructose

It has been shown that a good separation of a three sugar component mixture can be achieved using the CCC equipment. It was noted that using the Purolite resin, the sucrose exits the annulus at a smaller angle from the fixed feed point than either glucose or fructose. The bandwidth for sucrose was always found to be smaller than that of the glucose and the fructose. The reason for this is that the sucrose having a

larger molecular size is excluded from the pores of the resin to a greater extent than the other sugars. The usual trends outlined earlier applied to these separations.

The distribution coefficient for fructose was found to increase during these separations probably because the total concentration of fructose in the feed had been reduced allowing greater interaction with the Ca^{2+} ions on the packing.

9.5 The separation of glucose and fructose in a natural feed solution; enzyme inverted beet molasses

Using beet molasses which had the sucrose present inverted to glucose and fructose as feed created two problems: the first was an increase in the growth of micro-organisms which was controlled by use of sodium azide solutions to flush out the equipment after use. The second problem was that of poor separation particularly at high feed concentrations. Concentrations of sugar above 30% w/v in the feed were found to give solutions of very high viscosity. At 20°C the separation was very poor. Regeneration of the ion exchange resin using calcium nitrate solution was found to increase the resolution obtained using 30% w/v sugars in feed from 0.38 to 0.63 by moving the fructose band further from the feed entry point. This gave a good separation of glucose from fructose and from betaine or trimethylglycine; a partial separation of the conductivity band and glucose was achieved. The equipment has therefore been shown to be capable of resolving natural and multicomponent feedstocks.

9.6 The separation of sucrose, non-sugars and betaine from beet molasses

This separation has been achieved quite successfully using 30% w/v sucrose in the feed. The Na^+ form resin has the effect of repelling ions and retaining sucrose, hence sucrose exits the annulus at higher θ values than the ionic components. The betaine appears at greater θ values than the sucrose. Similar effects were noticed for the molasses experiments on increasing the feed rate or increasing rotational speed as noted with the glucose/fructose separations.

9.7 Computer modelling

A computer simulation program has been developed in conjunction with Mr S Bridges, a fellow research student, named CHROMA which can be used to predict the peak positions of solutes leaving the annulus, the exit bandwidths of solute peaks, product purities, throughputs and yields. The program also has the facility of superimposing the computer predicted results over the experimentally determined chromatograms. Predictions of $\bar{\theta}$, the peak position is fairly simple since the theoretical plate model can be used to good effect. If an average value of the distribution coefficient is taken from all the experiments using a particular feed solution with the appropriate ion exchange resin, the computer predicted θ values are very close to the experimental values. Obviously the more data available the more reliable is the prediction of θ.

Where the 'plate' theory is limited is in the prediction of exit bandwidths, W. When feed flowrate is increased the increase in W is much greater than predicted by the theory and when rotational speed is increased the increase in W is smaller than predicted. The computer model requires the input of a dispersion factor which is essentially a lumped parameter which depends on temperature, particle size for the resin, eluent properties and velocity etc. The dispersion factor ultimately determines the bandwidth for each solute. A dispersion factor was found for each solute under each of the experimental conditions such that the computer predicted exit bandwidth matched the experimentally determined exit bandwidth. It was then discovered that with the data available there appeared to be a linear relationship between bed loading and the dispersion coefficient. Hence it should now be possible to use the program to predict the θ and W values provided the relationship between the bed loading and the dispersion coefficient is known and also the distribution coefficient of a solute at known feed concentration using specific resins. Once the θ and W values are known it is then possible to evaluate purity, throughput and yield under any desired conditions.

9.8 Recommendations for Future Work

The major problem encountered with the CCC equipment is that of dilution of products. To produce economically viable sugar solutions, product concentrations need to be as high as possible to cut down

evaporation costs. Dilution of products is related to bandspreading. Reducing bandspreading not only reduces dilution it also increases resolution and allows much greater feed flowrates to be used. The following are a series of recommendations for improvements to the design of the equipment in order to improve product concentration and resolution.

1 An increase in the diameter of the exit holes from the base of the annulus and a more of a gradual change from the base of the annulus to the hole. This should have the effect of reducing the plate pressure drop.

2 The second suggestion is the replacement of the porous plugs within the baseplate with a porous ring set into a V-groove. These two idea should reduce suspected radial mixing at the exit caused by disturbance of flow and hold-up.

3 The use of drip tubes beneath the baseplate to prevent product mixing under the plate.

4 The incorporation of a moveable feed nozzle which can be adjusted either upwards or downwards depending on the height of the packing on the day of the experiment. Using very porous resins and resins which compress with use causes vertical

movement of the packing. A means of quickly adjusting the height of the feed nozzle would not only save time but also produce more consistent results, since the feed nozzle could be set to an accurate height above the resin before each experiment.

4 Some form of backwashing device should be constructed to remove fires or debris from the resin. This would probably consist of a split polypropyiene ring with a channel set into one side to evenly distribute water to all parts of the equipment. The device would have to be screwed to the stainless steel baseplate and sealed with 'O'-rings.

5 The use of smaller particle size resins although causing increased pressure drop could be very beneficial in that mass transfer area is greatly improved and voidage is reduced. This would give significant improvements in resolution and/or product concentrations.

NOMENCLATURE

K'	Capacity factor = $\frac{\text{total moles of solute in the stationary phase}}{\text{total moles of solute in the mobile phase}}$
u_x	average velocity of solute x
t_R	retention time of a solute
t_o	time taken by the solvent to traverse a column
L	column length (m)
F	flowrate of a solute through a column
V_R	retention volume
V_m	total volume of solvent within a column
t_W	bandwidth in a conventional column
N	number of theoretical plates
H	the height equivalent to a theoretical plate
σ_z^2	length based second moment, variance
Z	distance along a column of length L
C	solute concentration
C_o	concentration at the peak
V_o	mobile phase velocity
$t_{w(h/e)}$	bandwidth at the peak height divided by the base of the natural logorithm, e
u	mobile phase velocity
A	eddy diffusion component
B	longitudinal diffusion terms

C	mass transfer term
α	separation factor
R_s	resolution or degree of separation between two solutes
θ	angular displacement of peak from feed entry point
V	superficial eluent velocity (mh^{-1})
ε	void fraction $= \dfrac{\text{volume of voids}}{\text{empty column volume}}$
D_f	dilution factor = W/Wo
W_o	initial feed bandwidth (degrees)
Q_f	feed flowrate ($cm^3\ h^{-1}$)
Q_E	eluent flowrate ($cm^3\ h^{-1}$)
ω	rotational speed ($deg\ h^{-1}$)
λ_c	Langmuir isotherm
n_i	solute i concentration in the solid phase ($mol\ l^{-1}$)
C_i	solute i concentration in the liquid phase ($mol\ l^{-1}$)
N_c	Langmuir isotherm parameter
ρ	number of solutes
D_z	dispersion factor

REFERENCES

1 RENDELL M "The Real Future of Large-scale Chromatography", Proc Eng, London, 66-70, (1975)

2 SUSSMAN MV "Continuous Chromatography", Chem Tech 6, (4), 260-264, (1976)

3 SUSSMAN MV & RATHORE RNS "Continuous Modes of Chromatography", Chromatographia 8(2), 55-59, (1975)

4 BARKER PE "Developments in Continuous Chromatographic Refining" Dev Chromatogr, 1, 41-86 (Birmingham), 1978

5 MARTIN AJP and SYNGE RLM, Biochem J (London) 35, 1358, (1941)

6 GLUECKAUF E, Transactions of the Faraday Society, 60, 729-734 (1964)

7 LAPIDUS L & AMUNDSON NR, "Mathematics of adsorption in Beds. VI. The Effect of Longitudinal Diffusion in Ion Exchange and Chromatographic Columns", J Phys Chem 56, 984-988 (1952)

8 VAN DEEMTER JJ, Zuiderweg FJ and Klinkerberg A, Chem Eng Sci, 5, 271-281, (1956)

9 GIDDINGS JC "Theoretical basis for a continuous large capacity gas chromatographic apparatus", J Chromatogr, 43, 48-65, (1969)

10 SNYDER LR & KIRKLAND JJ, "Introduction to modern liquid chromatography", Wiley-Interscience, New York, (1974)

11 MOSKIN LN, GUMEROV MF & GORSHKOV AI "Continuous composition monitoring for permanent gases in reactors", At Energy USSR 39 (2), 707-709 (1975)

12 WANKAT PC "The relationship between one-dimensional and two dimensional separation processes", AIChE J, 23 (6), 859, (1977)

13 SCOTT CD, SPENCE RD & SISSON WG "Pressurized annular chromatograph for continuous separations", J Chromatogr 126, 381-400 (1976)

14 BEGOVICH JH "Multicomponent separations using a continuous annular chromatograph", Oak Ridge National Laboratory Report ORNL-5915, Oak Ridge, Tennesee (Dec 1982)

15 HONGISTO HJ & HEIKKILA H "Desugarisation of cane molasses by Finn Sugar Chromatographic Separation Processes, 16th Congress, 1977 (78)

16 BROUGHTON DB, Chem Eng Progr 64, (8), 60-61, 1968

17 PICHLER H, SCHULTZ H, Brennst-Chem 39, 48-52 (1958)

18 Gulf Research and Development, US Patent: 289355

19 LUFT L, Mine safety appliances, US Patent: 3016107

20 BARKER PE & DEEBLE RE, Anal Chem 45, (1973)

21 BARKER PE, ELLISON JF & HATT BW "Continuous Chromatography of Macro-molecular Solutes" Chromatogr Synth Biol Polym, Elect Chem Soc Int Symp 3, 1, 281-39 (1976)

22 BARKER PE & CHUAH CH "A Continuous Chromatographic Process for obtaining Fructose from a Glucose-Dextran Contaminated Carbohydrate Mixture", Inst Chem Eng Symp Ser, 76, 313-37 (1982)

23 GOULD JC, PhD thesis, University of Aston in Birmingham, (1981)

24 MARTIN AJP, "Summarising Paper", Disc Faraday Soc (London) 2, 332 (1949)

25 DUNNIL P, LILLEY MD "Continuous enzyme isolation", Biotechnol and Bioeng Symp No 3, 97-113 (1972)

26 CHO BK, CARR RW & ARIS R "A new continuous flow reactor for simultaneous reaction and separation", Sep Sci Technol 15 (3) 679-696 (1980)

27 BYALI AL & GANITSKII MB "Continuous flow chromatograph for preparative purposes", USSR Patent No 257 134 (Nov 11, 1969)

28 WICHTERLE O & COUPEK J "Continuous chromatographic separation of mixtures", Czech Patent No 152, 620 (April 15, 1974)

29 ANDREW SPS "Some problems and opportunities in separation process technology in chemicals manufacturing", paper presented at the International Conference on Separation Process Technology, Plymouth, (Nov 13-15, 1979)

30 SVENNSON H & BRATTSEN CE Science tools 2, 17-22 (1955)

31 GRASSMAN W & HANNIG K, Agnew Chem 62 170-172 (1950)

32 SVENSSON H, Swed Patent 133,851 (1951)

33 DINELLI D, POLEZZO S & TARAMASSO M, J Chromatog 7, 477-484 (1962)

34 POLEZZO S & TARAMASSO M "Rotating unit for the preprative-scale gas chromatography, Part II - Theoretical aspects" J Chromatogr 11, 19-26 (1963)

35 TARAMASSO M "Considerations for the design of a rotating unit for continuous production by gas chromatography and its applications", J Chromatogr 49 27-35 (1970)

36 SOLMS JJ, Brit Patent 786, 896 (1957)

37 STRAIN HH & SULLIVAN JC, Anal Chem 189, 100-105 (1962)

38 DURRUM EL, J Am Chem Soc 73, 4875-9 (1951)

39 MICHEL F, VAN DER KAMP FP, Angew Chem 64, 607 (1952)

40 HEATON WB, US Patent 3, 077, 103 (1963)

41 MOSHIR LD, Ibid 3, 078, 647 (1963)

42 HALL LG, Ibid 2, 891., 680 (1959)

43 SUSSMAN MV, HUANG CC, Science 156 974 (1967)

44 SUSSMAN MV, ASTILL KN & RATHORE RNS, J Chromatog Sci 12, 91-102 (1974)

45 SUSSMAN MV, ASTILL KN, ROMBACH R & CARRULO A Chem SS Ind Eng Chem Fundam 5, 141-147 (1974)

46 SUSSMAN MV, ASTILL KN & RATHORE RNS, J Chromatog Sci 12, 91 (1974)

47 FOX JB "Apparatus for continuous liquid chromatography", US Patent No 3, 666, 105 (May 30, 1972)

48 FOX JB, CALHOUN RI, EGLINGTON NJ & NICHOLAS RA "Continuous chromatography apparatus" J Chromatog 43, 48-55, (1969)

49 FOX JB, CALHOUN RC, EGLINGTON NJ & NICHOLAS RA "Continuous chromatography apparatus", J Chromatogr 43, 55-65, (1969)

50 TUTHILL EJ & FIELDMAN J, Ibid 3527350, (1970)

51 TUTHILL EJ, J Chromatogr Sci 8, 285-291, (1970)

52 MOSKIN LN & MEL'NIKOV VA "Continuous isolation of Rubidium and Caesium from solution", J Anal Chem USSR 33 (1), 28-31 (1978)

53 CANON RM & SISSON WG "Operation of an improved continuous annular chromatograph", J Liq Chromatogr 1 (4), 427-441 (1978)

54 CANON RM, BEGOVICH JM & SISSON WG "Pressurized continuous chromatography", Sep Sci Technol 15 (3), 655-678 (1980)

55 BRATZLER RL & BEGOVICH JM "A mathematical model for multicomponent separations on the continuous annular chromatograph" Oak Ridge National Laboratory Report ORNL/TM-6706, Oak Ridge, Tennesee

56 BEGOVICH JM, BYERS CH & SISSON WG, "A high capacity pressurized continuous chromatograph" Sep Sci Technol Div, Oak Ridge National Laboratory, Sep Sci Technol, 18, (12-13), 1167-91 (1983)

57 McGINNIS RA (Ed) Beet Sugar Technology, (1971)

58 DOFNER K "Ion exchangers, properties and applications", Ann Arbor Science, Michigan (1972)

59 JONES GC, British Sugar plc, Norwich, Private communication

60 CHARLEY PJ, Abstract from Rendleman JA, Adv in Carbohydrate Chem and Biochem, 24, 209-214, (1966)

61 ANGYL SJ, J Chem 25, 1957-1961 (1972)

62 ANGYL SJ, J Chem 27, 1947-1953 (1974)

63 ANGYL SJ, J Chem 28, 1279-84 (1975)

64 ANGYL SJ, J Chem 28, 1541-49 (1975)

65 ANGYL SJ, OLIS J, JAMES VU & POJER PM, Carbohydrate Res 60, 219-229 (1978)

66 ANGYL SJ, EVANS ME & BEVERIDGE RJ, Methods in carbohydrate chromatography 8, 233-256 (1980)

67 JONES GJ, British Sugar plc Norwich, Private communication (1985)

68 BEGOVICH JM & SISSON WG "Pressurized continuous chromatograph", Sep Sci Technol 15 (3), 655-78 (1980)

69 BARKER PE & THAWAIT SJ, Chromatogr 295 479-486 (1984)

70 STARK JB, Am Chem Soc 14th Meeting Abstract of papers (Sept 1963)

71 SUGINO N & TAKAHASHI K, Japanese Patent No 19596/68 (Appl 11.6.64)

72 TAKAHASHI K & TAKIKAWA T, Process Res Soc Japan Sugar Refineries Technol 16 51-63 (1965)

73 SCHNEIDER HG & MIKULE J, German patent Appl 2231784, 223 2093 and 2257664

74 MUNIR M, SCHIACEK H & WEINZ HW "Process for the treatment of molasses", Suddeutche Zucker AG Ger OLS 2362211 Appl 14 Dec/published 19.6.75

75 MUNIR M, SCHIACEK H, WEINZ HW & WARM F Ger OLS 2511904 (19.3.75)

76 MUNIR M, International Sugar Journal 78, 100-106 (1976)

77 HONGISTO HJ & HEIKKILA H, Process International Society Sugar Cane Technology 16th Congress 3, 3031-3038 (1978)

78 HONGISTO HJ, Tech Pap Proc Annual Meeting of the Sugar Industry, 38, 22-38 (1979)

79 HONGISTO JH Proc Int Soc Sugar Cane Technol, 17th Congress, 3, 2029-2042 (1981)

80 HONGISTO HJ, Brit Sugar Corp, 23rd Technical Conference (1976) DI-024

81 HONGISTO HJ & HEIKKILA H, Proc 16th Congress 3031-3038 (1977)

82 SAYAMA K, SENBA Y & KAWAMOTO T Proc Res Soc Japan Sucrose Refineries Technol, 29, 1-29 (1980)

83 SAYAMA K, SENBA Y & KAWAMOTO T Proc Res Soc Japan Sucrose Refineries Technol, 30, 64-87 (1982)

84 ASADI M "Desaccharification of molasses by ion-exclusion chromatography", Listy Cukrov 99 (12), 275-84 (1983)

85 MATTILA M "Chromatographic separation of sugar from green syrup and molasses" Ind Sacc Ital 78, (6) 1183-8 (1985)

86 OSTANIEWICZ A & FOUNALE W "Development of a method of recovery of part of the sucrose contained in molasses by ion exclusion", Gaz Cukrov 88 (2), 45, (1980)

87 HOUGHTON G "Band shapes in non-linear chromatography with axial dispersion", J Phys Chem 67, 84-88 (1963)

Page 1 of HIJO.FOR

```
      PROGRAM CHROMA
      CHARACTER LINE(70)
      CHARACTER IB,IG,IF,II,PLUS,ANG
      DIMENSION CE(4),DIFFY(4),X(3200),CGRID(3200,4),PKPRD(4),
     1 W(4),PKCON(4),DILF(4),RES(3)
      DIMENSION K1(4),K0(4),K2(4)
      DIMENSION YSC(4),MAXH(4)
      COMMON CAPU(4),SLAM(4),EC(4),CI(4)
      PARAMETER(IB=' ',IG='S',IF='IO',PLUS='+',ANG='*')
      DATA DELTAT/.25/
      REAL K1,K0,K2
      OPEN(21,FILE='RESU',STATUS='NEW')
      OPEN(23,FILE='SIM',STATUS='NEW')
      DO 2001 IK=1,10
      PRINT*,'READ IN ROT,ANULL,ANULD,V,EPS,QE,QF,M'
      WRITE(21,810)
  810 FORMAT('ROT AUNLL ANULD V EPS QE QF M')
      READ*,ROT,ANULL,ANULD,V,EPS,QE,QF,M
      WRITE(21,*) ROT,ANULL,ANULD,V,EPS,QE,QF,M
      PRINT*,'READ IN FEED CONC. (G/CM3) '
      WRITE(21,811)
  811 FORMAT('FEED CONC')
      READ*,(CE(I),I=1,M)
      WRITE(21,*) (CE(I),I=1,M)
      PRINT*,'READ IN DIFFUSIVITIES (CM2/MIN) '
      WRITE(21,812)
  812 FORMAT('DIFFYS')
      READ*,(DIFFY(I),I=1,M)
      WRITE(21,*) (DIFFY(I),I=1,M)
      PRINT*,'READ IN K2 VALUES'
      WRITE(21,813)
  813 FORMAT('K2')
      READ*,(K2(I),I=1,M)
      WRITE(21,*) (K2(I),I=1,M)
      PRINT*,'READ IN K1 VALUES'
      WRITE(21,814)
  814 FORMAT('K1')
      READ*,(K1(I),I=1,M)
      WRITE(21,*) (K1(I),I=1,M)
      PW=360*(QF/(QF+QE))
      DQ=(QF+QE)/1440.0
      HGHPW=PW*3.142*ANULD/360
      HGHROT=ROT/60
      HGHV=V/EPS
      CALL SETHGH(HGHV,EPS,DIFFY,M,CE,K1,K2)
      NDIM=800/DELTAT+0.5
      DO 20 IT=1,NDIM
      X(IT)=IT*DELTAT
   20 CONTINUE
      DO 30 IE=1,M
      CALL HOUGH(CGRID,X,NDIM,IE,HGHROT,ANULL,PW,HGHPW,MAXH,CE)
   30 CONTINUE
      DO 90 IE=1,M
      PKCON(IE)=0.0
      PKPRD(IE)=0.0
```

```
      DO 40 IT=1,MAXH(IE)
      IF (CGRID(IT,IE).LE.PKCON(IE)) GO TO 40
      PKCON(IE)=CGRID(IT,IE)
      PKPRD(IE)=X(IT)
   40 CONTINUE
      HPRD=PKCON(IE)*0.60653
      DO 50 IT=1,MAXH(IE)
      IF (CGRID(IT,IE).GT.HPRD) GO TO 60
   50 CONTINUE
      IT=MAXH(IE)
   60 IF (IT.EQ.1) IT=IT+1
      IF (IT.EQ.MAXH(IE)) IT=MAXH(IE)-1
      SY=(CGRID(IT+1,IE)-CGRID(IT-1,IE))
      SX=(X(IT+1)-X(IT-1))
      SLOPE=SY/SX
      XP1L=X(IT)-CGRID(IT,IE)/SLOPE
      DO 70 ITT=1,MAXH(IE)
      IT=MAXH(IE)-ITT+1
      IF (CGRID(IT,IE).GT.HPRD) GO TO 80
   70 CONTINUE
      IT=1
   80 IF (IT.EQ.1) IT=IT+1
      IF (IT.EQ.MAXH(IE)) IT=MAXH(IE)-1
      SY=(CGRID(IT+1,IE)-CGRID(IT-1,IE))
      SX=X(IT+1)-X(IT-1)
      SLOPE=SY/SX
      Z=CGRID(IT,IE)/SLOPE
      Y=X(IT)
      XP1R=Y-Z
      XP1R=X(IT)-Z
      W(IE)=XP1R-XP1L
      DILF(IE)=W(IE)/PW
   90 CONTINUE
      ICNTT=0
      MM1=M-1
      DO 100 IE=1,MM1
      ICNTT=ICNTT+1
      INEXT=IE+1
      RES(ICNTT)=2.0*(PKPRD(INEXT)-PKPRD(IE))/(W(INEXT)+W(IE))
      RES(ICNTT)=ABS(RES(ICNTT))
  100 CONTINUE
      WRITE(21,819)
  819 FORMAT('COMPONENT PEAK POS. BANDWIDTH PEAK CONC. DF')
      DO 110 IE=1,M
      YSC(IE)=69/PKCON(IE)
      WRITE(21,*) IE,PKPRD(IE),W(IE),PKCON(IE),DILF(IE)
  110 CONTINUE
      OPEN(20,FILE='RESUL',STATUS='NEW')
      YSCA=YSC(1)
      DO 313 IE=1,M-1
      YSC(IE+1)=69/PKCON(IE+1)
      IF (YSC(IE+1).LT.YSCA) YSCA=YSC(IE+1)
  313 CONTINUE
      WRITE(20,213)
  213 FORMAT(30X,'CONC(%W/V)')
```

```
      A=6900/YSCA
      B=0.2*A
      C=0.4*A
      D=0.6*A
      E=0.8*A
      WRITE(20,215) B,C,D,E
  215 FORMAT(1X,4F13.2)
      WRITE(20,212)
  212 FORMAT(1X,65('+'))
      WRITE(21,667)
  667 FORMAT('RESOLUTION')
      PRINT*,'RESOLUTION=',(RES(IE),IE=1,ICNTT)
      WRITE (21,*) (RES(IE),IE=1,ICNTT)
      AONE=1.0/DELTAT
      GRIM=0.0
      DO 622 I=1,M
      IF(MAXH(I).GT.GRIM) THEN
      GRIM=MAXH(I)
      ENDIF
  622 CONTINUE
      WRITE(23,666)
  666 FORMAT('DEGREES  GLUC  FRUC')
      DO 130 AT=AONE,GRIM,40
      DO 214 L=1,70
  214 LINE(L)=IB
      AICOLG1=100*CGRID(AT,1)
      AICOLF1=100*CGRID(AT,2)
      ICOLG=YSCA*CGRID(AT,1)-0.5
      ICOLF=YSCA*CGRID(AT,2)-0.5
      WRITE(23,*) AT/4,AICOLG1,AICOLF1
      LINE(ICOLG)=IG
      LINE(ICOLF)=IF
      LINE(1)=PLUS
      A=AT/180.0
      I=AT/180
      IF(A.EQ.I) THEN
      LINE(1)=ANG
      ENDIF
      WRITE(20,217) LINE
  130 CONTINUE
  217 FORMAT(1X,70A1)
      AM1=0.0
      AM2=0.0
      C=0.0
      DO 75 J=1,NDIM
      IF(CGRID(J,1).GE.0.01.AND.CGRID(J,1).GE.1.857*CGRID(J,2))THEN
      AM1=AM1+CGRID(J,1)*DQ
      AM2=AM2+CGRID(J,2)*DQ
      C=C+1
      ENDIF
   75 CONTINUE
      IF(C.EQ.0.0) THEN
      PRINT*,'PRODUCT CONC TOO LOW I.E PEAK CONC IS BELOW
     1       1.0 %W/V.'
      GO TO 2001
```

```
      ENDIF
      S=AM1-1.8571*AM2
      Y=AM1/(CE(1)*QF)
      TNP=AM1+AM2
      VNP=C*DQ
      AN=TNP/VNP
      P=AM1/TNP
      WRITE(21,872)
  872 FORMAT('THRUPUT(GMMIN YIELD SOLID CONC PURITY')
      WRITE(21,*) S,Y,AN,P
 2001 CONTINUE
      END
      SUBROUTINE SETHGH(V,EPS,D,M,CE,K1,K2)
      DIMENSION K1(4),K2(4),CE(4),D(4)
      COMMON CAPU(4),SLAM(4),EC(4),CI(4)
      REAL K1,K2
      ALPHA=EPS
      DO 200 IE=1,M
      CI(IE)=CE(IE)
      SLAM(IE)=2.0*K2(IE)/(ALPHA*(1+K1(IE)/ALPHA))
      EC(IE)=D(IE)/(1+K1(IE)/ALPHA)
      CAPU(IE)=V/(1+K1(IE)/ALPHA)
  200 CONTINUE
      RETURN
      END
      SUBROUTINE HOUGH(CGRID,X,NDIM,IE,OMEGA,Z,PW,CL,MAXH,CE)
      DIMENSION CGRID(3200,4),X(3200)
      DIMENSION CE(4),MAXH(4)
      COMMON CAPU(4),SLAM(4),EC(4),CI(4)
      CUL=CI(IE)*CAPU(IE)*SLAM(IE)
      DO 10 IT=1,NDIM
      CGRID(IT,IE)=0.0
      IF (X(IT).EQ.0.0) GO TO 10
      T=X(IT)/OMEGA
      CZ=Z-CAPU(IE)*T
      SQ=SQRT(EC(IE)*T)
      IF (SQ.NE.0.0) P=(CZ+.5*CL)*.5/SQ
      IF (SQ.NE.0.0) Q=(CZ-.5*CL)*.5/SQ
      IF (T.NE.0.0) G=CUL*(2.0*T*CZ+CUL*T*T)/(4.0*EC(IE)*T)
      IF (SQ.NE.0.0) H=CUL*T/(2.0*SQ)
      RM=CUL*CL/(2.0*EC(IE))
      PPH=P+H
      QPH=Q+H
      PPHE=ERF(PPH)
      QPHE=ERF(QPH)
      CONS=PPHE-QPHE
      RNUM=0.0
      IF (ABS(CONS).GT.1.0E-20) RNUM=EXP(G)*CONS
      DNUM=1.0-ERF(P)+RNUM
      IF (ABS(ERF(Q)+1.0).GT.1.0E-20) DNUM=
     1 DNUM+EXP(RM)*(1.0+ERF(Q))
      IF (ABS(DNUM).LT.1.0E-6) GO TO 10
      CGRID(IT,IE)=RNUM/DNUM
      IF (CGRID(IT,IE).GT.0.0) MAXH(IE)=IT
   10 CONTINUE
```

```
      CURAR=0.0
      XL=X(1)
      YL=CGRID(1,IE)
      DO 20 J=2,MAXH(IE)
      XN=X(J)
      YN=CGRID(J,IE)
      CALL AREA(XL,YL,XN,YN,AC)
      CURAR=CURAR+AC
      XL=XN
      YL=YN
   20 CONTINUE
      ACTAR=PW
      CORR=ACTAR/CURAR
      DO 30 J=1,MAXH(IE)
      CGRID(J,IE)=CGRID(J,IE)*CORR*CE(IE)
   30 CONTINUE
      RETURN
      END
      SUBROUTINE AREA(XL,YL,XR,YR,AC)
      DIFFX=XR-XL
      DIFFY=YR-YL
      IF (DIFFY.LT.0.0) GO TO 10
      AC=DIFFX*YL
      AC=AC+0.5*DIFFX*DIFFY
      RETURN
   10 DIFFY=-DIFFY
      AC=DIFFX*YR
      AC=AC+0.5*DIFFX*DIFFY
      RETURN
      END
      FUNCTION ERF(UN)
      IF (UN.LE.1.95.AND.UN.GE.-1.75) THEN
      E=0.0
      DO 20 I=0,12
      A=UN**(2*I+1)
      B=(-1.0)**I
      C=2.0*I+1.0
      IF (I.LE.1) THEN
      K=1
      GO TO 17
      ENDIF
      K=I
      DO 15 J=1,I-1
      K=K*J
   15 CONTINUE
   17 E=(B*A)/(C*K)+E
   20 CONTINUE
      ERF=1.1283792*E
      ELSE
      A=1.0/UN
      DO 56  J=1,5
      K=1.0
      DO 66 I=J,1,-1
      K=(2*I-1)*K
   66 CONTINUE
```

```
      A=(K*((-1)**J))/((2**J)*(UN**(2*J+1)))+A
   56 CONTINUE
      E=0.5641895*(EXP(-(UN*UN))*A)
      IF (UN.GT.1.75) THEN
      ERF=1-E
      ELSE
      ERF=-1-E
      ENDIF
      ENDIF
      RETURN
      END
```